



North American Neuro-Ophthalmology Society 36th Annual Meeting

March 6-11, 2010 • JW Starr Pass Marriott Resort & Spa, Tucson, AZ
Educational Program Schedule

THURSDAY, MARCH 11

LOCATION

6:30 a.m. – 12:30 p.m.	Registration	Arizona Ballroom Foyer
6:30 a.m. – 7:30 a.m.	Continental Breakfast	Arizona Salon
8:30 a.m. – 10:30 a.m.	Spouse/Guest Hospitality Suite	Signature Grill
7:30 a.m. – 9:30 a.m.	OCT IN NEURO-OPHTHALMOLOGY PRACTICE [2 CME] <i>Moderators: Laura J. Balcer, MD, MSCE and Fiona Costello, MD</i>	Arizona Salons 1-6

This half-morning symposium will review the current knowledge concerning the use of optical coherence tomography (OCT) in patients with neuro-ophthalmologic disorders. The session will discuss the history of OCT and the evolution of the underlying technology. The currently available and future equipment will be discussed and evaluated. The evidence regarding the use of OCT in the diagnosis and follow/up of optic neuritis, chiasmal lesions, multiple sclerosis and other neurologic diseases will be reviewed. A perspective on the clinical utilization of OCT drawing on experience from its place in glaucoma management will be presented. The potential of OCT for monitoring possible neuro-protective treatment of optic nerve and macular disease will be reviewed.

At the conclusion of the symposium, the attendees should be able to: 1) Describe the principle of OCT and the forms of equipment available to perform the test; 2) Discuss the currently available evidence about the use of OCT in evaluating optic neuritis, MS, chiasmal lesions, and other neuro-ophthalmologic disorders; 3) Explain the lessons available from the use of OCT in management of glaucoma; and 4) Discuss the potential use of OCT in monitoring the effects of therapy of anterior visual pathway disease, including neuroprotective agents.

PAGES

7:30 a.m. – 7:50 a.m.	OCT Technologies: Past, Present, and What's New? – <i>Joel Schuman, MD</i>	327
7:50 a.m. – 8:10 a.m.	OCT in Neurologic Disease – <i>Eric Eggenberger, DO, MSEpi</i>	335
8:10 a.m. – 8:30 a.m.	Lessons from Glaucoma: Use of OCT in the Clinic and Trials – <i>Joel Schuman, MD</i>	343
8:30 a.m. – 8:50 a.m.	Linking Axons and Neurons: Unveiling Mysteries of the Macula and Modeling Neuroprotection – <i>Randy Kardon, MD, PhD</i>	369
8:50 a.m. – 9:05 a.m.	Platform Presentation: Ganglion Cell Layer Volume by Spectralis Optical Coherence Tomography (OCT) in Multiple Sclerosis – <i>Emma Davies, MD</i>	375
9:05 a.m. – 9:20 a.m.	Evidence Meets Practice: Take-Home Points on OCT – <i>Thomas Hedges, III, MD</i>	377
9:20 a.m. – 9:30 a.m.	Questions and Discussion	
9:30 a.m. – 10:00 a.m.	Coffee Break	

10:00 a.m. – 12:00 p.m.	<p>THYROID EYE DISEASE UPDATE [2 CME] <i>Moderators: Steven Feldon, MD and Madhu Agarwal, MD</i></p>	Arizona Salons 1–6
	<p>This course will review the latest concepts in the evaluation and treatment of the often vexing disease process of thyroid orbitopathy. The immunology of the condition as well as potential new treatments and their indications will be discussed. Speakers will further discuss newer modalities for assessing disease progression, evaluating strabismus, and surgical and pharmacologic treatment options. A panel discussion will consider these topics, as well as the potential for clinical trial in this area.</p> <p>At the conclusion of the symposium, the attendees should be able to: 1) Understand the latest diagnostic and assessment tools for thyroid eye disease; and 2) Discuss both medical and surgical treatment options.</p>	
		PAGES
10:00 a.m. – 10:30 a.m.	<p>Immunology of Thyroid Eye Disease: New Treatments on the Horizon? – <i>Raymond Douglas, MD, PhD</i></p>	383
10:30 a.m. – 10:50 a.m.	<p>Objective Markers for Thyroid Eye Disease (TED) Activity, Severity and Progression – <i>Kim Cockerham, MD, FACS</i></p>	387
10:50 a.m. – 11:20 am.	<p>Surgical Techniques for Anatomic Restoration – <i>Raymond Douglas, MD, PhD</i></p>	391
11:20 a.m. – 11:40 a.m.	<p>Ocular Motility in Thyroid Eye Disease –Evaluation and Surgery – <i>Steven Feldon, MD</i></p>	395
11:40 a.m. – 12:00 p.m.	<p>Panel Discussion: Impediments to Formulating a Meaningful Clinical Trial</p>	
12:00 p.m.	<p>Meeting adjourns</p>	

OCT TECHNOLOGIES: PAST, PRESENT, AND WHAT'S NEW?

Joel S. Schuman, MD, FACS,^{1,2,3} Michelle Gabriele, BS, MS,^{1,2,3} Gadi Wollstein, MD¹

¹UPMC Eye Center, Eye and Ear Institute, Ophthalmology and Visual Science Research Center, Department of Ophthalmology, University of Pittsburgh School of Medicine, Pittsburgh, PA;

²Department of Bioengineering, Swanson School of Engineering, University of Pittsburgh;

³Center for the Neural Basis of Cognition, Carnegie Mellon University and University of Pittsburgh

LEARNING OBJECTIVES

- The attendee will be able to describe the basic principles of optical coherence tomography.
- The attendee will be able to explain how OCT can be used in the detection of ocular diseases.
- The attendee will be know the utility and potential utility of OCT in the assessment of longitudinal change in diseases of the eye.

CME QUESTIONS AND ANSWERS

1. What is the basic physical principle underlying optical coherence tomography (OCT)?
2. How can OCT be used to detect eye disease, and is there any evidence that it can do so?
3. How can OCT be used to assess change over time in eye disease?

KEY WORDS

- Optical Coherence Tomography (OCT)
- Optic Nerve Head (ONH)
- Retinal Nerve Fiber Layer (RNFL)
- Macula
- Ganglion Cell Complex (GCC)

Supported in part by National Institutes of Health contracts R01-EY13178-10, R01-EY11289-24, and P30-EY08098-21 (Bethesda, MD), The Eye and Ear Foundation (Pittsburgh, PA), and unrestricted grants from Research to Prevent Blindness, Inc. (New York, NY).

Corresponding Author: Joel S. Schuman, MD, UPMC Eye Center, Eye and Ear Institute, Department of Ophthalmology, University of Pittsburgh School of Medicine, 203 Lothrop Street, Suite 816, Pittsburgh, PA 15213; schumanjs@upmc.edu.

Conflict of Interest Statement: Dr. Schuman receives royalties for intellectual property licensed by Massachusetts Institute of Technology to Carl Zeiss Meditec. Dr. Wollstein received research funding from Carl Zeiss Meditec and Optovue. Dr. Schuman received honoraria from Carl Zeiss Meditec, Heidelberg Engineering and Optovue. Ms. Gabriele reports no conflicts.

INTRODUCTION

The development of optical coherence tomography (OCT) began with a team comprised of clinician-scientists and a physicist at Massachusetts Eye and Ear Infirmary (MEEI), Harvard University and engineers at the Massachusetts Institute of Technology (MIT). Remarkably, one member of this group was a graduate student, one a postdoctoral fellow, and another was a predoctoral fellow. OCT actually began as optical coherence domain ranging (OCDR), essentially a single A-scan in what we now know as OCT. OCDR was being developed by James Fujimoto and Carmen Puliafito for corneal ranging. Joel Schuman was a fellow in Puliafito's laser laboratory at MEEI and David Huang an MD, PhD student in the Harvard-MIT Health Sciences Technology (HST) program, working in Fujimoto's laboratory at MIT. Eric Swanson was an engineer at MIT-Lincoln Laboratories, Charles Lin a physicist in Puliafito's lab and William Stinson a preresidency fellow working in Puliafito's lab as well. These seven people were the key persons involved in the development of this technology.

Joel Schuman, while working on other projects in the laser laboratory, became aware of the OCDR corneal ranging target. It occurred to Schuman that the near infrared wavelength of OCDR would be able to safely measure retinal thickness, and would perhaps be useful for measuring retinal layers. After discussing this idea with Puliafito, Schuman pursued the concept together with Fujimoto and Huang. Schuman, Huang, Lin and Stinson did the very first retinal ranging experiments in James Fujimoto's laboratory at MIT.

David Huang, while an MD-PhD student, had the insight that an OCDR A-scan was similar to an ultrasound A-scan, and that creating a tomographic cross-sectional image similar to an ultrasound B-scan would be possible. The technology was refined to create tomography, and was renamed Optical Coherence Tomography (OCT). In 1991 the first scientific paper regarding OCT was published, describing the use of an optical detection technique called low coherence interferometry to acquire cross-sectional images of the peripapillary region of the human retina *ex vivo*.¹ Low coherence tomography refers to the detection of light that has been split, reflected off of an object of interest and a reference mirror and recombined. This recombination produces an interference pattern with an amplitude proportional to the reflectivity of the corresponding location (same optical path length) within tissue of interest. Individual axial scans, or A-scans, are

acquired at a given location in tissue and correspond to a reflectivity profile in depth. Multiple neighboring A-scans can be acquired to build up a B-scan that represents an optical cross-section of the tissue.

OCT was described in vivo in 1993² and quickly used in human subjects as a research tool to investigate retinal and glaucomatous abnormalities.³⁻⁶ During this time the technology was transferred to industry. The OCT patent was granted in 1994 to Fujimoto, Huang, Lin, Puliafito, Schuman and Swanson, and was licensed by what is now Carl Zeiss Meditec, Inc. (Dublin, CA), allowing the creation of a device that could be broadly used for patient care.

The first commercial system became available in 1996 and was a time-domain OCT system (TD-OCT). This means A-scans are acquired by moving the interferometer's reference mirror, which changes the reference path length and enables the detection of reflectivity from different depths in a given structure. Hence, in TD-OCT imaging, the time of flight of the light reflected from the retinal structures determines the OCT measurements. The commercial time-domain OCT system has an axial resolution of approximately 10 μ m.

The first commercial two iterations of OCT were not particularly successful, in part because of the novelty of the technology, but also because systems were big, slow and difficult to use. This changed in 2002 with the introduction of Stratus OCT. The Stratus system acquired 400 A-scans per second, compared with 100 per second in prior versions. Stratus OCT also had a normative database, making clinical use considerably more practical, and the system was now ergonomically designed. Finally, a billing code for scanning computerized ocular diagnostic imaging was introduced around the time that Stratus came to market. All of these factors contributed to the rapid adoption of the technology; by 2008 10,000 OCT devices were in worldwide clinical use.

OCT underwent further evolution with the clinical availability in 2006 of spectral-domain OCT (SD-OCT).⁷⁻¹¹ SD-OCT introduced in 2006 was 40–60 times faster than TD-OCT, allowing the collection of large amounts of clinical data, permitting increased scan densities and three dimensional imaging. SD-OCT refers to the measurement of tissue thickness using not time of flight but reflected wavelengths (frequencies). Using SDOCT, an entire A-scan can be collected simultaneously, and the optical frequencies analyzed using fast Fourier transformation and mathematical algorithms to create a tomographic image and determine depth information, converting from the frequency domain to the time domain. Because optical frequencies from different depths are detected at once and used to determine the spatial locations of reflections in the A-scans, a moving reference mirror is not required: conversion from the frequency domain to the time domain occurs after acquisition. This means SD-OCT systems can acquire A-scans much faster than time-domain systems. SD-OCT systems have recently been commercialized by several companies, and most of these systems have an axial resolution of approximately 3.5 – 6 μ m and

acquisition speeds of 24,000 – 55,000 A-scans per second. Axial resolution improvements in these systems can be attributed to broader bandwidth light sources.

HEALTHY EYES

This section provides representative ocular OCT images, both time-domain and spectral domain, from healthy subjects. Figure 1a shows a representative SD-OCT image through the macular region of a healthy subject, while the Figure 1b shows a representative TDOCT image from the same subject. Note that the time-domain image contains 128 A-scans and the SD-OCT image contains 1000 A-scans; however, the TD-OCT image required 0.32 seconds to acquire, while the SD-OCT image, with eight times more A-scans, took 0.04 seconds.

FIGURE 1: (a) Vertical SD-OCT cross-section through the macula of the same subject. The white box with vertical line indicates the orientation of SD-OCT image. (b) Vertical TDOCT cross-section through the macula.

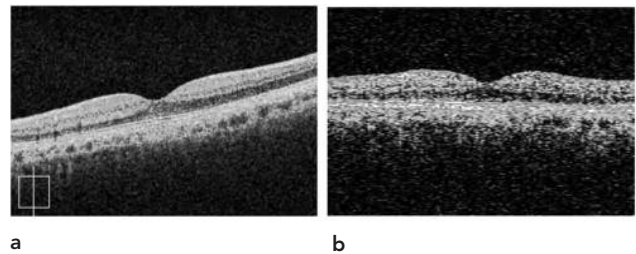
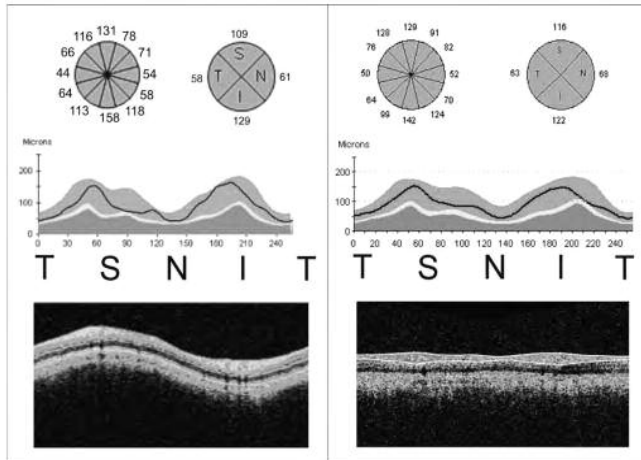


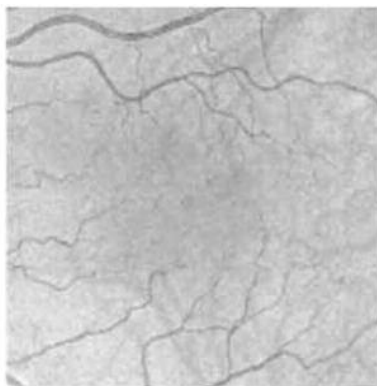
Figure 2 shows spectral domain (left panel) and time-domain (right panel) OCT retinal nerve fiber layer (RNFL) assessments. With time-domain devices, a 3.4-mm circular scan centered on the optic nerve head (ONH) is used to assess peripapillary RNFL thickness. Typically, three OCT scans (with 256 A-scans per scan) are acquired in succession, the RNFL is segmented, and thickness measurements along the scan are compared to a normative database. Using spectral-domain three-dimensional tissue volumes from around the optic nerve, one can reconstruct the RNFL peripapillary scan by resampling the tissue volume along a 3.4 mm circle centered on the ONH. An extracted RNFL scan can be seen in Figure 2, bottom left. Above it, an RNFL thickness overlay on a normative database is shown along with clock-hour and quadrant RNFL thickness measurements. One peripapillary TD-OCT scan, with RNFL segmentation (white line), is shown in Figure 2, bottom right. Above it lie the normative database with an overlay of RNFL thickness and clock-hour and quadrant RNFL thickness measurements.

FIGURE 2: (Left) SD-OCT RNFL thickness clock-hour and quadrant measurements (top), comparison to normative database (middle), and resampled 3.4-mm RNFL B-scan (bottom). (Right) TD-OCT RNFL thickness measurements (top), comparison to normative database (middle) and 3.4-mm RNFL peripapillary scan (bottom). Both images were acquired from the same subject, same day.



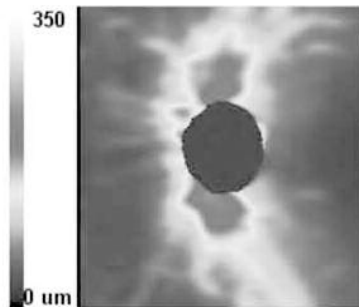
In SD-OCT, after multiple B-scans are acquired in raster fashion and a three-dimensional volume of tissue is acquired, *en-face* (OCT fundus) images can be generated by summing intensity values along the z-direction (in depth). An example SD-OCT fundus image through the macular region of a healthy subject is seen in Figure 3.

FIGURE 3: SD-OCT fundus image of the macular region of the left eye of a healthy subject, created by taking the sum of the reflections along the direction of each individual A-scans in the 200 x 200 A-scan volume. This creates a picture-like image due to the total reflection at each scan location being viewed in the *en-face* composite, much the same as in a photograph.



When three-dimensional tissue volumes have been acquired around the optic nerve head region using SD-OCT, RNFL thickness maps can be created by segmenting the RNFL in each frame of the volume, excluding the optic nerve head region. This provides easy visualization of areas of thinning around the optic nerve. Example RNFL thickness maps from a healthy subject can be seen in Figure 4.

FIGURE 4: RNFL thickness map of the left eye of a healthy subject created from a 200 x 200 A-scan scanning (6 x 6 mm) of the optic nerve head region. Thicker areas are red and thinner areas are blue. The uniform blue area towards the center of each map indicates the optic nerve head region, where no thickness measurements are made.



In addition to posterior segment imaging, images of the cornea and anterior chamber can be acquired with OCT. Figure 5 shows a horizontal TD-OCT image through the cornea of a healthy subject. Figure 6 shows an anterior chamber TD-OCT image from the same subject.

FIGURE 5: TD-OCT image through the cornea of a healthy subject.

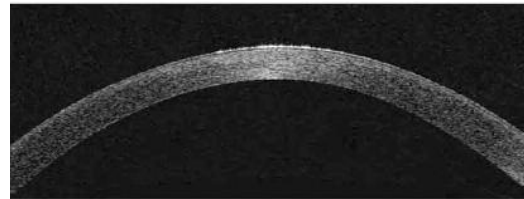


FIGURE 6: TD-OCT image through the anterior chamber of a healthy subject.



GLAUCOMA

A 58-year-old woman with a history of primary open angle glaucoma presented with an IOP of 30 in the right eye (VA 20/20). Visual field testing showed a superior arcuate defect, with a glaucoma hemifield test outside normal limits, mean deviation of -1.25 dB, and pattern standard deviation of 4.37 dB (Figure 7). Widespread inferior nerve fiber layer thinning can be seen in the SD-OCT RNFL thickness map (Figure 8). Figure 9, top, shows clock hour and quadrant thicknesses from SD-OCT (left panel) and TD-OCT (right panel). A comparison to a normative database is shown below the segment measurements. Both spectral- and time-domain measurements show inferior thinning of the RNFL, as indicated by red quadrant and clock hour segments. Looking at individual spectral- domain and time domain OCT cross sections (bottom left and bottom right, respectively), thinning of the RNFL can be seen (arrows). Note that the white line outlining the RNFL in the time-domain image indicates segmentation of the RNFL; this line is not present in the spectral-domain image. In addition, the spectral-domain image has not been flattened using image filtering techniques while the time-domain image has.

FIGURE 7: Visual field test showing a superior arcuate defect from a patient with primary open angle glaucoma.

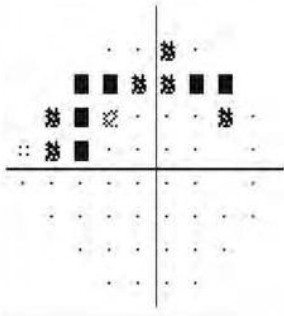


FIGURE 8: RNFL thickness map of patient with primary open angle glaucoma showing inferior thinning of the RNFL (map created from 200 x 200 A-scans, 6x6 mm region around the optic nerve head). The uniform blue region towards the center of the image represents the optic nerve head while black region is the result of RNFL detection algorithm failure.

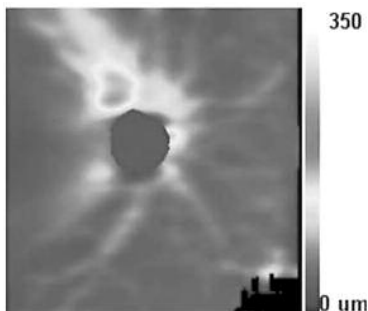
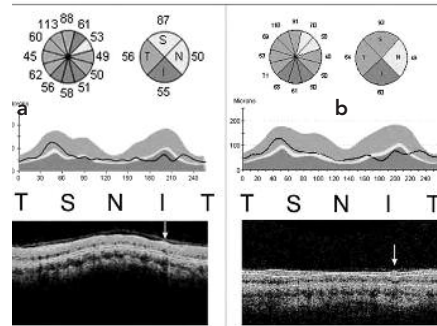


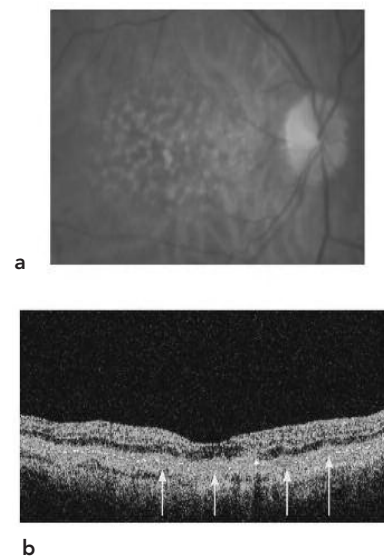
FIGURE 9: (Left) SD-OCT RNFL thickness clock-hour and quadrant measurements (top), comparison to normative database (middle), and resampled 3.4-mm RNFL B-scan (bottom) in patient with primary open angle glaucoma and inferior RNFL loss. (Right) TD-OCT RNFL thickness measurements (top), comparison to normative database (middle) and 3.4-mm RNFL peripapillary scan (bottom). Both images were acquired from the same subject, same day.



AGE-RELATED MACULAR DEGENERATION

Figure 10 shows a fundus photograph and slow macular (512 A-scans) TD-OCT scan from an 84-year-old female with exudative age-related macular degeneration; she had with 20/40 vision in the right eye. Drusen and RPE changes were noted upon clinical examination. The fundus photograph (Figure 10a) shows numerous drusen in the macular region. Similarly, irregularities in the RPE can be seen in the horizontal OCT cross-section though the macular region (Figure 10b, arrows).

FIGURE 10: (a) Fundus photograph of age-related macular degeneration patient with drusen (b) Horizontal TD-OCT scan (512 A-scans). Arrows indicate areas that are likely drusen.



MACULAR HOLE

A 72-year-old male presented with a distorted vision in the right eye (VA 20/200) and 20/50 vision in the left eye. Both spectral-domain and TD-OCT images showed a large macular hole in the right eye with posterior hyaloid partially attached to edge of the hole (Figure 11, spectral-domain horizontal and vertical cross-sections on left and time-domain horizontal and vertical cross-sections on right). Small cystoid changes with a vitreous traction were seen in the left eye along with posterior hyaloid traction in the foveal center (Figure 12). Three-dimensional reconstructions of the thickness maps of the macular region are also shown (Figure 11 and 12, top) and were created by segmenting three-dimensional data volumes (200 x 200 A-scans in a 6 x 6 mm region of the retina) from the ILM to the RPE. The blue lines on each thickness map correspond to the location of the horizontal spectral-domain cross-sections (1000 A-scans each), while the purple lines correspond to the location of vertical cross-sections (1000 A-scans).

FIGURE 11: Right eye (Top) Three-dimensional reconstruction of macular region showing foveal thickening (red) that corresponds to the location of a macular hole and corresponding edema (Middle and Bottom, left) Horizontal and vertical SD-OCT (1000 A-scans) cross-sections through the macular hole (Middle and Bottom, right) Horizontal and vertical TD-OCT (512 A-scans) cross-sections through the macular hole.

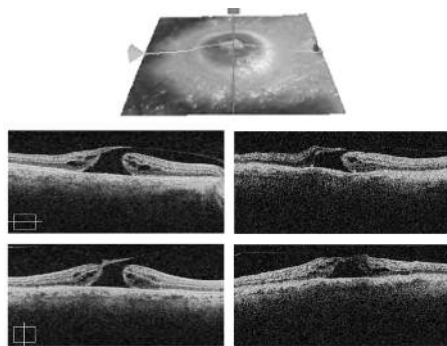
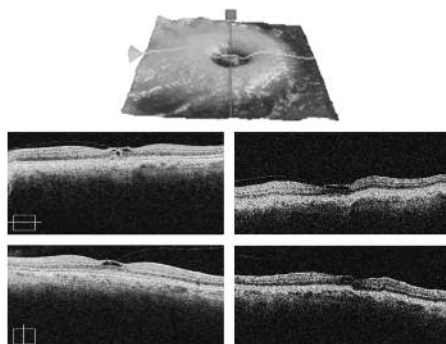


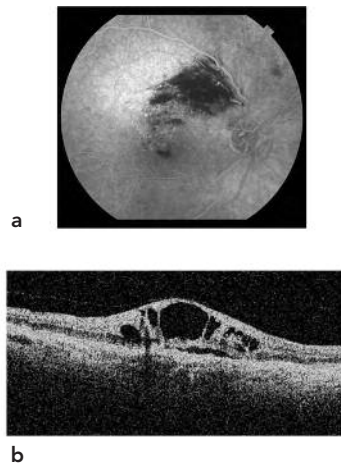
FIGURE 12: Left eye. (Top) Three-dimensional reconstruction of macular region showing slight foveal thickening (green) that corresponds to the location of small cystoid changes (Middle and Bottom, left) Horizontal and vertical SD-OCT (1000 A-scans) cross-sections through the macula (Middle and Bottom, right) Horizontal and vertical TD-OCT (512 A-scans) cross-sections through the macula.



BRANCH RETINAL VEIN OCCLUSION

Figure 13a shows a late-phase angiograph from an 82-year-old male with branch retinal vein occlusion in the right eye. He presented with a visual acuity of 20/400 and clinical examination showed hemorrhage and macular edema in the right eye. A slow macular (512 A-scans) horizontal TD-OCT image showed clinically significant macular edema (Figure 13b).

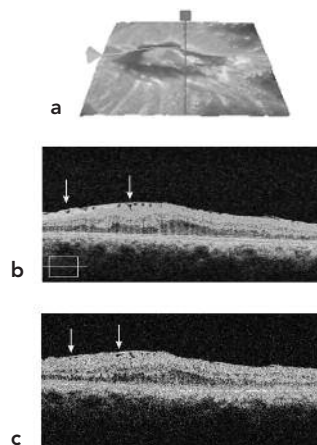
FIGURE 13: (a) Late-phase angiograph showing branch retinal vein occlusion (b) Horizontal TD-OCT image (512 A-scans) through the macular region showing edematous changes.



MACULAR PUCKER

A 60-year-old woman with 20/70 vision in the left eye showed a pronounced epiretinal membrane with posterior vitreous detachment. A three-dimensional reconstruction of the macular thickness map illustrates the extent of macular puckering (Figure 14a). The epiretinal membrane can be seen in individual horizontal spectral-domain (Figure 14b) and time-domain (Figure 14c) OCT images (arrows).

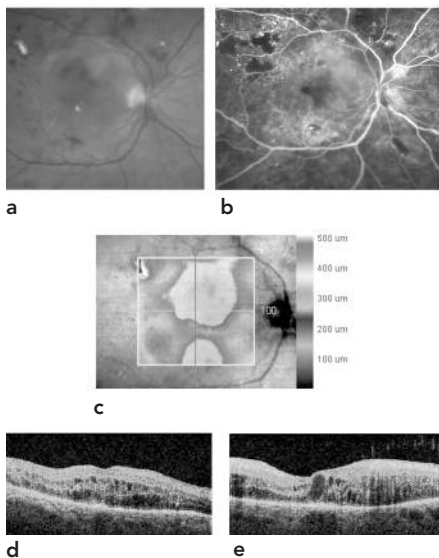
FIGURE 14: (a) Three-dimensional reconstruction of macular region showing macular puckering (b) Horizontal SD-OCT (1000 A-scans) and (c) time-domain (512 A-scans) OCT images through the macula, with arrows indicating epiretinal membrane.



DIABETIC MACULAR EDEMA

Figure 15 (a) and (b) show a fundus and red-free photograph, respectively, from a 65-year-old male with moderate nonproliferative diabetic retinopathy and clinically significant diabetic macular edema in the right eye. He presented with 20/160 vision in this eye. Scattered blot hemorrhages and hard exudates can be seen in the fundus photograph, and microaneurysms in the red-free photograph. A SD-OCT macular thickness map (200 x 200 A-scans covering 6x6 mm region, segmented from the ILM to the RPE) superimposed on a fundus photograph (Figure 15c) shows a region of thickening that corresponds to the macular edema, with thicker areas represented as hotter colors. Horizontal (Figure 15 d) and vertical (Figure 15e) spectral-domain crosssectional OCT images show the extent of fluid accumulation in the macular region.

FIGURE 15: (a) Fundus photograph of patient with diabetic retinopathy and clinically significant macular edema. (b) Red-free photograph. (c) SD-OCT thickness map of macular region superimposed onto fundus photograph, with thicker areas white/red. (d) Horizontal and (e) vertical SD-OCT images (1000 A-scans each), the location of each corresponding to the blue and purple lines on the macular thickness map.



POTENTIAL DIAGNOSTIC POWER

Since its commercialization in 1996, OCT has increasingly become a valuable tool for ophthalmologists. Posterior segment imaging has improved the quantification of RNFL damage in glaucoma and the visualization of changes due to age-related macular degeneration, macular hole, epiretinal membrane and macular puckering, macular edema and more. In addition, anterior segment imaging allows clinicians to monitor patients after LASIK (not shown here) and corneal injury, and provides a non-invasive alternative to ultrasound biomicroscopy for anterior chamber imaging.

While OCT offers several advantages to clinicians, certain limitations need to be kept in mind. This technique, especially spectral-domain imaging, is still rather new and longitudinal studies are required to evaluate its objective monitoring capabilities. In addition, high-speed imaging is very sensitive to eye motion and large movements may make measurements inaccurate. Fortunately, however, solutions to these restrictions are currently being pursued by several research groups.

In sum, OCT offers clinicians a new perspective on structural damage caused by disease. This may lead to enhanced diagnostic power — not only through objective quantification but through synergy with other methods of evaluation that are presently available to clinicians.

CME ANSWERS

1. OCT is based on interferometry
2. Measurements of various ocular structures demonstrate differences in disease and health. There are numerous articles showing the usefulness of OCT in disease detection for glaucoma and other optic neuropathies, macular degeneration and other retinal diseases, as well as diseases of the anterior segment and anterior chamber angle.
3. Change can be measured in the RNFL, macula and optic nerve head using software algorithms, some of which exist already and others in development. The relevant tissue should be evaluated when investigating longitudinally.

REFERENCES

1. Huang D, Swanson EA et al. Optical coherence tomography. *Science*. 1991; 254(5035): 1178–81.
2. Fercher AF et al. In vivo optical coherence tomography. *Am J Ophthalmol*. 1993;116(1):113–4.
3. Schuman JS, Hee MR, Arya AV, Pedut-Kloizman T, Puliafito CA, Fujimoto JG, Swanson EA. Optical coherence tomography: a new tool for glaucoma diagnosis. *Curr Opin Ophthalmol*. 1995;6(2):89–95.
4. Puliafito CA, Hee MR, Lin CP, Reichel E, Schuman JS, Duker JS, Izatt JA, Swanson EA, Fujimoto JG. Imaging of macular diseases with optical coherence tomography. *Ophthalmology*. 1995;102(2):217–29.
5. Hee MR, Puliafito CA, Wong C, Duker JS, Reichel E, Schuman JS, Swanson EA, Fujimoto JG. Optical coherence tomography of macular holes. *Ophthalmology*. 1995 May;102(5):748–56.
6. Hee MR, Puliafito CA, Duker JS, Reichel E, Coker JG, Wilkins JR, Schuman JS, Swanson EA, Fujimoto JG. Topography of diabetic macular edema with optical coherence tomography. *Ophthalmology*. 1998;105(2):360–70.
7. Leitgeb R, Wojtkowski M, Kowalczyk A, Hitzenberger CK, Sticker M, Fercher AF. Spectral measurement of absorption by spectroscopic frequency-domain optical coherence tomography. *Opt Lett*. 2000;25(11):820–2.
8. de Boer JF, Cense B, Park BH, Pierce MC, Tearney GJ, Bouma BE. Improved signal-to-noise ratio in spectral-domain compared with time-domain optical coherence tomography. *Opt Lett*. 2000;28(21):2067–9.
9. Nassif N, Cense B, Park BH, Yun SH, Chen TC, Bouma BE, Tearney GJ, de Boer JF. In vivo human retinal imaging by ultrahigh-speed spectral domain optical coherence tomography. *Opt Lett*. 2004;29(5):480–2.
10. Wojtkowski M, Bajraszewski T, Gorczyńska I, Targowski P, Kowalczyk A, Wasilewski W, Radzewicz C. Ophthalmic imaging by spectral optical coherence tomography. *Am J Ophthalmol*. 2004 ;138(3):412–9.
11. Wojtkowski M, Srinivasan V, Fujimoto JG, Ko T, Schuman JS, Kowalczyk A, Duker JS. Three-dimensional retinal imaging with high-speed ultrahigh-resolution optical coherence tomography. *Ophthalmology*. 2005;112(10):1734–46.

OCT IN NEUROLOGIC DISEASE

Fiona Costello, M.D.; Adnan Subie, D.O.; Eric Eggenberger, D.O., MSEpi

Michigan State University
East Lansing MI

LEARNING OBJECTIVES

The attendee will be able to:

1. Understand OCT as it applies to optic neuropathy-related neurologic diseases such as MS.
2. Understand OCT applications to CNS diseases associated with disc edema.
3. Understand relationships between OCT measures and other CNS measures including clinical optic nerve function.

CME QUESTIONS

1. OCT works by:
 - a. light reflectivity
 - b. echo location
 - c. birefringence of the retinal axons
 - d. xray imaging
 - e. magnetic imaging
2. OCT has demonstrated retinal nerve fiber loss in which of the following conditions:
 - a. optic neuritis
 - b. MS
 - c. Alzheimer's disease
 - d. NAION
 - e. All of the above
3. OCT is an emerging non-invasive technology that at present is a useful tool in the GROUP analysis of neuro-ophthalmic conditions, rather than the basis for INDIVIDUAL clinical decisions. True or False

KEY WORDS

1. OCT
2. Optic Neuritis
3. Multiple Sclerosis
4. Papilledema

INTRODUCTION

Optical coherence tomography (OCT) has evolved dramatically since the first reports of this technology in 1991, and has become an integral part of the ophthalmology evaluation. In addition to providing an indispensable service for the retina physician, the ability to quantify the retinal nerve fiber layer has begun to change neuro-ophthalmic practice. In this regard, OCT has the potential to change qualitative, subjective descriptive reporting into reproducible quantitative science.

Quantification of the RNFL has several clinical applications, including numerous diseases of the optic nerve, both in documentation of edema and quantification of optic atrophy; OCT has also become a viable study outcome in treatment trials. This review will focus on current OCT applications as they apply to neuro-ophthalmic clinical practice.

RETINAL IMAGING METHODOLOGIES

In addition to OCT, commercially available retinal imaging devices also include Heidelberg Retinal Tomography (HRT), and scanning laser polarimetry (GDx). Each of these instruments has inherent advantages and disadvantages, and results obtained from 1 instrument do not translate into results from another imaging technique. The Heidelberg Retina Tomograph (HRT) is a confocal laser scanning system to acquisition three dimensional retinal images. GDx relies on birefringence of the retinal ganglion cell axon microtubules and filaments. Monteiro and Moura compared GDx with variable corneal compensation (VCC) against TD-OCT in patients with band atrophy (BA) from chiasmal compression, and reported GDx appeared to underestimated the temporal quadrant by an average of 22 μ m; conversely, Zaveri et al found OCT and GDx-VCC equally able to measure RNFL thickness in MS patients experiencing acute optic neuritis; by virtues of assessing retinal ganglion cell axon microtubule density, GDx changes appeared earlier than OCT-demonstrable RNFL thinning. The remainder of this review will focus on OCT as the most common methodology employed in neuro-ophthalmic practice.

OCT METHODOLOGY

Time-domain OCT (TD-OCT), the 3rd generation instrument, is able to record a series of 512 x 1024 A-scan images within 2 seconds with approximately 10 μ m resolution. Several studies have demonstrated TD-OCT's reproducibility in assessing the RNFL thickness in normal eyes, glaucoma, and various non-glaucomatous optic

neuropathies. The next generation of OCT, Spectral-domain OCT (SD-OCT), has significantly improved the speed of image acquisition; the SD-OCT captures approximately 27,000 scans per second with a resolution of 5µm, and has the ability to form a 3-dimensional map of the retina and optic nerve, allowing more accurate distinctions between retinal layers. In addition, SD-OCT automatically centers the scan on the optic disc with the use of optic nerve landmarks to decrease scan — rescan variability. Although measurements with the TD-OCT and SD-OCT instruments correlate well, the RNFL and retinal thickness results are not interchangeable.

OCT VS Histology

Blumenthal et al compared OCT-derived RNFL measurements to histology-derived measurements (exenterated orbit secondary to an infiltrative squamous cell carcinoma), and reported OCT outcomes mirrored the histology, but actual measurements differed by 10–40µm. This discrepancy likely reflects identification of the RNFL layers via staining techniques versus optical reflectance.

FACTORS INFLUENCING SCAN ACCURACY

Several factors influence the quality of OCT images. The 3.4 mm laser reticule must be centered on the optic nerve; decentered scans preferentially affect quadrant thicknesses, especially the vertical quadrants, while total RNFL remains relatively stable. Surprisingly, use of the OCT scan tracking coordinates only provided a statistically significant effect on the temporal quadrant. Signal strength also positively correlates with the observed RNFL thickness; many studies require signal strength of 7. Pupil size is not generally a significant factor as long as size is ≥ 3mm. Lens opacities are inversely correlated with the measurement of RNFL thickness (effect size <12%); similarly, contact lenses use is associated with decrease in signal strength (7.8 to 7.1; P=0.011) and the measured average RNFL thickness (average RNFL 105.3 to 102.8µm; P=0.001).

OCT IN CNS DISEASE/OPTIC NEUROPATHIES

Anterior Ischemic Optic Neuropathy (AION)

AION is a disease characterized by disc edema at onset with subsequent optic atrophy. Contreras and colleagues used OCT to study 27 patients with NAION at baseline, 6-weeks; and 3, 6, and 12 months after onset. The initial mean RNFL of 201µm represented a 96.4% increase relative to the fellow eye. Percentages of RNFL loss 3, 6, and 12 months after onset were 38.9%, 42.3%, and 43.9%, respectively. Regression analysis revealed a 2-dB decrease in visual field function for every 1-µm of mean RNFL thickness loss, and a 1-line drop in Snellen visual acuity for every 1.6µm deficit.

Bellusci et al documented RNFL edema followed by thinning in the superior optic nerve among acute NAION patients with inferior altitudinal defects; conversely, patient with diffuse visual field (VF) loss had extensive RNFL thinning. Temporal quadrant RNFL thinning (papillomacular fibers) correlated with central field defects. Chan et al used OCT to investigate the optic disc in 22 NAION patients; smaller cups and C:D ratios were more common in NAION eyes compared to control eyes; additionally, a smaller cup was present in the non-affected fellow eye of NAION patients (C:D 0.103) compared to the affected NAION eye (C:D 0.135; P=0.04), suggesting a small degree of cup enlargement after NAION.

These studies indicate that OCT-measured RNFL values correlate with the topographical representation of visual field defects in eyes with NAION. Further, reduced RNFL values can help predict recovered visual function in NAION patients.

Optic Neuritis (ON) & Multiple Sclerosis (MS)

Several investigators have demonstrated RNFL loss in MS patients even without a history of optic neuritis, while superimposed optic neuritis produces additional RNFL decline. There is a clinical-OCT paradox concerning optic neuritis, similar to the MRI-clinical paradox within MS. MRI T2 lesion load does not correlate with overall neurologic function, with MS patients often exhibiting MRI lesions out of proportion to their clinical condition (especially as assessed by the EDSS). Similarly, OCT RNFL loss appears out of proportion to the clinical visual assessments. Although the majority of patients lose RNFL following an episode of optic neuritis, most recover “normal” visual function (despite the patients’ perception that the ‘recovered’ eye is not normal). Costello et al documented an OCT injury threshold of 75µm before a linear decline in visual field was apparent. Several studies have investigated RNFL quadrant data after optic neuritis, and there appears to be a predilection for the infero-temporal quadrants.

Costello et al investigated OCT findings in CIS optic neuritis. There was no significant difference in RNFL thickness between CIS progressing to MS versus CIS without MS at 2 years follow up; however, progressive RNFL thinning was more apparent in CIS patients progressing to MS.

OCT has been used to investigate MS subtypes; RNFL loss is generally greater in progressive MS than RRMS (somewhat duration of disease dependent).

Neuromyelitis Optica (NMO)

In most reports, NMO is associated with greater RNFL loss than optic neuritis or MS. De Seze et al reported RNFL thickness of 29 NMO patients had significantly reduced RNFL values (77.9 µm) compared to controls. OCT is not specific enough to distinguish NMO from ON/MS, but NMO should be considered in ON patients with poor recovery, or dramatic RNFL thinning <50µm.

Papilledema/Pseudotumor Cerebri (PTC)/Idiopathic Intracranial Hypertension (IIH)

Patients with idiopathic intracranial hypertension (IIH) typically present with headache, pulsatile tinnitus, transient visual obscurations, and papilledema usually with relatively preserved visual acuity.

Intuitively, we expect elevated RNFL values at presentation when optic disc edema is maximal, and decreasing RNFL elevation with effective treatment.

Rebolleda and Munoz-Negrete studied 22 PTC patients, and noted the initial increase in RNFL correlated well with visual field mean deviation (MD) ($P=0.002$) and pattern standard deviation (PSD; $P=0.013$). At 1 year follow-up, perimetry demonstrated a 0.6dB MD decline with a $10\mu\text{m}$ RNFL decrease. It should be noted that OCT alone is unable to distinguish resolving edema from emerging optic atrophy, and therefore OCT needs to be incorporated into the remainder of the clinical exam. Additional information on OCT in IIH will emerge from the OCT substudy of the Idiopathic Intracranial Hypertension Treatment Trial (IIHTT).

Optic Nerve Head Drusen

Johnson et al applied the TD-OCT “fast optic disc” protocol to differentiate disc drusen from disc edema. Drusen appeared more “lumpy-bumpy” with RNFL thinner than $86\mu\text{m}$ nasally in contrast to the smooth and elevated contour of true disc edema.

Compressive Optic Neuropathy (CON)

Danesh-Meyer et al investigated OCT's ability to predict visual recovery from CON. Thirty five patients with various etiologies of CON were evaluated with OCT and visual fields pre- and post-surgical decompression. The patients were divided into 2 groups: “normal” RNFL and “thin” RNFL (defined as pre-op RNFL $<97.5\%$ of normal values). Patients with reduced VA and VF but normal RNFL thickness had significant improvement of VA (mean of 20/40 to 20/25; $P=0.028$) post-decompression than those with “thin” RNFL (20/80 to 20/60; $P=0.177$). Although the mean improvement in the “thin” RNFL group of 2 lines was statistically insignificant, this degree of improvement may well be clinically significant. The analysis found an increased likelihood of post-op improvement with a thicker pre-op RNFL until approximately $85\mu\text{m}$, after which there was no additional benefit was observed; this likely reflects the fact that patients with RNFL of $85\mu\text{m}$ have relatively preserved visual function. While pre-op measurements of RNFL do not necessarily change our management of patients with CON, such studies enhance our ability to predict visual outcome post decompression in CON.

Hereditary Optic Neuropathies/Leber Hereditary Optic Neuropathy (LHON)

Leber hereditary optic neuropathy (LHON) is a mitochondrially inherited degeneration of retinal ganglion cells and their axons that leads to an acute or subacute loss of central vision. Affected patients are predominantly males, mutations in the mitochondrial genome from their

mother. LHON is usually due to one of three pathogenic mitochondrial DNA (mtDNA) point mutations: at nucleotide positions 11778 G to A, 3460 G to A and 14484 T to C, respectively, in the ND4, ND1 and ND6 subunit genes of complex I of the oxidative phosphorylation chain in mitochondria. Clinically, patients may develop often acute onset visual loss in one eye, followed by fellow eye involvement months to weeks later. Vision loss typically occurs in young adulthood. In the acute stage, the affected eye demonstrates telangiectatic and tortuous peripapillary vessels; and with time, optic atrophy ensues.

Seo et al. studied RNFL in LHON patients with the 11778 and 14484 mutations. Patients were divided into early (≤ 6 months) and late (> 6 months) categories. In the late stage, the RNFL thickness was greater in the 14484 group (average RNFL $81\mu\text{m}$) compared to the 11778 (average RNFL $65.6\mu\text{m}$; $P=0.02$), thus supporting severe atrophy in the late 11778 group. Comparisons between the 2 mutations in the early stage may be misleading, since there can be considerable variability within this time frame as thinning occurs. Overall, these OCT findings are in agreement with the clinical impression that the 11778 mutation is associated with worse visual outcome than the 14484 mutation.

Savini et al used OCT to study RNFL thickness in unaffected carriers with LHON mutations. Sixty-six unaffected carriers (44 females and 22 males) were analyzed and compared with an age-matched control group of 70 patients (40 females and 30 males). As compared to the control group, unaffected male carriers showed thicker RNFL measurements in the temporal and inferior RNFL quadrants and in the 360 degrees average measurements. These differences reached statistical significance in subjects carrying the 11778 mutation, whereas only a trend was detected in those with the 3460 mutation. Unaffected female carriers had an increased thickness in the temporal quadrant when compared with the control group ($P = 0.003$). The increase in temporal sectors was statistically significant in females with the 11778 mutation, whereas a trend was detected in those with the 3460 mutation. A thickening of the temporal fibers was detected in all subgroups of unaffected carriers.

Migraine

Martinez et al used OCT to study 70 patients with migraine, and noted a significant RNFL reduction in the temporal quadrants of migraineurs compared to healthy controls; additionally, the RNFL in migraine with aura (average RNFL $96.5\mu\text{m}$) was significantly less than migraine without aura (average RNFL of $102.9\mu\text{m}$; $P=0.0189$). Significantly thinner RNFL was found in patients with migraine ≥ 15 years. These investigators found a correlation between RNFL thickness and migraine disability assessment (MIDAS) scores.

Neurodegenerative disease/Alzheimer Disease

There is both histologic and retinal imaging evidence of retinal ganglionic cell (RGC) in patients with Alzheimer disease (AD). Danesh-Meyer et al used HRT scanning laser ophthalmoscopy (SLO) to investigate 40 patients with AD compared to age- and sex-matched controls, and found that clinical and SLO vertical cup-to-disc ratio was significantly different between the groups (AD 0.4, control 0.27–0.31); additionally, these authors reported decreased rim volume, RNFL thickness and rim area in AD compared to controls.

CONCLUSION

OCT has enhanced our assessment, management, and understanding of neuro-ophthalmic diseases, and has potential to further our understanding of other CNS-based diseases. OCT has the advantages of reproducibility, ease of use, non-invasive nature and relatively low cost, makes it an asset to several clinical situations. With its advancement into spectral domain, OCT has wide use in evaluating the optic nerve and the visual system.

CME ANSWERS

1. A
2. E
3. True

REFERENCES

1. Albrecht P, Frohlich R, Hartung HP, Kieseier BC, Methner A. Optical coherence tomography measures axonal loss in multiple sclerosis independently of optic neuritis. *J Neurol* 2007;254:1595–1596.
2. Balcer LJ, Galetta SL, Calabresi PA, et al. Natalizumab reduces visual loss in patients with relapsing multiple sclerosis. *Neurology* 2007;68:1299–1304.
3. Balcer LJ, Markowitz CE. Optical coherence tomography to monitor neuronal integrity in multiple sclerosis. In: Rudick RA, Cohen JA, editors. *Multiple Sclerosis Therapeutics*, 3rd ed. Oxon, UK: Informa Healthcare, 2007:251–265.
4. Beck RW, Cleary PA, Anderson MM et al. A Randomized Controlled Trial of Corticosteroids in the Treatment of Acute Optic Neuritis. *N Engl J Med* 1992; 326:581–8.
5. Beck RW, Cleary PA, et al. The 5-year risk of MS after optic neuritis Experience of the Optic Neuritis Treatment Trial Optic Neuritis Study Group *Neurology* 1997; 49:1404–1413.
6. et al. Retinal nerve fiber layer thickness in nonarteritic anterior ischemic optic neuropathy: OCT characterization of the acute and resolving phases. : 2008;246(5):641–7.
7. OCT and PVEP examination in eyes with visible idiopathic optic disc drusen. 2006;223(12):993–6.
8. Blumenthal EZ, Parikh RS, Pe'er J, et al. Retinal nerve fibre layer imaging compared with histological measurements in a human eye. *Eye*. 2009;23(1):171–5.
9. Blumenthal EZ, Williams JM, Weinreb RN, et al. Reproducibility of nerve fiber layer thickness measurements by use of optical coherence tomography. *Ophthalmology*. 2000;107:2278–82.
10. Budenz D, Chang R, Huang X, et al. Reproducibility of nerve fiber thickness measurements using stratus OCT in normal and glaucomatous eyes. *Invest Ophthalmol Vis Sci*. 2005;46:2440–3.
11. Bulens C, Meerwaldt JD, Van der Wildt CJ, Van Deursen JB. Effect of levodopa treatment on contrast sensitivity in Parkinson's disease. *Ann Neurol* 1987;22:365–369.
12. Carpineto P, Ciancaglini M, Zuppari E, et al. Reliability of nerve fiber layer thickness measurements using optical coherence tomography in normal and glaucomatous eyes. *Ophthalmology*. 2003;110:190–5.
13. Cettomai D, Pulicken M, Gordon-Lipkin E, et al. Reproducibility of optical coherence tomography in multiple sclerosis. *Arch Neurol*. 2008;65:1218–22.
14. Cettomai D, Pulicken M, Gordon-Lipkin E, Salter A, Frohman T, Conger A, Zhang X, Cutter G, Balcer L, Frohman E, Calabresi P. Cross center and inter-rater reproducibility of optical coherence tomography in multiple sclerosis. *Arch Neurol* 2008;65:1218–1222.
15. Decreased retinal nerve fibre layer thickness detected by optical coherence tomography in patients with ethambutol-induced optic neuropathy. : 2007; 91(7):895–7.
16. Chan CK, Cheng AC, Leung CK, et al. Quantitative assessment of optic nerve head morphology and retinal nerve fibre layer in non-arteritic anterior ischaemic optic neuropathy with optical coherence tomography and confocal scanning laser ophthalmoscopy. *Br J Ophthalmol*. 2009;93(6):731–5.
17. Chen J, Lee L. Clinical applications and new developments of optical coherence tomography: an evidence-based review. *Clin Exp Optom*. 2007;90(5):317–35.
18. Chen TC, Cense B, Miller JW, et al. Histologic correlation of in vivo optical coherence tomography images of the human retina. *Am J Ophthalmol* 2006;141(6):1165–1168.
19. Cheung CY, Leung CK, Lin D, et al. Relationship between retinal nerve fiber layer measurement and signal strength in optical coherence tomography. *Ophthalmology*. 2008;115(8):1347–51.
20. Cheung CY, Yiu CK, Weinreb RN, et al. Effects of scan circle displacement in optical coherence tomography retinal nerve fibre layer thickness measurement: a RNFL modelling study. *Eye*. 2008;23(6):1436–41.
21. et al. Fourier-domain optical coherence tomography and adaptive optics reveal nerve fiber layer loss and photoreceptor changes in a patient with optic nerve drusen. 2008 Jun;28(2):120–5.
22. Choi SS, Zawadzki RJ, Keltner JL, Werner JS. Changes in cellular structures revealed by ultra-high resolution retinal imaging in optic neuropathies. *Invest Ophthalmol Vis Sci* 2008;49:2103–2119.
23. Cleary PA, Beck RW, Bourque LB, Backlund JC, et al. Visual Symptoms After Optic Neuritis Results from the Optic Neuritis Treatment Trial. *J Neuroophthalmol* 1997; 17: 18–28.
24. Cohen MJ, Kaliner E, Frenkel S, Kogan M, Miron H, Blumenthal EZ. Morphometric analysis of human peripapillary retinal nerve fiber layer thickness. *Invest Ophthalmol Vis Sci* 2008;49:941–944.

25. Follow-up of nonarteritic anterior ischemic optic neuropathy with optical coherence tomography. 2007;114 (12):2338-44.
26. Contreras I, Rebolleda G, Noval S, Muñoz-Negrete. Optic disc evaluation by optical coherence tomography in nonarteritic anterior ischemic optic neuropathy. *Invest Ophthalmol Vis Sci* 2007;48(9):4087-4092.
27. Cormack FK, Tovee M, Ballard C. Contrast sensitivity and visual acuity in patients with Alzheimer's disease. *In J Geriatr Psychiatry* 2000;15:614-620.
28. Costello F, Coupland S, Hodge W, et al. Quantifying axonal loss after optic neuritis with optical coherence tomography. *Ann Neurol*. 2006;59(6):963-9.
29. Costello F, Coupland S, Hodge W, Lorello GR, Koroluk J, Pan YI, Freedman MS, Zackon DH, Kardon RH. Prognostic consequences of axon loss after optic neuritis: a prospective study using optical coherence tomography (OCT). *Ann Neurol* 2006;59:963-969.
30. Costello F, Hodge W, Pan YI, et al. Tracking retinal nerve fiber layer loss after optic neuritis: a prospective study using optical coherence tomography. *Mult Scler* 2008;14(7): 893-905.
31. Costello F, Hodge W, Pan YI, et al. Differences in retinal nerve fiber layer atrophy between multiple sclerosis subtypes. *J Neurol Sci*. 2009;281(1-2):74-9.
32. Costello F, Hodge W, Pan YI, et al. Retinal nerve fiber layer and future risk of multiple sclerosis. *Can J Neurol Sci*. 2008;35(4):482-7.
33. et al. Relationship between retinal nerve fiber layer and visual field sensitivity as measured by optical coherence tomography in chiasmal compression. *I* 2006 Nov;47(11): 4827-35.
34. Danesh-Meyer HV, Papchenko T, Savino PJ, et al. In vivo retinal nerve fiber layer thickness measured by optical coherence tomography predicts visual recovery after surgery for parachiasmal tumors. *Invest Ophthalmol Vis Sci*. 2008;49(5):1879-85.
35. Danis RP, Fisher MR, Lambert E, Goulding A, Wu D, Lee LY. Results and repeatability of retinal thickness measurements from certification submissions. *Arch Ophthalmol* 2008;126:45-50.
36. Davis MD, Bressler SB, Aiello LP, Bressler NM, Browning DJ, Flaxel CJ, Fong DS, Foster WJ, Glassman AR, Hartnett MER, Kollman C, Li HK, Qin H, Scott IU, and the Diabetic Retinopathy Clinical Research Network Study Group. Comparison of time-domain OCT and fundus photographic assessments of retinal thickening in eyes with diabetic macular edema. *Invest Ophthalmol Vis Sci* 2008;49: 1745-1752.
37. de Seze J, Blanc F, Jeanjean L, et al. Optical coherence tomography in neuromyelitis optica. *Arch Neurol*. 2008;65(7):920-3.
38. DeLeon-Ortega J, Carroll KE, Arthur SN, Girkin CA. Correlations Between Retinal Nerve Fiber Layer and Visual Field in Eyes with Non-Arteritic Anterior Ischemic Optic Neuropathy. *Am J Ophthalmol* 2007;143(2): 288-294.
39. Della Mea G, Bacchetti S, Zappieri M, et al. Nerve fiber layer analysis with GDx with a variable corneal compensator in patients with multiple sclerosis. *Ophthalmologica*. 2007;221(3):186-189.
40. Diabetic Retinopathy Clinical Research Network, Krzystolik MG, Strauber SF, et al. Reproducibility of macular thickness and volume using Zeiss optical coherence tomography in patients with diabetic macular edema. *Ophthalmology*. 2007;114:1520-5.
41. Diabetic Retinopathy Clinical Research Network, Krzystolik MG, Strauber SF, et al. Reproducibility of macular thickness and volume using Zeiss optical coherence tomography in patients with diabetic macular edema. *Ophthalmology*. 2007;114:1520-5.
42. et al. Optic disc size is associated with development and prognosis of Leber's hereditary optic neuropathy. *i* 2008 Dec 20. [Epub ahead of print]
43. Drexler W, Fujimoto JG. State-of-the-art. retinal optical coherence tomography. *Prog Retin EyeRes* 2008;27:45-88.
44. Dutta R, Trapp BD. Pathogenesis of axonal and neuronal damage in multiple sclerosis. *Neurology* 2007;68(Suppl 3):S22-S31.
45. Elbol P, Work K. Retinal nerve fiber layer in multiple sclerosis. *Acta Ophthalmol*.1990; 68:481-48.
46. Evangelou N, Konz D, Esiri MM, Smith S, Palace J, Matthews PM. Size-selective neuronal changes in the anterior optic pathways suggest a differential susceptibility to injury in multiple sclerosis. *Brain* 2001;124:1813-1820.
47. Fisher JB, Jacobs DA, Markowitz CE, et al. Relation of visual function to retinal nerve fiber layer thickness in multiple sclerosis. *Ophthalmology*. 2006;113:324-32.
48. Fisher JB, Jacobs DA, Markowitz CE, Galetta SL, Volpe NJ, Ligia Nano-Schiavi M, et al. Relation of visual function to retinal nerve fiber layer thickness in multiple sclerosis. *Ophthalmology* 2006;113:324-325.
49. Measurement of the scleral canal using optical coherence tomography in patients with optic nerve drusen. 2005; 139(4):664-9.
50. Fortune B, Wang L, Cull G, Cioffi GA. Intravitreal colchicine causes decreased RNFL birefringence without altering RNFL thickness. *Invest Ophthalmol Vis Sci* 2008;49:255-261.
51. Frisen L, Hoyt WF. Insidious atrophy of retinal nerve fibers in multiple sclerosis. Funduscopy identification in patients with and without complaints. *Arch Ophthalmol* 1974;92:91-97.
52. Frohman E, Costello F, Zivadinov R, Stuve O, Conger A, Winslow H, et al. Optical coherence tomography in multiple sclerosis. *Lancet Neurol* 2006;5:853-863.
53. Frohman EM, Costello F, Stuve O, Calabresi P, Miller DH, Hickman SJ, et al. Modeling axonal degeneration within the anterior visual system. *Arch Neurol* 2008;65(1):26-35.
54. Frohman EM, Fujimoto JG, Frohman TC, et al. Optical coherence tomography: a window into the mechanisms of multiple sclerosis. *Nat Clin Pract Neurol*. 2008;4(12):664-75.
55. Frohman EM, Raine C, Racke MK. Multiple sclerosis: the plaque and its pathogenesis. *N Engl J Med* 2006;354: 942-955.
56. Methanol-induced retinal toxicity patient examined by optical coherence tomography. 2006;50(3):239-41.
57. Fujimoto JG, Hee MR, Huang D, Schuman JS, Pulifiato CA, Swanson E. Principles of optical coherence tomography. In: Schuman JS, Pulifiato CA, Fujimoto JG. *Ocular coherence tomography of ocular disease*. Second edition. Thorofare: Slack Inc., 2004.

58. Gordon-Lipkin E, Chodkowsky B, Reich DS, et al. Retinal nerve fiber layer is associated with brain atrophy in multiple sclerosis. *Neurology* 2007;69(16):1603-1609.
59. Grazioli E, Zivadinov R, Weinstock-Guttman B, Lincoff N, Baier M, Wong JR, Hussein S, Cox JL, Hojnacki D, Ramanathan M. Retinal nerve fiber layer thickness is associated with brain MRI outcomes in multiple sclerosis. *J Neurol Sci* 2008;268:12-17.
60. Hedges TR 3rd, Quireza ML. Multifocal visual evoked potential, multifocal electroretinography, and optical coherence tomography in the diagnosis of subclinical loss of vision. *Ophthalmol Clin North Am.* 2004;17(1):89-105.
61. et al. Subretinal fluid from anterior ischemic optic neuropathy demonstrated by optical coherence tomography. 2008;126(6):812-5.
62. Henderson AP, Trip SA, Schlottmann PG, et al. An investigation of the retinal nerve fibre layer in progressive multiple sclerosis using optical coherence tomography. *Brain.* 2008;131(Pt 1):277-87.
63. Henderson AP, Trip SA, Schlottmann PG, Altmann DR, Garway-Heath DF, Plant GT, Miller DH. An investigation of the retinal nerve fibre layer in progressive multiple sclerosis using optical coherence tomography. *Brain* 2008;131(1): 277-287.
64. Hickman SJ, Dalton CM, Miller DH, Plant GT. Management of acute optic neuritis. *Lancet* 2002; 360: 1953-1962.
65. et al. Retinal nerve fiber structure versus visual field function in patients with ischemic optic neuropathy. A test of a linear model. 2008;115(5):904-10.
66. Huang D, Swanson EA, Lin CP, et al. Optical coherence tomography. *Science.* 1991;22,254(5035):1178-81.
67. Huang X., Knighton RW. Microtubules contribute to the birefringence of the retinal nerve fiber layer. *Invest Ophthalmol Vis Sci* 2005;46(12):4588-4593.
68. et al. Predicting visual outcome after treatment of pituitary adenomas with optical coherence tomography. 2009 Jan;147(1):64-70.
69. Jaffe GJ, Caprioli J. Optical coherence tomography to detect and manage retinal disease and glaucoma. *Am J Ophthalmol* 2004;137:156-69.
70. Johnson LN, Diehl ML, Hamm CW, et al. *Arch Ophthalmol.* 2009;127(1):45-9.
71. Kakinoki M, Sawada O, Sawada T, et al. Comparison of macular thickness between Cirrus HD-OCT and Stratus OCT. *Ophthalmic Surg Lasers Imaging.* 2009;40(2):135-40.
72. Kallenbach K, Frederiksen J. Optical coherence tomography in optic neuritis and multiple sclerosis: a review. *Eur J. Neurol* 2007;14:841-849.
73. Kanamori A, Escano MF, Eno A, et al. Evaluation of the effect of aging on retinal nerve fiber layer thickness measured by optical coherence tomography. *Ophthalmologica* 2003;217:273-278.
74. Kanamori A, Nakamura M, Matsui N, et al. Optical coherence tomography detects characteristic retinal nerve fiber layer thickness corresponding to band atrophy of the optic discs. *Ophthalmology.* 2004;111(12):2278-2283.
75. Optical coherence tomography of the retinal nerve fibre layer in mild papilloedema and pseudopapilloedema. 2005;89(3):294-8.
76. Visual field defects and retinal nerve fiber layer defects in eyes with buried optic nerve drusen 2006;141(2):248-253.
77. Kiernan DF, Hariprasad SM, Chin EK, et al. Prospective comparison of cirrus and stratus optical coherence tomography for quantifying retinal thickness. *Am J Ophthalmol.* 2009;147(2):267-275.
78. Stratus OCT in dominant optic atrophy: features differentiating it from glaucoma. 2007;16 (8):655-8.
79. Klistorner A, Arvind H, Nguyen T, et al. Multifocal VEP and OCT in optic neuritis: a topographical study of the structure-function relationship. 2009;118(2):129-37.
80. et al. Axonal loss and myelin in early ON loss in postacute optic neuritis. 2008 Sep; 64(3):325-31.
81. Kupersmith MJ, Gal RL, Beck RW, et al. Visual function at baseline and a 1 month in acute optic neuritis: predictors of visual outcome. *Neurology* 2007;69:508-514.
82. Retinal nerve fiber layer loss documented by Stratus OCT in patients with pituitary adenoma: case report. 2006; 69(2):251-4.
83. Lynch DR, Farmer JM, Rochestie D, Balcer LJ. Contrast letter acuity as a measure of visual dysfunction in patients with Friedreich ataxia. *J Neuro-Ophthalmol* 2002;22:270-274.
84. Lynch DR, Farmer JM, Wilson RL, Balcer LJ. Performance measures in Friedreich ataxia: potential utility as clinical outcome tools. *Mov Disord* 2005;20:777-782.
85. MacFadyen DJ, Drance SM, Douglas GR, Airaksined PJ, et al. The retinal nerve fiber layer, neuroretinal rim area, and visual evoked potentials in MS. *Neurology* 1988; 38:1353-1358
- Kerrison JB, Flynn T, Green R. Retinal Pathologic Changes in Multiple Sclerosis. *Retina* 1994; 14:445-451.
86. Martinez A, Proupim N, Sanchez M. Retinal nerve fibre layer thickness measurements using optical coherence tomography in migraine patients. *Br J Ophthalmol.* 2008;92(8):1069-75.
87. Medeiros FA, Moura FC, Vessani RM, Susanna R. Axonal loss after traumatic optic neuropathy documented by optical coherence tomography. *Am J Ophthalmol* 2003;135: 406-408.
88. Menke MN, Fekke GT, Trempe CL. OCT measurements in patients with optic disc edema. *Invest Ophthalmol Vis Sci* 2005;46:3807-3811.
89. Merle H, Olindo S, Donnio A, et al. Retinal peripapillary nerve fiber layer thickness in neuromyelitis optica. *Invest Ophthalmol Vis Sci.* 2008;49(10):4412-7.
90. et al. Retinal peripapillary nerve fiber layer thickness in neuromyelitis optica. 2008;49(10):4412-7.
91. Miller D, Barkhof F, Montalban X, Thompson A, et al. Clinically isolated syndromes suggestive of multiple sclerosis, part I: natural history, pathogenesis, diagnosis, and prognosis. *Lancet Neurol* 2005; 4: 281-288.
92. Monteiro ML, Leal BC, Rosa AA, Bronstein MD. Optical coherence tomography analysis of axonal loss in band atrophy of the optic nerve. *Br J Ophthalmol* 2004;88: 896-899.
93. Monteiro ML, Medeiros FA, Ostroscki MR. Quantitative analysis of axonal loss in band atrophy of the optic nerve using scanning laser polarimetry. *Br J Ophthalmol.* 2003; 87(1):32-37.

94. Monteiro ML, Moura FC, Medeiros FA. Diagnostic ability of optical coherence tomography with a normative database to detect band atrophy of the optic nerve. *Am J Ophthalmology* 2007;143:896–899.
95. Monteiro ML, Moura FC. Comparison of the GDx VCC scanning laser polarimeter and the stratus optical coherence tomograph in the detection of band atrophy of the optic nerve. *Eye*. 2008;22(5):641–8.
96. Morgan JE, Waldock A, Jeffery G, Cowey A. Retinal nerve fibre layer polarimetry: histological and clinical comparison. *Br J Ophthalmol*. 1998;82(6):684–690.
97. Moura FC, Medeiros FA, Monteiro ML. Evaluation of macular thickness measurements for detection of band atrophy of the optic nerve using optical coherence tomography. *Ophthalmology* 2007;114:175–181.
98. Mumcuoglu T, Wollstein G, Wojtkowski M, Kagemann L, Ishikawa H, Gabriele ML, Srinivasan V, Fujimoto JG, Duker JS, Schuman JS. Improved visualization of glaucomatous retinal damage using high-speed ultrahigh-resolution optical coherence tomography. *Ophthalmology* 2008;115:782–789.
99. Nagai-Kusuhara A, Nakamura M, Kanamori A, et al. Evaluation of optic nerve head configuration in various types of optic neuropathy with Heidelberg Retina Tomograph. *Eye*. 2008;22(9):1154–60.
100. Nagai-Kusuhara A, Nakamura M, Tatsumi Y, et al. Disagreement between Heidelberg Retina Tomograph and optical coherence tomography in assessing optic nerve head configuration of eyes with band atrophy and normal eyes. *Br J Ophthalmol*. 2008;92(10):1382–6.
101. Disagreement between Heidelberg Retina Tomograph and optical coherence tomography in assessing optic nerve head configuration of eyes with band atrophy and normal eyes. 2008 Oct; 92(10):1382–6.
102. Naismith RT, Tutlam NT, Xu J, et al. Optical coherence tomography differs in neuromyelitis optica compared with multiple sclerosis. *Neurology*. 2009;72(12):1077–82.
103. Newman NJ. Driving with Parkinson's disease: more than meets the eye [editorial]. *Ann Neurol* 2006;60:387–388.
104. Noval S, Contreras I, Rebolleda G, Munoz-Negrete FJ. Optical coherence tomography versus automated perimetry for follow-up of optic neuritis. *Acta Ophthalmol Scand* 2006; 84: 790–794.
105. Optic Neuritis Study Group. High and Low Risk Profiles for the Development of Multiple Sclerosis Within 10 Years After Optic Neuritis. *Arch Ophthalmol*. 2003; 121: 944–949.
106. Osborne B, Jacobs D, Markowitz C, Galetta S, Volpe N, Nano-Schiavi L, Winslow H, Fisher JB, Baier M, Frohman T, Calabresi P, Maguire MG, Cutter GR, Balcer LJ, Frohman EM. Relation of macular volume to retinal nerve fiber layer thickness and visual function in multiple sclerosis. *Neurology* 2006;66 (Suppl 2):A14.
107. Paquet C, Boissonnot M, Roger F, Dighiero P, Gil R, Hugon J. Abnormal retinal thickness in patients with mild cognitive impairment and Alzheimer's disease. *Neurosci Lett* 2007;420:97–99.
108. Parikh RS, Parikh SR, Sekhar GC, Prabakaran S, Ganesh Babu J, Thomas R. Normal age-related decay of retinal nerve fiber layer thickness. *Ophthalmology* 2007;114:921–926.
109. Parisi V, Manni G, Spadaro M, et al. Correlation between morphological and functional retinal impairment in multiple sclerosis patients. *Invest Ophthalmol Vis Sci* 1999;40: 2520–7.
110. Patel PJ, Chen FK, Ikeji F, et al. Repeatability of stratus optical coherence tomography measures in neovascular age-related macular degeneration. *Invest Ophthalmol Vis Sci*. 2008;49:1084–8.
111. Paunescu LA, Schumann JS, Price LL, Stark PC, Beaton S, Ishikawa, et al. Reproducibility of nerve fiber layer thickness, macular thickness, and optic nerve head measurements using StratusOCT. *Invest Ophthalmol Vis Sci* 2004;45: 1716–1724.
112. Pro MJ, Pons ME, Liebmann JM, et al. Imaging of the optic disc and retinal nerve fiber layer in acute optic neuritis. *J Neurol Sci* 2006;250(1–2):114–119.
113. Pulicken M, Gordon-Lipkin E, Balcer LJ, et al. Optical coherence tomography and disease subtype in multiple sclerosis. *Neurology*. 2007;69:2085–92.
114. Pulicken M, Gordon-Lipkin E, Balcer LJ, Frohman E, Cutter G, Calabresi PA. Optical coherence tomography and disease subtype in multiple sclerosis. *Neurology* 2007;69(22): 2085–2092.
115. Rebolleda G, Munoz-Negrete FJ. Follow-up of Mild Papilledema in Idiopathic Intracranial Hypertension with Optical Coherence Tomography. *Invest Ophthalmol Vis Sci*. 2008 Nov 14. [Epub ahead of print]
116. Sakata LM, Deleon-Ortega J, Sakata V, Girkin CA. Optical coherence tomography of the retina and optic nerve – a review. *Clin Experiment Ophthalmol*. 2009;37(1):90–9.
117. et al. Utility of optical coherence tomography (OCT) in the follow-up of idiopathic intracranial hypertension in childhood 2006; 7:383–9.
118. et al. Retinal nerve fiber layer evaluation by optical coherence tomography in unaffected carriers with Leber's hereditary optic neuropathy mutations. 2005;112(1):127–31.
119. et al. Detection and quantification of retinal nerve fiber layer thickness in optic disc edema using stratus OCT. 2006;124(8):1111–7.
120. Savini G, Zanini M, Barboni P. Influence of pupil size and cataract on retinal nerve fiber layer thickness measurements by Stratus OCT. *J Glaucoma*. 2006;15(4):336–40.
121. Schrems WA, Mardin CY, Horn FK, et al. Comparison of Scanning Laser Polarimetry and Optical Coherence Tomography in Quantitative Retinal Nerve Fiber Assessment. *J Glaucoma*. 2009 Apr 15. [Epub ahead of print]
122. Schuman JS, Pedut-Koizman T, Pakter H, et al. Optical coherence tomography and histologic measurements of nerve fiber layer thickness in normal and glaucomatous monkey eyes. *Invest Ophthalmol Vis Sci* 2007;48(8): 3645–3654.
123. Seo JH, Hwang JM, Park SS. Comparison of retinal nerve fibre layers between 11778 and 14484 mutations in Leber's hereditary optic neuropathy. *Eye*. 2009 Feb 27. [Epub ahead of print]
124. Sepulcre J, Fernandez MM, Salinas – Alaman A, et al. Diagnostic accuracy of retinal abnormalities in predicting disease activity in MS. *Neurology* 2007; 68: 1488–1494.

125. Sergott RC, Frohman E, Glanzman R, Al-Sabbagh A ; On behalf of the OCT in MS Expert Panel. The role of optical coherence tomography in multiple sclerosis: expert panel consensus. *J Neurol Sci* 2007;263(1-2):3-14.
126. Sergott RC, Piette S, Etter J, Savino PJ, Affel L. In vivo neuroprotection with high-dose, high-frequency interferon therapy: a serial optical coherence tomography study in multiple sclerosis and optic neuritis. Abstract presented at the 21st Congress of the European Committee for Treatment and Research in Multiple Sclerosis, 2005.
127. Sergott, RC. Optical coherence tomography: measuring in-vivo axonal survival and neuroprotection in multiple sclerosis and optic neuritis. *Curr Opin Ophthalmol* 2005;16:346-350.
128. Soderstrom M, Ya-Ping J, Hillert J, Link H. Optic Neuritis Prognosis for multiple sclerosis from MRI, CSF, and HLA findings. *Neurology* 1998; 50:708-714.
129. Soderstrom M. Optic neuritis and multiple sclerosis. *Acta Ophthalmol Scand* 2001: 79; 223-227.
130. Subei AM, Antonio-Santos AA, Morehouse J, et al. Reproducibility of Optical Coherence Tomography in Non-glaucomatous Optic Nerve Pathologies. Poster presented at NANOS, 2009.
131. Trapp BD, Peterson J, Ransohoff RM, Rudick R, Mörk S, Bo L. Axonal transection in the lesions of multiple sclerosis. *N Engl J Med* 1998;338:278-285.
132. Trip SA, Schlottmann PG, Jones SJ et al. Optic nerve magnetization transfer imaging and measures of axonal loss and demyelination in optic neuritis. *Mult Scler* 2007;13: 875-9.
133. Trip SA, Schlottmann PG, Jones SJ, et al. Optic nerve atrophy and retinal nerve fiber layer thinning following optic neuritis: evidence that axonal loss is a substrate of MRI-detected atrophy. *Neuroimage* 2006; 31: 286 - 293.
134. Trip SA, Schlottmann PG, Jones SJ, et al. Retinal nerve fiber layer axonal loss and visual dysfunction in optic neuritis. *Ann Neurol* 2005;58:383-391.
135. Tzamalís A, Kynigopoulos M, Schlote T, Haefliger I. Improved reproducibility of retinal nerve fiber layer thickness measurements with the repeat-scan protocol using the Stratus OCT in normal and glaucomatous eyes. *Graefes Arch Clin Exp Ophthalmol*. 2009;247:245-52.
136. Uc EY, Rizzo M, Anderson SW, et al. Impaired visual search in drivers in Parkinson's disease. *Ann Neurol* 2006;60:387-388.
137. van Velthoven ME, Faber DJ, Verbraak FD, et al. Recent developments in optical coherence tomography for imaging the retina. *Prog Retin Eye Res*. 2007;26(1):57-77. Epub 2006 Dec 8.
138. Reversible dysfunction of retinal ganglion cells in non-secreting pituitary tumors. 2008 Aug 1 [Epub ahead of print]
139. Vizzeri G, Bowd C, Medeiros FA, et al. Effect of improper scan alignment on retinal nerve fiber layer thickness measurements using Stratus optical coherence tomograph. *J Glaucoma*. 2008;17(5):341-9.
140. Vizzeri G, Bowd C, Medeiros FA, et al. Scan tracking coordinates for improved centering of Stratus OCT scan pattern. *J Glaucoma*. 2009;18(1):81-7.
141. Vizzeri G, Bowd C, Medeiros FA, et al. Scan tracking coordinates for improved centering of Stratus OCT scan pattern. *J Glaucoma*. 2009;18(1):81-7.
142. Vizzeri G, Weinreb RN, Gonzalez-Garcia AO, et al. Agreement between Spectral-Domain and Time-Domain OCT for measuring RNFL thickness. *Br J Ophthalmol*. 2009;93(6): 775-81.
143. Wu GF, Schwartz ED, Lei T, et al. Relation of vision to global and regional brain MRI in multiple sclerosis. *Neurology* 2007;69:2128-2135.
144. Youm DJ, Kim JM, Park KH, Choi CY. *Curr Eye Res*. 2009;34(1):78-83.
145. Youm DJ, Kim JM, Park KH, Choi CY. *Curr Eye Res*. 2009;34(1):78-83.
146. Zaveri MS, Conger A, Salter A, et al. Retinal imaging by laser polarimetry corroborates optical coherence tomography evidence of axonal degeneration in multiple sclerosis. *Arch Neurol* 2008;65(7):924-928.
147. Zaveri MS, Conger A, Salter A, et al. Retinal imaging by laser polarimetry and optical coherence tomography evidence of axonal degeneration in multiple sclerosis. *Arch Neurol*. 2008;65(7):924-8.
148. Optical coherence tomography can measure axonal loss in patients with ethambutol-induced optic neuropathy. 2005;243(5):410-6.

LESSONS FROM GLAUCOMA: USE OF OCT IN THE CLINIC AND TRIALS

Joel S. Schuman, MD, FACS, Allison K. Ungar, Gadi Wollstein

*Department of Ophthalmology, UPMC Eye Center, Eye and Ear Institute,
Ophthalmology and Visual Science Research Center, University of Pittsburgh School of Medicine,
Pittsburgh, PA*

LEARNING OBJECTIVES

1. The participant will be able to describe the two types of optical coherence tomography devices.
2. The participant will be able to explain the advantages of Spectral-Domain Optical Coherence Tomography in comparison to Time-Domain Optical Coherence Tomography.
3. The participant will be able to describe five different scenarios where OCT would be clinically useful in glaucoma diagnosis and management.

CME QUESTIONS

1. What are the most clinically relevant parameters collected from an OCT scan for glaucoma?
2. Name the three main scans from time domain OCT.
3. Name 4 advantages of Spectral-Domain Optical Coherence Tomography in comparison to Time-Domain Optical Coherence Tomography

KEY WORDS

- Optical Coherence Tomography (OCT)
- Time-Domain Optical Coherence Tomography (TD-OCT)
- Spectral-Domain Optical Coherence Tomography (SD-OCT)
- Retinal Nerve Fiber Layer (RNFL)
- Circumpapillary Scan
- Ganglion Cell Complex (GCC)
- Glaucoma Progression Analysis (GPA)
- Visual Field Index (VFI)
- Pre-perimetric
- Central Island

ABSTRACT

Glaucoma is the second leading cause of blindness worldwide. It is characterized by the accelerated death of retinal ganglion cells and presents as progressive functional damage to the visual field. There is no formal screening method for glaucoma. Disease detection is solely dependent on the clinical capabilities of the eye

care provider. The first-line diagnostic tools for identifying glaucoma are clinical examination with direct or indirect ophthalmoscopy and/or stereoscopic optic nerve head photographs. Unfortunately, these tools are prone to high intra- and inter-observer variability. Recently, a number of imaging devices have been introduced with the goal of early detection and quantification of structural glaucomatous changes in the retinal nerve fiber layer and optic nerve head. One of the commercially available glaucoma imaging devices is optical coherence tomography (OCT). OCT generates cross-sectional and three-dimensional images of retinal structures. Its application in glaucoma diagnostics and monitoring will be discussed in this chapter.

INTRODUCTION

Glaucoma is the second leading cause of blindness worldwide. It is characterized by the accelerated death of retinal ganglion cells and presents as progressive functional damage to the visual field. The World Health Organization (WHO) has projected this disease to affect 60.5 million individuals by the year 2010, leaving 8.4 million blind. With the world's aging population, the burden of disease is predicted to grow exponentially, affecting 80 million people by 2020¹.

With this understanding, the WHO has made it a priority eye disease to address with their program Vision 2020, which aims to prevent avoidable blindness. One of their specific objectives is to develop adequate training methods in the diagnosis of glaucoma, as early intervention has been shown to slow disease progression and preserve functional sight². The NIH National Eye Institute has also set improved glaucoma diagnostic measures as a part of their National Plan for Eye and Vision Research.

Unfortunately, early detection of glaucoma remains a challenge. No symptoms appear until there is advanced retinal ganglion cell death and visual field loss. Estimates of undiagnosed glaucoma range from 40 to 90%, with higher percentages found in underdeveloped nations^{4,5}.

There is no formal screening method for glaucoma. Disease detection is solely dependent on the clinical capabilities of the eye care provider. The first-line diagnostic tools for identifying structural changes in glaucoma are clinical examination with direct or indirect ophthalmoscopy and/or stereoscopic ONH photographs. These tools are mostly qualitative thus prone to high intra- and inter-observer variability⁷⁻⁹. The functional

damage caused by glaucoma which causes characteristic patterns of VF loss is often quantified through the use of standard automated perimetry (SAP). SAP is a threshold test that determines the eye's sensitivity to light throughout the central visual field (VF). This commonly used clinical test has a high test-retest variability, and multiple VF tests are required to confirm damage^{10,11}. Also, significant structural loss may occur before changes are detected by VF¹².

A number of ocular imaging devices have been introduced which provide reproducible quantification of the retinal nerve fiber layer (RNFL) and ONH. The commercially available glaucoma imaging devices (GIDs) include: optical coherence tomography (OCT), confocal scanning laser ophthalmoscopy (CSLO) and scanning laser polarimetry (SLP).

Using the best parameters of each GID has been shown to have specificity and sensitivity similar to that of glaucoma experts in detecting glaucomatous ONH abnormalities^{40,41}. Studies directly comparing these three technologies have not found significant differences in their diagnostic ability⁴²⁻⁴⁶. In 2007, the American Academy of Ophthalmology suggested that information from imaging printouts is best used in conjunction with other clinical parameters⁴⁷.

BASICS OF OCT

OCT generates cross-sectional and three-dimensional (3D) images of retinal structures by detecting coherent (non-scattered) light echoes with an interferometer. The most important glaucoma application of the device is the measurement of RNFL thickness. Thinning of the RNFL has been well correlated with the fundamental pathophysiology of glaucoma namely the destruction of the ganglion cell layer of the retina²⁰.

The commercial time-domain OCT (TD-OCT) system (StratusOCT, Carl Zeiss Meditec, Dublin, CA (CZMI)), has an axial resolution of 8–10 μ m and obtains scans at a rate of 400 axial scans/second. A newer model of OCT, Spectral Domain OCT (SD-OCT), is able to detect all of the light echoes simultaneously rather than sequentially, as in time domain detection. This enables a dramatic increase in resolution and scanning speed, most offering a 5–7 μ m axial resolution and 25,000 scans per second. The increase in resolution is advantageous in following small changes in progression.

OCT provides reproducible quantification of the RNFL thickness¹³⁻¹⁵, a measurement that correlates with the fundamental pathophysiology of glaucoma, namely the destruction of the ganglion cell layer of the retina. OCT provides good glaucoma discriminatory power with an area under the receiver operating curve of 0.79 to 0.97, depending on the referenced sector²¹⁻²⁵.

COMMERCIAL TYPES OF OCT

TD-OCT

- Stratus (CZMI)

SD-OCT

- Cirrus (CZMI)
- Spectralis (Heidelberg Engineering, Heidelberg, Germany)
- RTVue (Optovue, Fairmont, CA)
- TopCon (Topcon Medical Systems, Inc, Paramus, NJ)
- Bioptogen (Research Triangle Park, Durham, NC)

FEATURED HIGHLIGHTS OF OCT DEVICES

When deciding on an device to use in the clinic or in research, consider that different instruments have different special features which make them unique.

Various imaging devices emphasize:

- Tracking to control for eye motion.
- 3-Dimensional reconstruction.
- Advanced visualization with cube data
- Averaging scan data to make for a visually appealing image.
- Fundus image either red-free or CSLO, which provides information about orientation.
- Quantification of various parameters.
- Comparison to a normative database to use clinically.
- A variety of scan patterns allowing for multiple means of visualizing any pathology.
- Automatic registration within a cube of data allowing for more accurate change analyses.

OCT SCAN PATTERNS

TD-OCT

- Peripapillary Circle Scan
 - This is relevant in glaucoma as it is a robust indicator of the nerve fiber layer thickness.
- ONH
 - Provides cup and disc parameters.
- Macula
 - This is an alternative to the circle scan which provides a statistically significant correlation with glaucoma.
 - Note: Correlation $r=.52$ between overall mean macular thickness and peripapillary RNFL thickness

In a longitudinal study published in 2005 by Wollstein, et al., OCT sensitivity using RNFL thickness was higher than that of SAP. [Reference]

SD-OCT

- 3-Dimensional Cube (multiple B-scans compiled)
 - Post-processing allows a misaligned scan to be fixed, removing a limitation of TD-OCT.
 - Increased reproducibility in comparison with TD-OCT [Reference: Kim JS, Br J Ophthalmol 2009]
 - Faster speed in comparison with TD-OCT reduces the number of motion artifacts

CASE 1: NORMAL EYE

This was a 45 year old Caucasian man with hypothyroidism and no ocular disease. Best corrected visual acuity in the left eye is 20/16 wearing a prescription of -2.00+1.50x174, intraocular pressure (IOP) was 12 millimeters of mercury (mmHg), and pachymetry showed a central corneal thickness (CCT) of 586. The anterior chamber was normal, and the dilated fundus exam revealed a normal appearing ONH with no other abnormalities (Fig. 1). Humphrey visual fields (HVF) were full (Fig. 2) and showed no progression over the span of 5 years (Fig. 3).

Imaging with OCT, both TD (Fig. 4-9) and SD (Fig. 10-15) revealed structures with parameters within the normal distribution. Confocal scanning laser ophthalmoscopy (CSLO) and scanning laser polimetry (SLP) confirmed normal ONH parameters (Fig. 17 and 18, respectively).

FIGURE 1: Normal color photo (left) and red-free photo (right) of a normal optic nerve head. The white arrow points to the normal coloration of the nerve fiber bundles in a red-free photo.

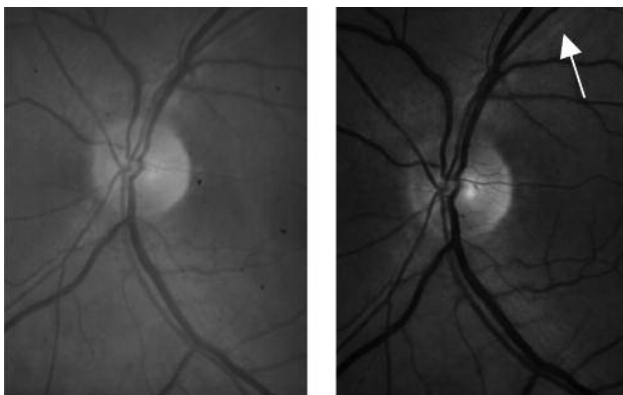


FIGURE 2: HVF – Normal gray scale (left) and pattern deviation (right).

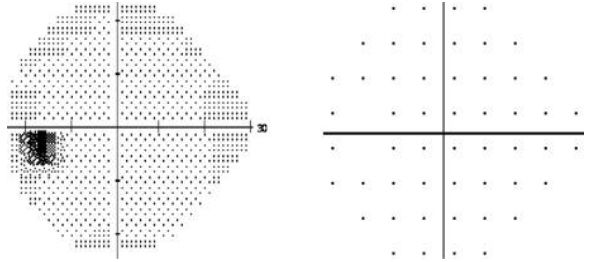


FIGURE 3: HVF – VFI graph over 5 years showing no progression.

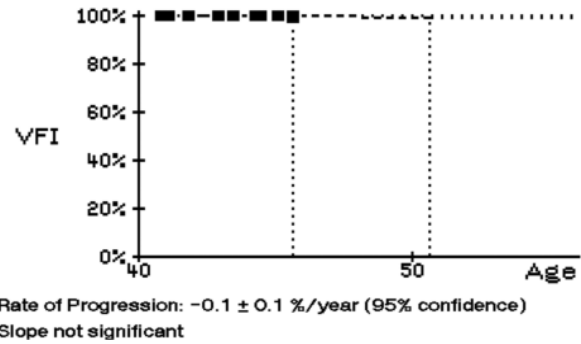


FIGURE 4: Stratus OCT - Circumpaillary B scan with excellent signal strength showing a normal retinal nerve fiber layer thickest in the superior and inferior regions.

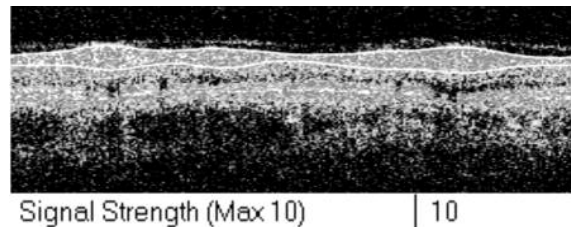


FIGURE 5: Stratus OCT Infrared Photo — Circumpaillary scan properly placed around the ONH (left) and off-centered, displaced nasally (right).

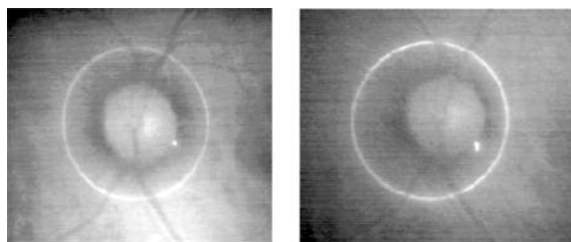
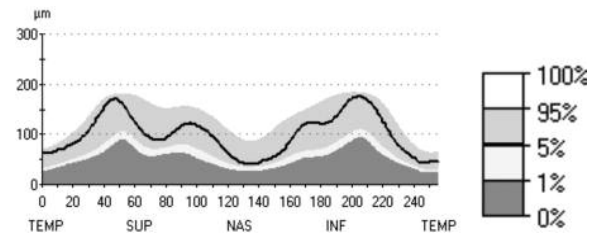
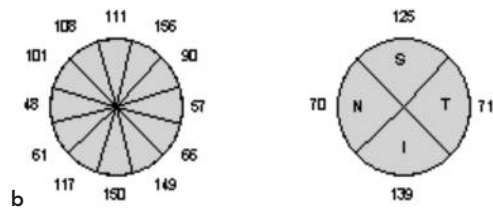


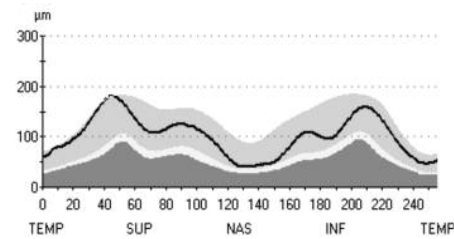
FIGURE 6: Stratus OCT circumpapillary thickness profiles for properly placed (A, B) and nasally displaced (C, D) scans compared with normal distribution percentiles. Note that the “double hump” pattern in C and D is spread apart. This changes the thickness, although remaining in the normal distribution.



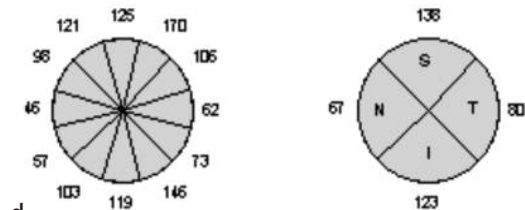
a



b

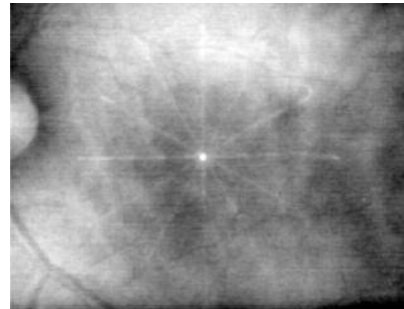


c

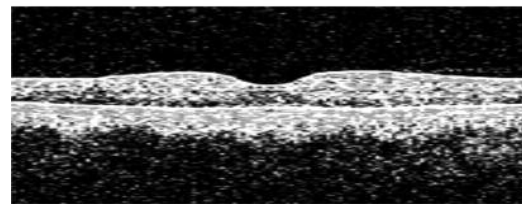


d

FIGURE 7: Well-centered Stratus OCT macula raster scan. (A) Infrared fundus image. (B) Normal vertical retinal B scan. Note the paucity of reflectance centrally at the foveal dip. (C) Thickness chart — overall retinal thickness compared to a normative database. (D) Retinal volume map quantitative color map (top) and sectoral comparison to a normative database (below). Note that the blue foveal thinning is placed centrally.

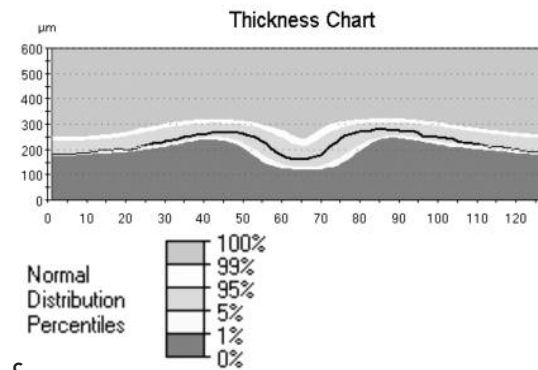


a

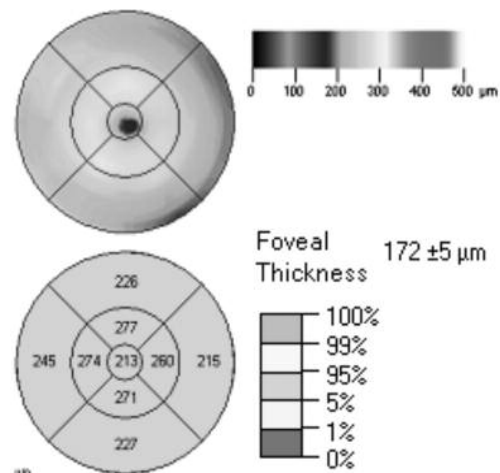


Signal Strength (Max 10) | 8

b

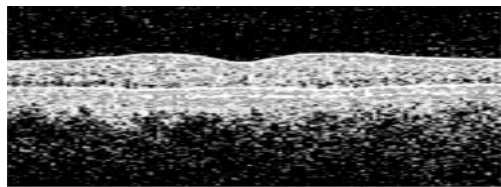


c



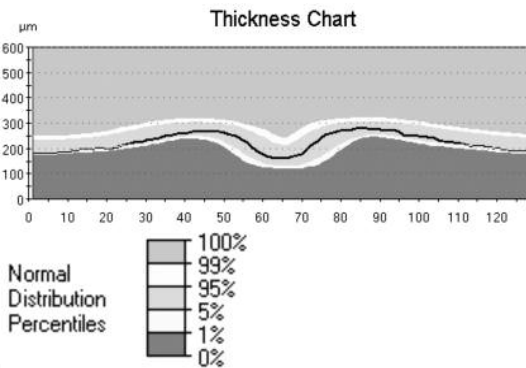
d

FIGURE 8: Nasally displaced Stratus OCT macula raster scan. (A) Vertical macular B scan. Note that the foveal dip has increased reflectance in comparison with the well-centered scan shown in Figure 7B. (B) Thickness chart with the scan displaced nasally. (C) Retinal volume map quantitative color map (top) and sectoral comparison to a normative database (below). Note that the blue foveal thinning is displaced. In this case, the quantitative assessment of the macula overall has not been compromised, however, the foveal thickness is significantly different (in comparison with Figure 7D).

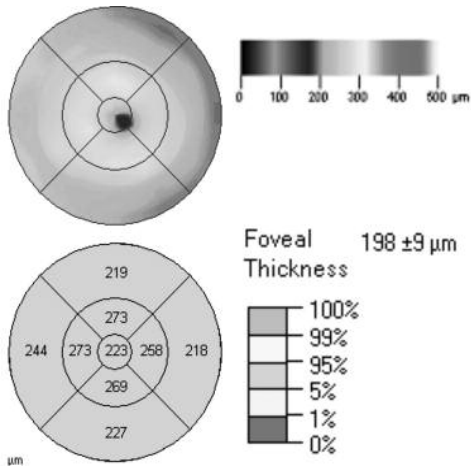


Signal Strength (Max 10) | 10

a

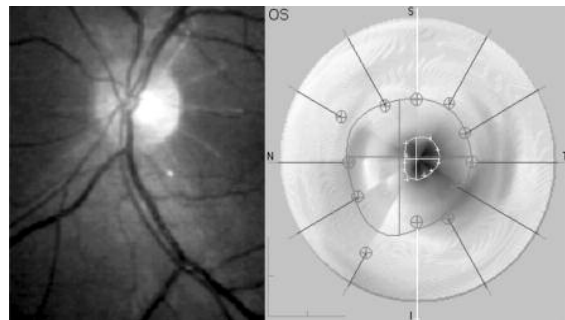


b



c

FIGURE 9: Normal ONH Scan from Stratus TD-OCT. (A) Infrared ONH image. (B) ONH parameter outlining a small cup-to-disc ratio (C/D). (C) ONH Analysis Results (D) Manually placed edges of retinal pigment epithelium (red-circles) allow for a computer generated disc (blue shaded area). (E) Vertical ONH B scan without any graphics shows a thick RNFL at the ONH.

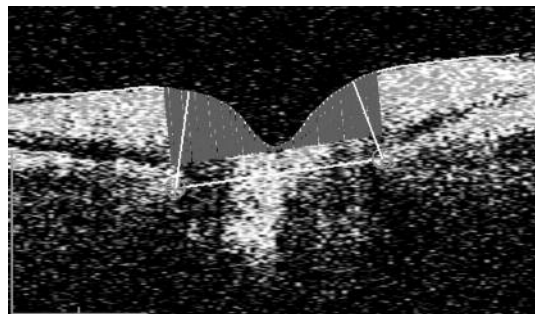


a

b

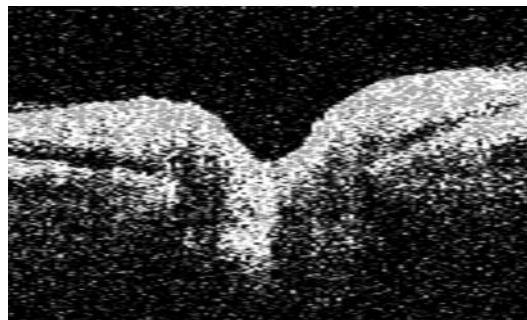
Optic Nerve Head Analysis Results	
Disk Area	2.182 mm ²
Rim Area	1.991 mm ²
Rim Cross Sectional Area	2.066 mm ²
Rim Volume	0.677 mm ³
Cup Area	0.191 mm ²
Cup Volume	0.006 mm ³
Cup/Disk Horiz. Ratio	0.276
Cup/Disk Vert. Ratio	0.312
Cup/Disk Area Ratio	0.088

c



Signal Strength (Max 10) | 9

d



e

FIGURE 10: Normal Optic Disc Cube 200x200 from Cirrus SD-OCT showing no progression. (A) RNFL Thickness Map. (B) En-face fundus image showing the location of the peripapillary circle scan location. (C) RNFL Tomogram extracted from the cube. (D) RNFL thickness profile compared to a normative database at the Temporal-Superior-Nasal-Inferior-Temporal (TSNIT) locations. (E) RNFL Thickness — Average, Quadrants, and Clock Hours. (F) Optic disc cube maps over 2 years showing no progression. These scan locations are automatically registered within the cube with the intent to have a consistent circle scan location in following progression. (G) Progression graph of average, superior, and inferior measurements. (H) Progression graph of RNFL thickness profile.

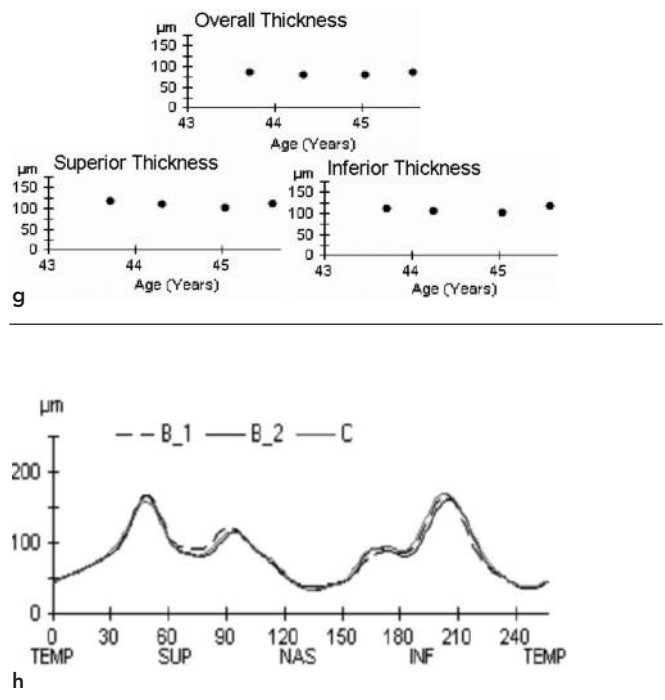
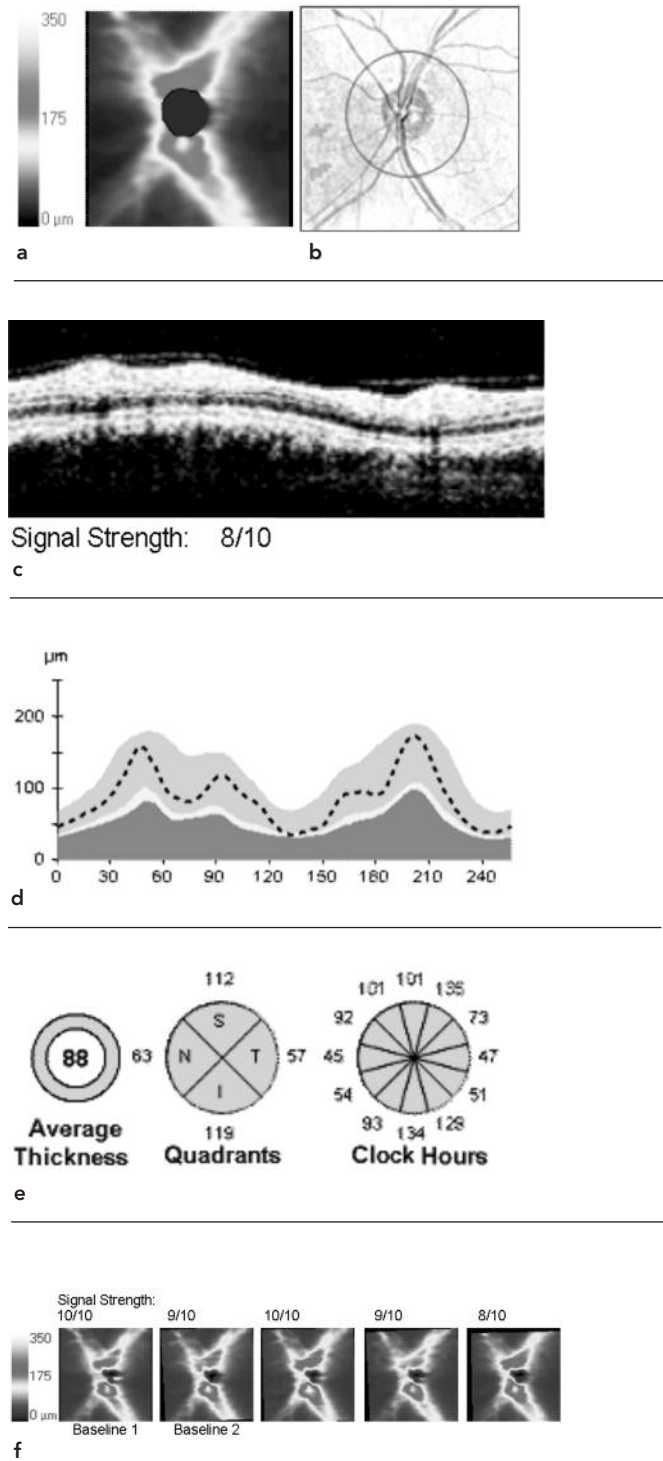


FIGURE 11: Normal Optic Disc Cube 200x200 from Cirrus SD-OCT, advanced visualization function. (A) CSLO fundus image showing the vertical (Purple line) and horizontal (blue line) scans available for viewing in the cube. (B) Vertical B Scan through the ONH. (C) Horizontal B Scan through ONH.

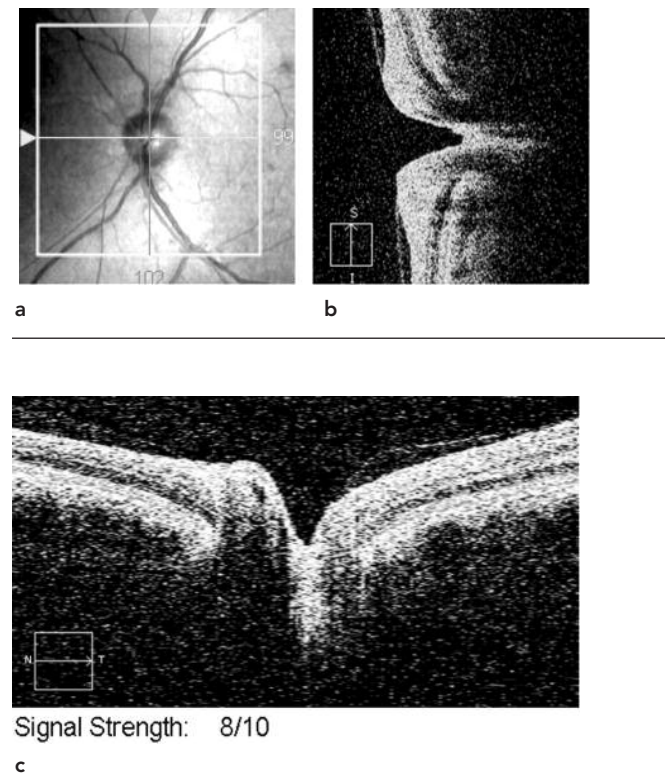
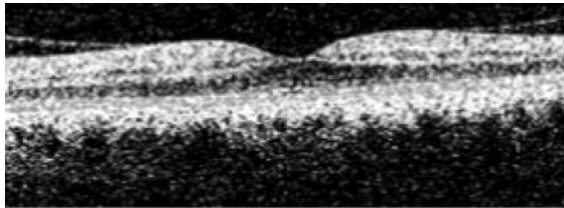
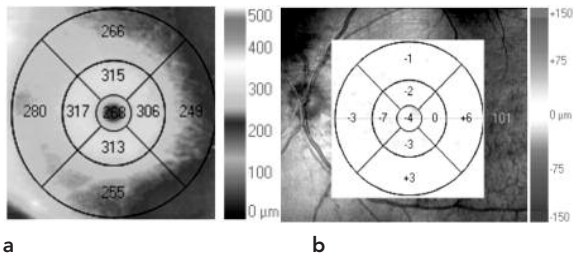


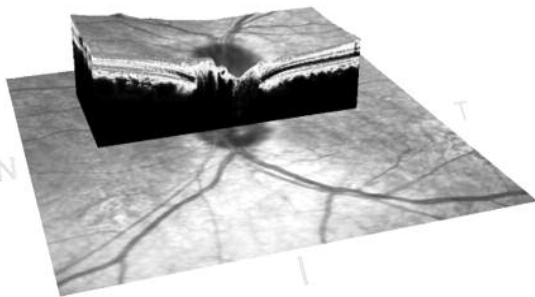
FIGURE 12: Normal Macular Cube 200x200 from Cirrus SD-OCT. (A) Macular thickness map. (B) Progression analysis map showing minimal change. (C) Horizontal B Scan from the macular cube.



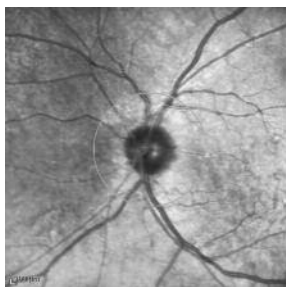
Signal Strength: 9/10

c

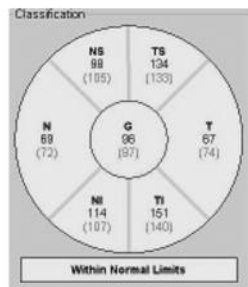
FIGURE 13: Normal Optic Disc from Spectralis SD-OCT. (A) Confocal Scanning Laser Ophthalmoscopy (CSLO) overlay and background with a 3-Dimensional horizontal B scan through the ONH. (B) SLO ONH Image with peripapillary circle in green. (C) Sectoral RNFL measurements compared to a normative database. (D) Peripapillary Circle Scan. (E) RNFL thickness profile compared to a normative database.



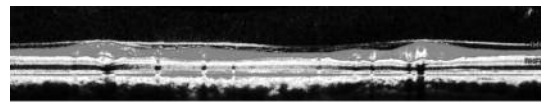
a



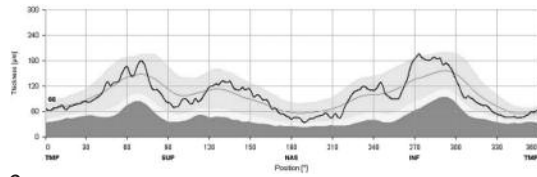
b



c

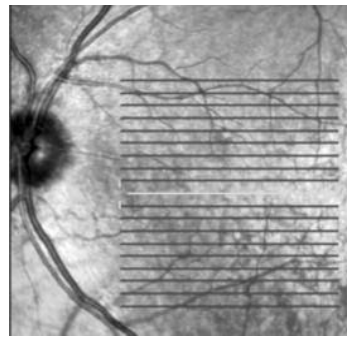


d

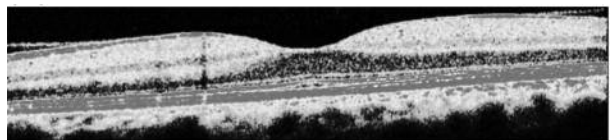


e

FIGURE 14: Normal Macula Images from Spectralis SD-OCT. (A) Confocal Scanning Laser Ophthalmoscopy (CSLO) background green lines indicating the individual B scans. The brightest line is the scan location seen in the image below. (B) Horizontal B-Scan through the macula.

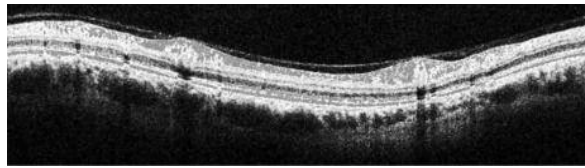


a



b

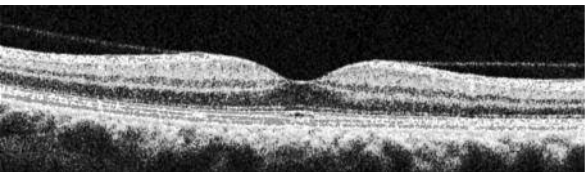
FIGURE 15: Normal Images from TopCon SD-OCT.
 (A) Peripapillary circle scan. (B) Vertical scan through ONH.
 (C) Macular scan.



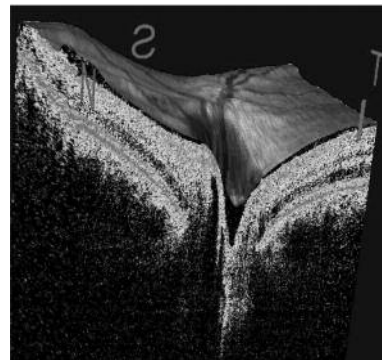
a



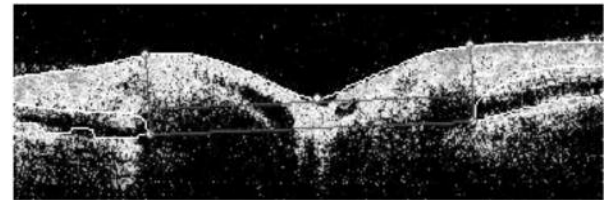
b



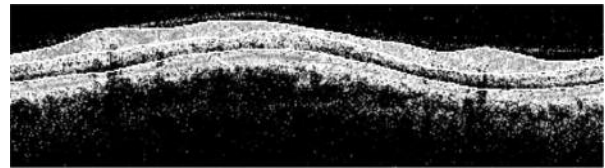
c



b

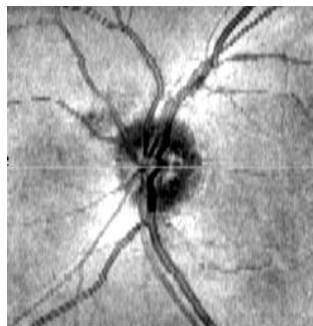


c

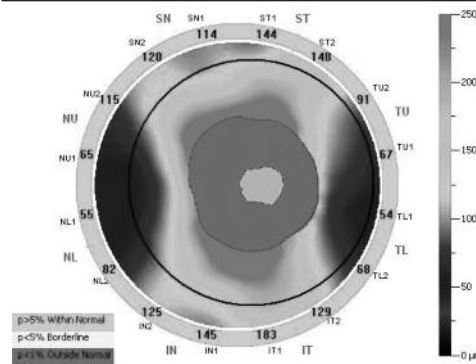


d

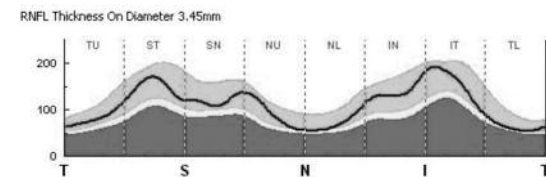
FIGURE 16: Normal Images from RTView SD-OCT. (A) En-face ONH Image. (B) 3-Dimensional horizontal ONH scan cube data with CLSO overlay. Green line in (A) indicating location of scan. (C) ONH scan. (D) Peripapillary circle scan. (E) Thickness map of ONH compared to a normative database. (F) RNFL profile scan compared to a normative database. (G) Horizontal cross-line scan of macula. (H) Vertical cross-line scan of macula. (I) Ganglion Cell Complex (GCC) Scan of the macula with thickness map (left) and significance map (right).



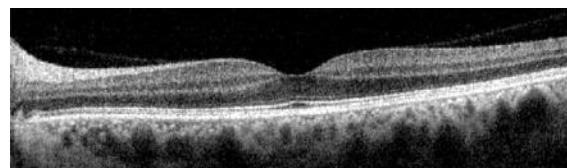
a



e



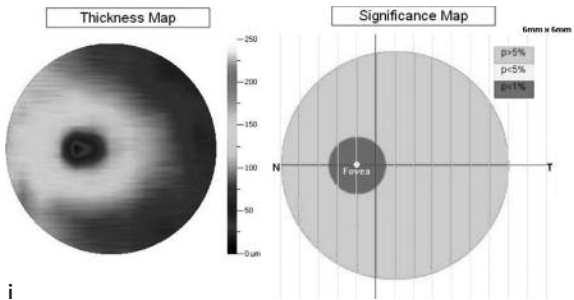
f



g

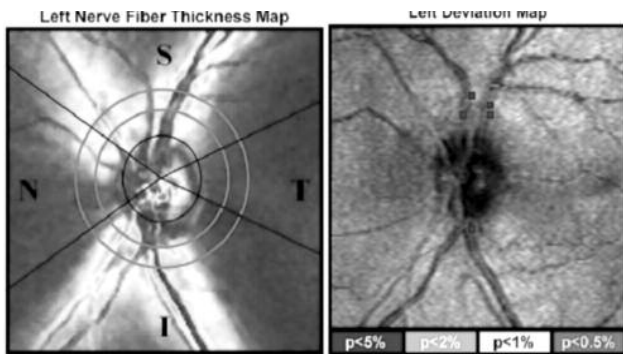


h



i

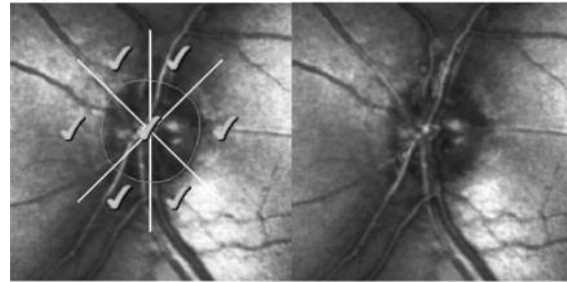
FIGURE 17: Normal Images from Scanning Laser Polarimetry with the highest quality (10/10). (A) Nerve fiber layer thickness map of the ONH. (B) Deviation map compared to a normative database.



a

b

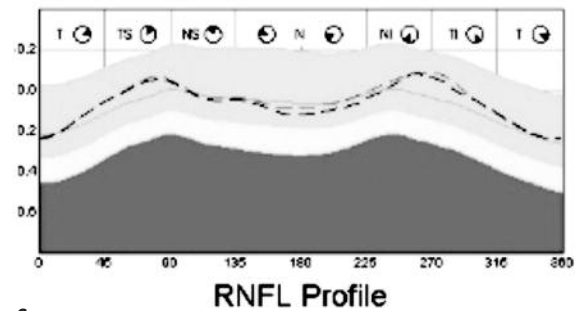
FIGURE 18: Normal Images from CSLO. (A) Moorfields Regression Analysis within normal limits within each sector. (B) Topographic Change Analysis over 8 years showing normal variation around blood vessels on a CSLO background. (C) RNFL Profile compared to a normative database.



Quality: Very good

a

b



c

TAKE HOME POINTS

1. Use OCT scans with a high quality signal strength.
2. Use OCT scans with good alignment around the ONH and on the macula.
3. It is beneficial to analyze data using the normative database.

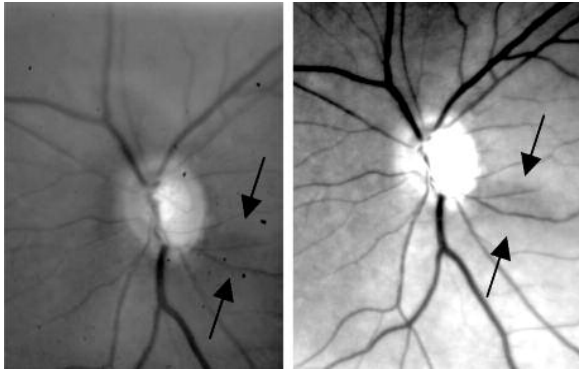
CASE 2: GLAUCOMA — THE FOCAL DEFECT WITH EXCELLENT CORRESPONDENCE BETWEEN STRUCTURE AND FUNCTION

This was the left eye of a 57 year old female with normal tension glaucoma treated with Lumigan, Cosopt, and Alphagan. Best corrected visual acuity was 20/30 wearing a prescription of +0.75+0.50x90 and the IOP was 11 mm. The anterior segment examination was normal with wide open angles. The dilated fundus exam revealed an ONH with C/D = 0.85x0.6 with no other abnormalities (Fig. 19 A).

Red-free photography reveals a RNFL wedge defect at 4:00 (Figure 19B black arrows). Humphrey visual fields (HVF) showed a superior nasal step and superior paracentral scotoma (Figure 20).

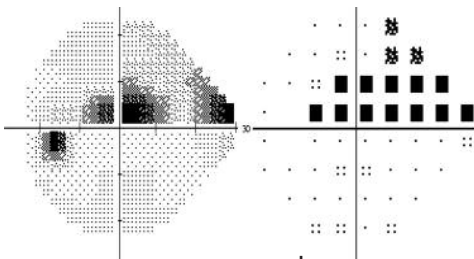
Imaging with OCT, both TD (Fig. 21–23) and SD (Fig. 24) confirm this defect. Confocal scanning laser ophthalmoscopy (CSLO) and Scanning Laser Polarimetry also confirms this defect (Fig. 25 A and B, respectively).

FIGURE 19: Color disc photo (left) and Red-Free photo (right) with discoloration indicating an area of defect (between black arrow), better seen in the red-free photo.



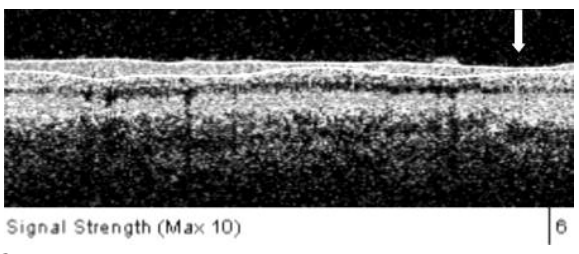
a b

FIGURE 20: HVF showing visual fields with a superior nasal step and superior paracentral scotoma. Grey scale (left) and pattern deviation (right). Glaucoma Hemifield Test (GHT) is outside of normal limits, visual field index (VFI) = 80%, mean deviation (MD) = -4.66 dB with $p < 0.5\%$, pattern standard deviation (PSD) = 8.63 dB with $p < 0.5\%$.

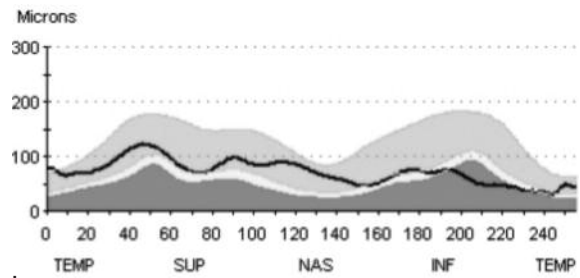


a b

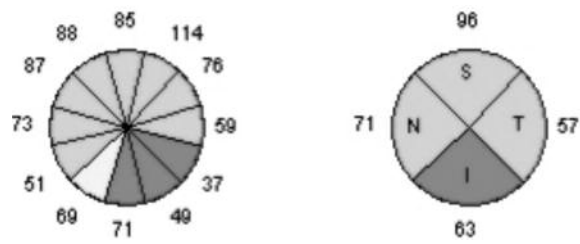
FIGURE 21: Images from Stratus TD-OCT Peripapillary Circle Scan. (A) B Scan showing focal RNFL inferiortemporal thinning (white arrow). (B) RNFL thickness profile comparison to a normative database confirming the inferiortemporal defect seen in (A). (C) Clock-hours (left) and quadrants (right) comparison to a normative database, again confirming the finding in (A).



a

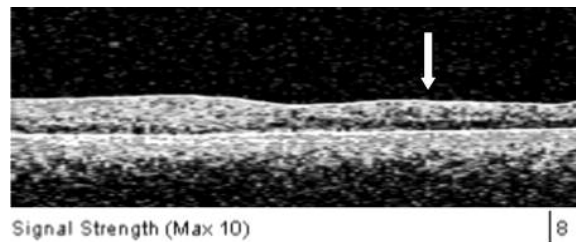


b

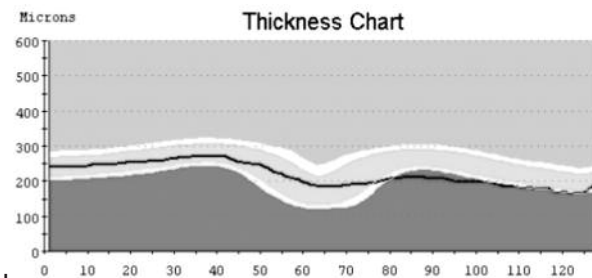


c

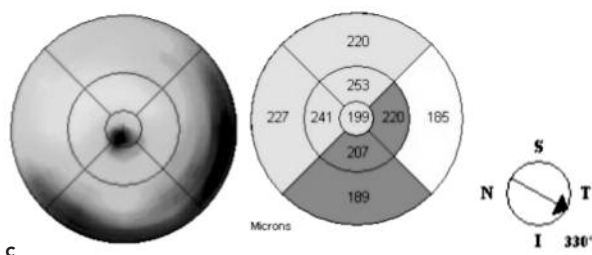
FIGURE 22: Stratus OCT macula raster scan. (A) Macular B scan at 330 degrees. Note the thin RNFL indicated by the white arrow. (B) Thickness chart - overall retinal thickness compared to a normative database. (C) Retinal volume map quantitative color map (left) and sectoral comparison to a normative database (right).



a

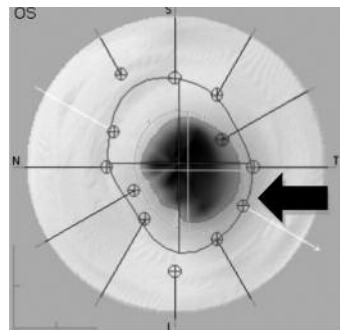


b

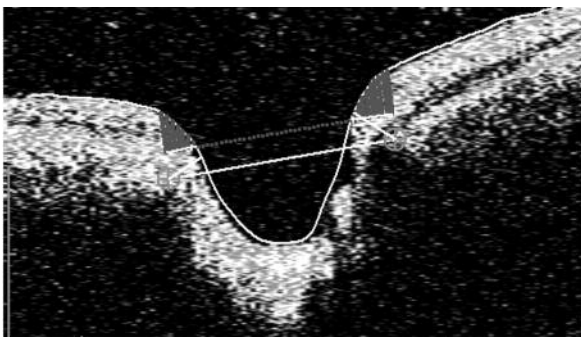


c

FIGURE 23: Stratus OCT Images (A) Optic Nerve Head Map. Black arrow indicating where the neuroretinal rim is thinnest, 4:00. (B) Radial B Scan through ONH 4:00 with manually placed edges of retinal pigment epithelium (red-circles) allow for a computer generated disc (blue shaded area). (E) Identical B scan as (B) without any graphics.



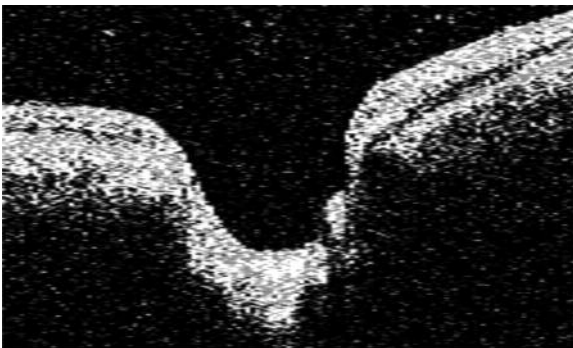
a



Signal Strength (Max 10)

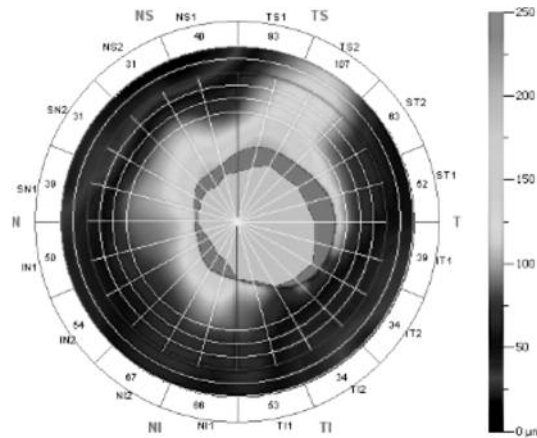
8

b

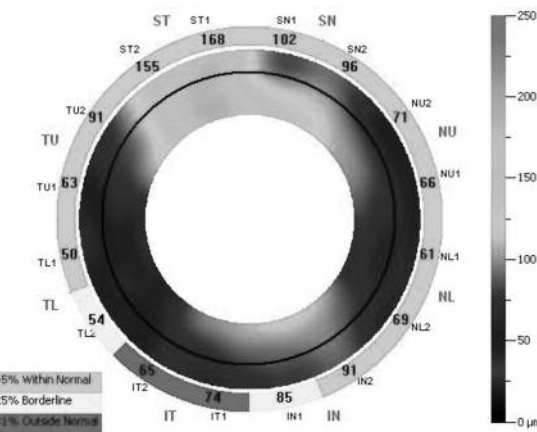


c

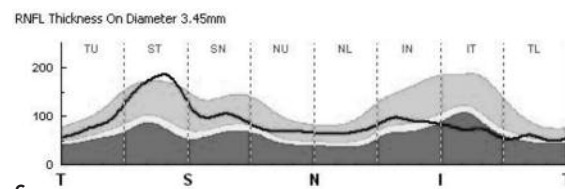
FIGURE 24: Images from RTView SD-OCT (A) "NHM4" ONH Scan showing a neuroretinal rim thinnest inferiorly. (B) ONH Scan with RNFL sector measurements along the 3.45mm diameter peripapillary circle. (C) RNFL Thickness Profile along the 3.45 mm circle. (D) Vertical Crossline through the macula showing decreased reflectance of the inferior RNFL.



a



b

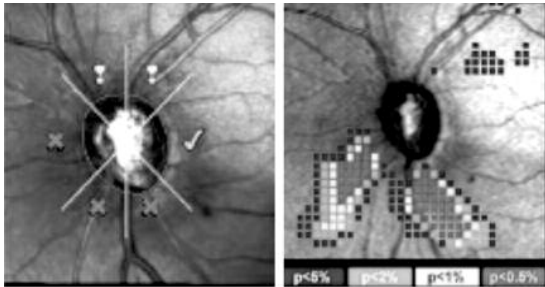


c



d

FIGURE 25: Other imaging modalities confirm the focal defect. (A) CSLO. (B) SLP.



TAKE HOME POINTS

1. Defects in the RNFL are displayed in the visual field inverted and reversed.
2. Red free photos are the best type of photo to view a focal neurofiber bundle defect.
3. The peripapillary circle, ONH, and macula scans can all provide information about RNFL wedge defects.

CASE 3: ADVANCED GLAUCOMA – THE CENTRAL ISLAND

This was the right eye of a 56 year old male with primary open angle glaucoma (POAG) treated with a trabeculectomy. All images are taken after the surgical treatment. Best corrected visual acuity was 20/30 and the IOP was 14 mm. The anterior segment examination was normal other than a flat bleb without leak superiorly and a patent peripheral iridotomy. The dilated fundus exam revealed an ONH with a barely perceptible neuroretinal rim (C/D = 0.99) with no other abnormalities.

Humphrey visual fields (HVF) showed a severely depressed field with only central vision spared (Figure 26).

Imaging with OCT, both TD (Fig. 27) and SD (Fig. 28) confirm this defect. Confocal scanning laser ophthalmoscopy (CSLO) and Scanning Laser Polarimetry also confirms this global defect (Fig. 30 and 31, respectively). The macula RNFL thickness remains normal (Figure 29), corresponding with the remaining central vision.

FIGURE 26: HVF Grey Scale. Pattern deviation is not commuted by the technology for severely depressed fields. GHT is outside of normal limits, VFI= 11%, MD=-29.59dB with $p < 0.5\%$, PSD=7.89dB with $p < 0.5\%$.

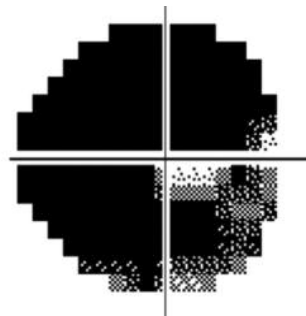
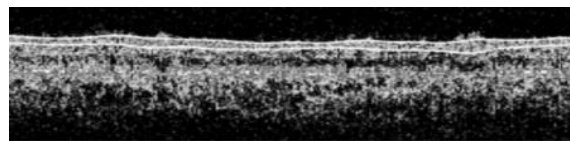
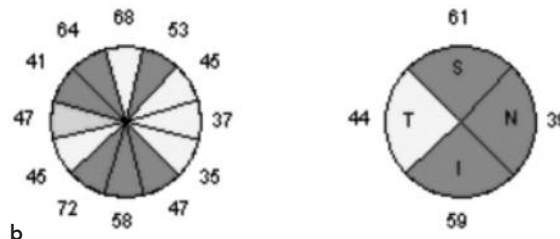
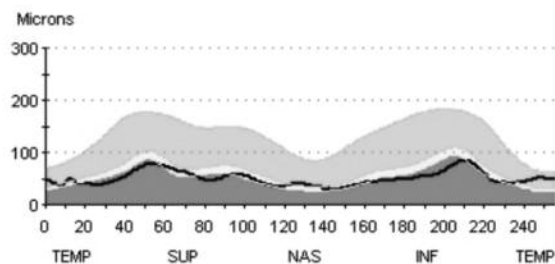


FIGURE 27: Images from Stratus TD-OCT Peripapillary Circle Scan. (A) B Scan showing global RNFL thinning. (B) RNFL thickness profile comparison to a normative database showing the topography to have thinned predominantly superiorly and inferiorly with relative temporal sparing. (C) Clock-hours (left) and quadrants (right) comparison to a normative database.



a



b

FIGURE 28: (A) Optic Disc Cube 200x200 from Cirrus SD-OCT. (A) RNFL Thickness Map displays global thinning (top). En-face fundus image showing thinning most prominent superiorly and inferiorly (bottom). (B) RNFL Thickness – Average (top), Quadrants (middle), and Clock Hours (bottom). (C) RNFL Tomogram extracted from the cube. (D) RNFL thickness profile compared to a normative database at the TSNIT locations.

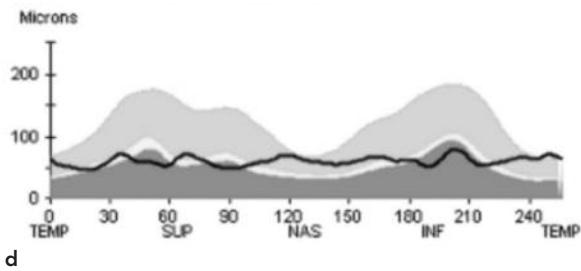
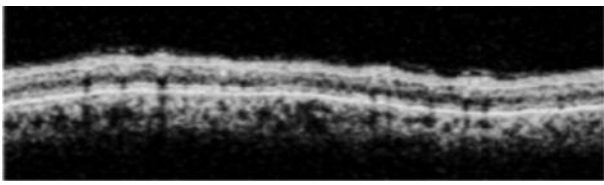
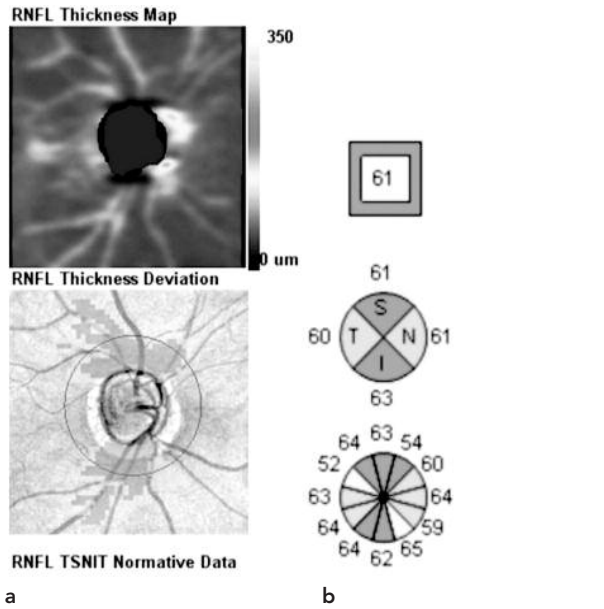


FIGURE 29: Macular Cube 200x200 from Cirrus SD-OCT. (A) Macular thickness map displaying that the macula has been spared from the otherwise global RNFL damage. (B) Horizontal (top) and vertical (bottom) B scans from the macular cube. (C) 3D segmentation of the macula showing the green circular island of retinal thickness at the macula surrounded by sea of thin (blue) retina.

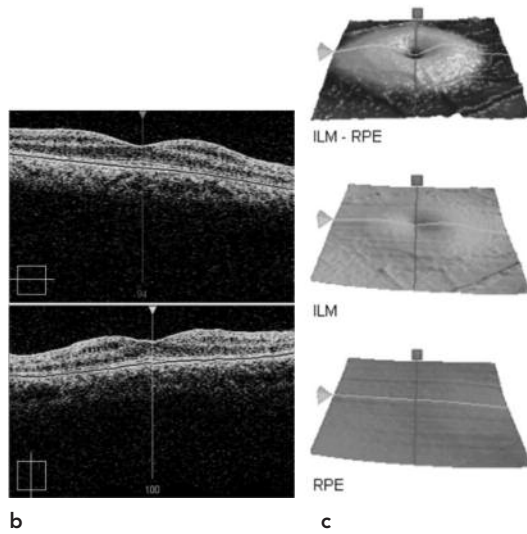
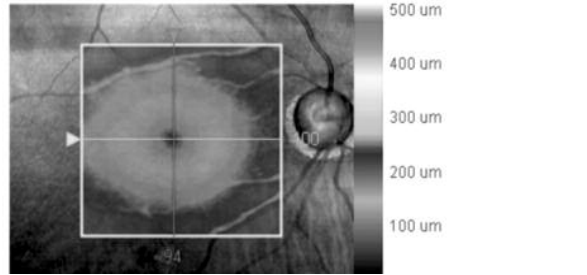


FIGURE 30: CLSO Moorfields Regression Analysis outside normal limits for each sector.

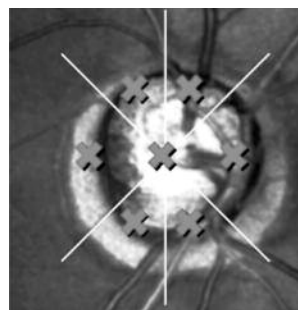
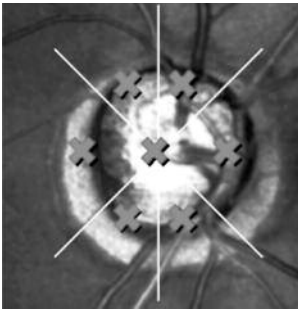


FIGURE 31: SLP image nerve fiber layer thickness map of the ONH showing a globally thin RNFL (blue).



TAKE HOME POINTS

1. The RNFL thickness “bottoms out” at 40 microns in severe damage.
2. Although the TD- and SD-OCT are not quantitatively identical, they can both provide into a RNFL defect location and severity.

CASE 4: GLAUCOMA — GLOBAL PROGRESSION

This was the left eye of a 52 year old female with juvenile glaucoma secondary to juvenile rheumatoid arthritis. She was treated with a trabeculectomy in 2004. She also has ocular rosacea and is pseudophakic. All images are taken after the surgical treatments. From 2005 to 2009 she progressed globally both structurally by OCT and functionally by HVF.

From 2005–2009, the patient’s exam remained stable. Best corrected visual acuity was 20/30 and the IOP was 12 mm Hg, and remained stable without drops. External exam was notable for telangiectasis on the lids. The anterior segment examination was normal other than a flat bleb without leak superior and a patent peripheral iridotomy. The posterior chamber intraocular lens was in place. The dilated fundus exam revealed a pale ONH with a thin neuroretinal rim (C/D = 0.9) with no other abnormalities.

Red-free photography clearly shows a loss of the neurofiber layer from 2005 to 2009. In 2005, clear neurofiber bundles are visualized following the vascular arches (Figure 32 B). In 2009, these striations have disappeared and the shadows of choroidal vessels are clear (Figure 32D).

In 2005 and 2009, HVF showed significantly depressed fields with both superior and inferior arcuate scotomas and superior and inferior nasal steps. (Figure 33). Glaucoma progression analysis showed a significant VF deterioration in the superior and inferior nasal step areas. (Figure 34A). The VFI analysis shows non-significant progression (Figure 34B).

Imaging with TD-OCT (Figure 35) shows a significant progression globally from 2005 to 2009 (Figure 36). The RNFL thins much more than the HVF would suggest.

The macula RNFL thickness remains normal (Figure 37), corresponding with the remaining central vision.

FIGURE 32: Color and Red-free photography. In 2005, clear neurofiber bundles are visualized following the vascular arches (B, between white arrows). In 2009, these striations have disappeared and the shadows of choroidal vessels are clear (D, between white arrows).

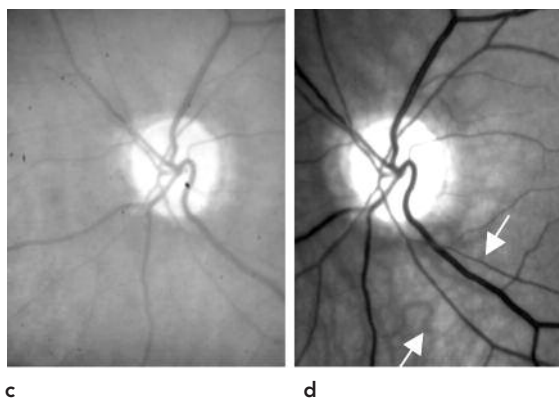
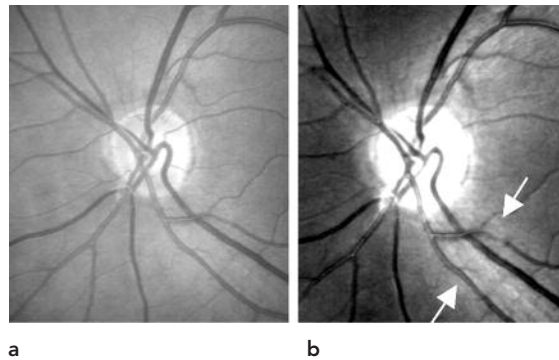


FIGURE 33: HVF grey scale (left) and pattern deviation (right) from 2005 (A and B) and 2009 (C and D) showing visual fields with a superior and inferior nasal step as well as a superior and inferior arcuate. In 2005, GHT is outside of normal limits, VFI= 77%, MD=-9.82 dB with p<0.5%, PSD=7.28dB with p<0.5%. In 2009, GHT is outside of normal limits, VFI=73%, MD=-11.53 dB with p<0.5%, PSD=8.13dB with p<0.5%.

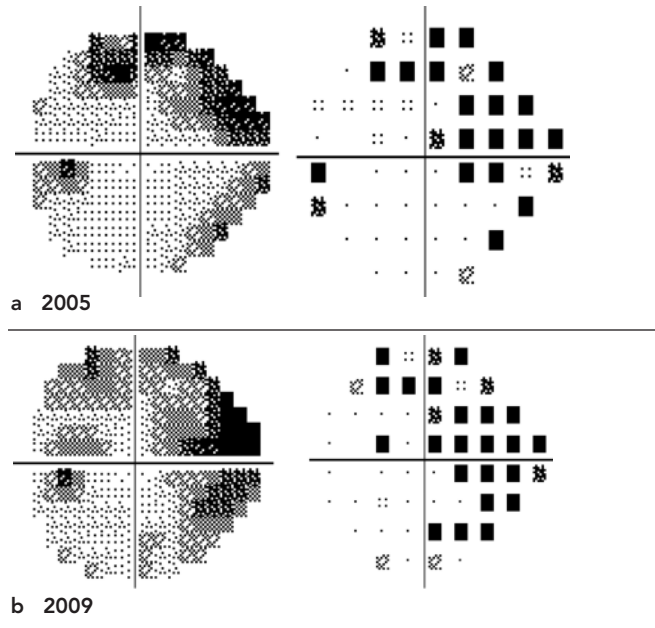


FIGURE 34: Glaucoma progression analysis (A) showed a significant VF deterioration in the superior and inferior nasal step areas. The VFI progression analysis shows non-significant progression (B).

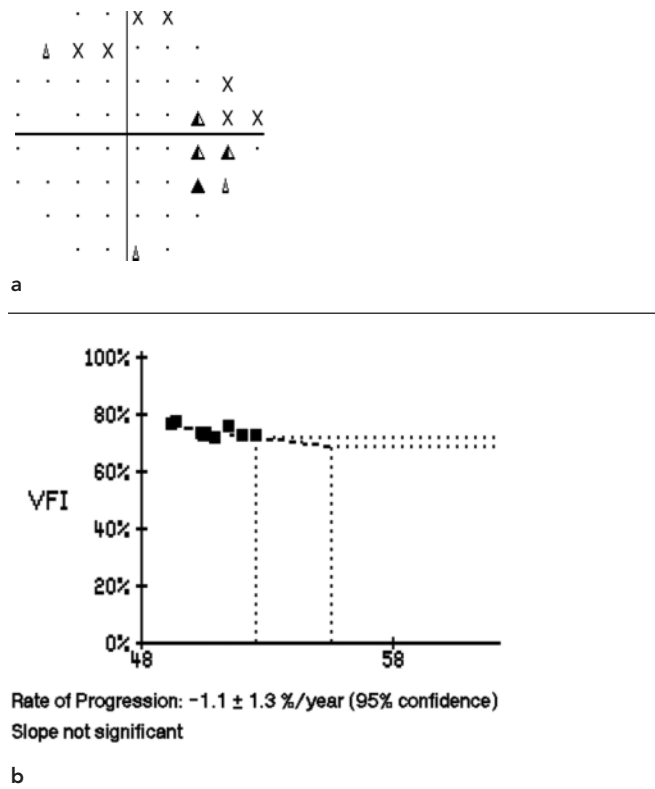
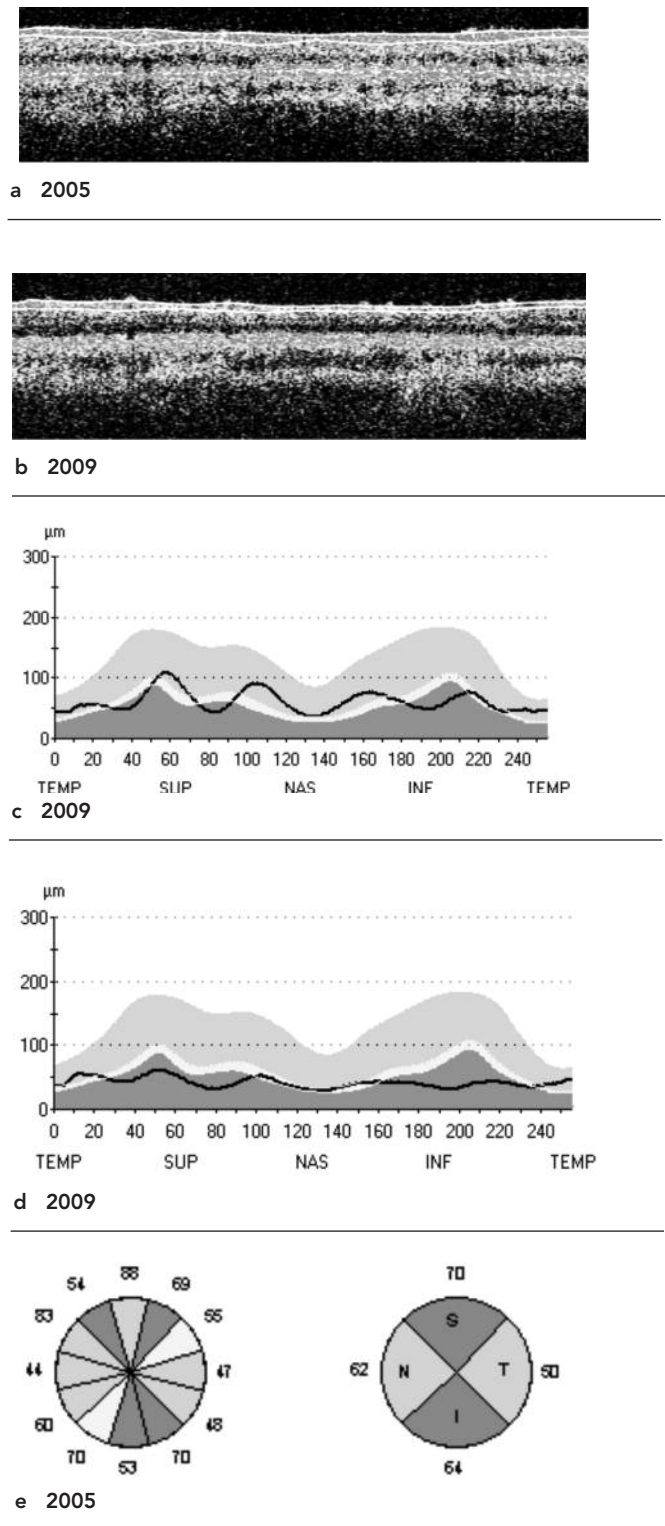


FIGURE 35: Stratus OCT TD-OCT Images in 2005 (A, C, and E) and 2009 (B, D, and F). Images (A) and (B) show the circumpaillary B scan in 2005 and 2009, respectively. Comparing (A) and (B) one can see the RNFL thinning globally. Images (C) and (D) show the RNFL thickness profile comparison to a normative database in 2005 and 2009, respectively. Images (E) and (F) show clock-hours (left) and quadrants (right) in comparison to a normative database in 2005 and 2009, respectively.



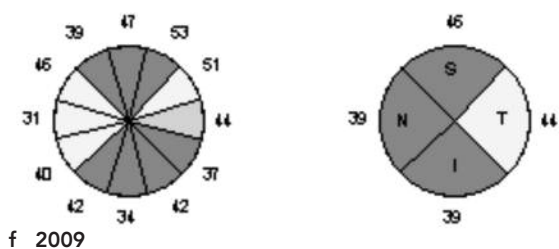
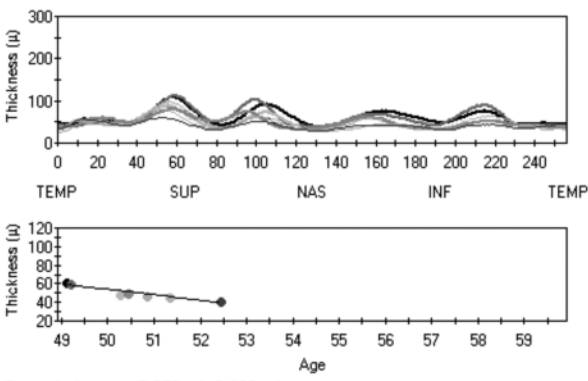


FIGURE 36: Stratus TD-OCT Progression Analysis. (A) RNFL Profiles color coded by date (top) and graph of average RNFL thickness (bottom) showing a significant rate of change. (B) Dates of scans color coded along with signal strengths and quantitative measurements of each scan.



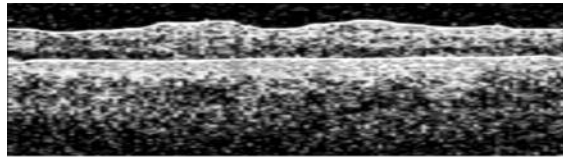
Rate of change: $-5.972 \pm 2.069 \mu/\text{year}^*$
 Statistically significant $P < 0.1\%$, seek clinical correlates

a

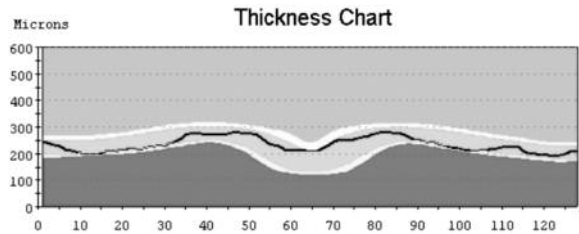
	SS,Q	AVG	SUP	INF
12/ /2005 (N=3)	9	61.74	70.00	64.00
1/ /2006 (N=3)	8	61.00	76.00	64.00
2/ /2007 (N=3)	6	49.46	60.00	43.00
4/ /2007 (N=3)	9	50.32	64.00	43.00
9/ /2007 (N=3)	8	48.20	63.00	44.00
3/ /2008 (N=3)	6	46.33	54.00	46.00
4/ /2009 (N=3)	6	42.21	46.00	39.00

b

FIGURE 37: Vertical Macular B Scan (A) and Retinal Thickness Map (B). The macula in this scenario has been preserved despite the global damage.



a



b

TAKE HOME POINTS

- OCT is a tool that is able to quantify progression, even when a clinical fundus exam remains stable.

CASE 5: GLAUCOMA — “PREPERIMETRIC”

This was the right eye of a 70 year old female with a history of ocular hypertension since 1994, referred to the glaucoma service in 2004 after a structural defect was seen on imaging. No visual field defects appeared until 2006. She was treated in 2008 and 2009 with Selective Laser Trabeculoplasty.

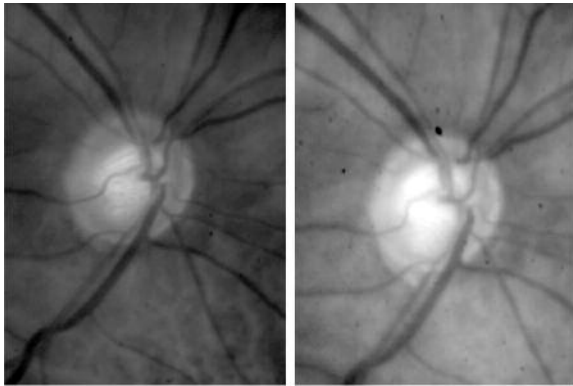
Best corrected visual acuity was 20/20 and the IOP was recorded as 24 mm Hg in 2004 and 13 mm Hg in 2009. The anterior segment examination was normal with open angles. The dilated fundus exam revealed an ONH with C/D = 0.9x0.8 in 2004 and 0.9x0.9 in 2009 with no other abnormalities (Figure 38 A and B, respectively).

Humphrey visual fields (HVF) in 2004 show a normal field and in 2009 shows a superior nasal and a superior arcuate scotoma. (Figure 39 A and B, respectively).

Imaging with TD-OCT (Figure 41) displays a progressing inferior RNFL defect from 2004–2009. The RNFL changes are significant and progressive (Figure 42). Confocal scanning laser ophthalmoscopy (CSLO) confirmed this defect in 2004 (Fig. 45).

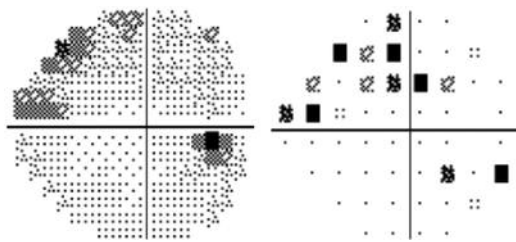
Imaging of the macula with OCT, both TD (Fig. 43) and SD (Fig. 44) also show an inferior defect. Figure 44 displays the progressive changes from 2006–2009.

FIGURE 38: Color ONH Photographs in 2004 (A) and 2009 (B). Note the barring of the lamina cribrosa inferiorly from and the superior neuroretinal thinning 2004 to 2009.

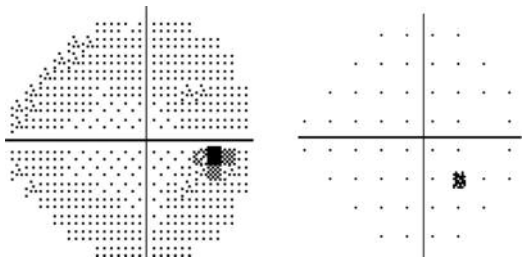


a 2004 b 2009

FIGURE 39: HVF from 2004 and 2009. HVF grey scale (left) and pattern deviation (right) from 2004 (A) and 2009 (B). In 2004, GHT is outside of normal limits, VFI= 100%, MD=+0.46 dB and PSD=1.78dB. In 2009, GHT is outside of normal limits, VFI=94%, MD=-2.73 dB with p<2%, and PSD=3.82dB with p<0.5%.

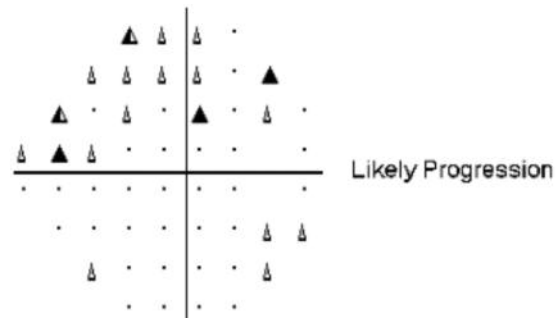


a 2004

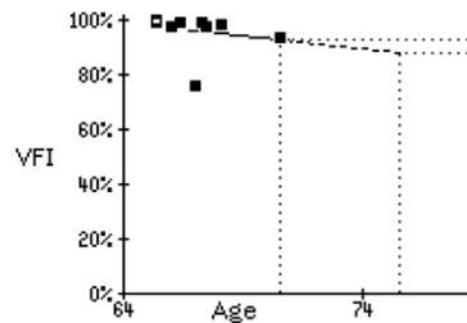


b 2009

FIGURE 40: Glaucoma progression analysis from 2004-2009 (A) showed a significant VF deterioration in the superior nasal step area. The VFI progression analysis from 2004-2009 shows non-significant progression (B).



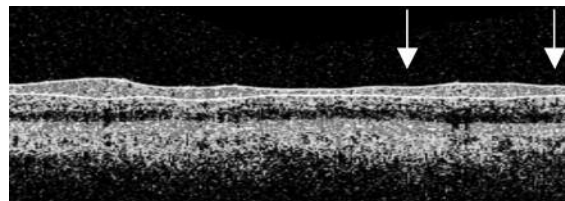
a



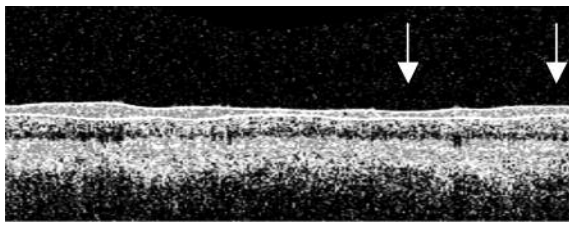
Rate of Progression: $-0.9 \pm 3.8 \%$ /year (95% confidence)
Slope not significant

b

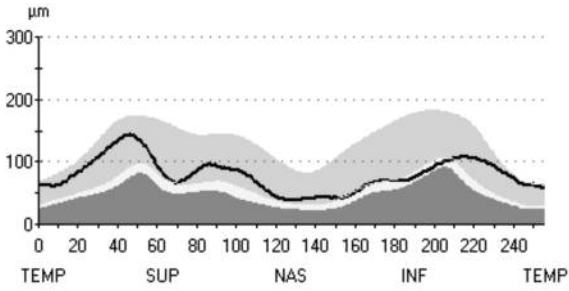
FIGURE 41: Stratus OCT TD-OCT Images in 2004 (A, C, and E) and 2009 (B, D, and F). Images (A) and (B) show the circumpaillary B scan in 2004 and 2009, respectively. Comparing (A) and (B) one can see the RNFL thinning inferiorly and inferiotemporally (between white arrows). Images (C) and (D) show the RNFL thickness profile comparison to a normative database in 2004 and 2009, respectively. Images (E) and (F) show clock-hours (left) and quadrants (right) in comparison to a normative database in 2004 and 2009, respectively.



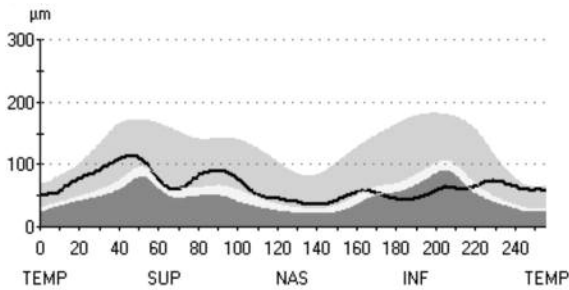
a 2004



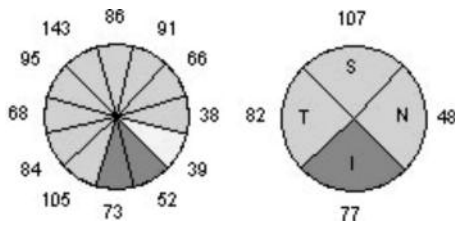
b 2009



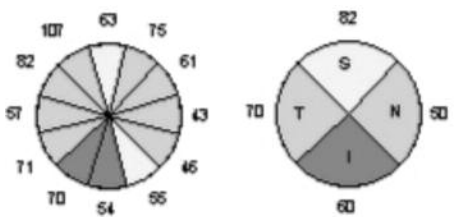
c 2004



d 2009

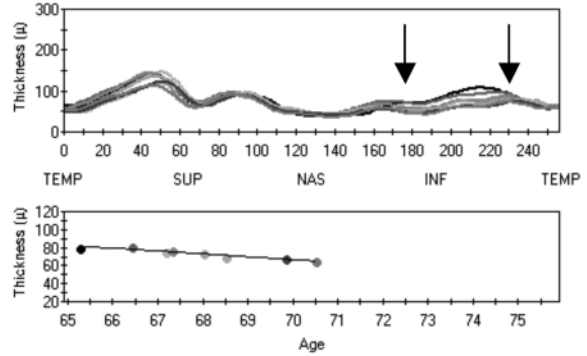


e



f

FIGURE 42: Stratus TD-OCT Progression Analysis. (A) RNFL Profiles color coded by date (top) and graph of average RNFL thickness (bottom) showing a significant rate of change. In between the black arrows, the graph highlights the inferior area that thins progressively from the first visit (black line) to the last visit (red line). (B) Dates of scans color coded along with signal strengths and quantitative measurements of each scan.



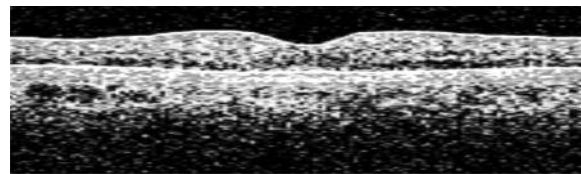
Rate of change: $-3.178 \pm 1.027 \mu\text{/year}^*$
 Statistically significant $P < 0.1\%$. seek clinical correlates

a

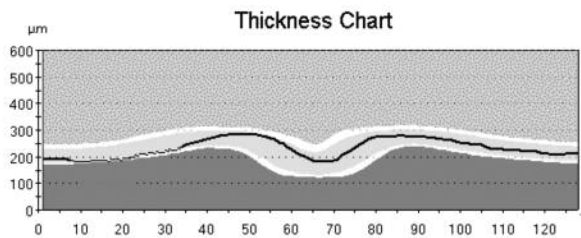
	SS,Q	AVG	SUP	INF
3/ /2004 (N=3)	9	79.98	103.00	85.00
5/ /2005 (N=3)	9	81.39	104.00	82.00
2/ /2006 (N=3)	10	74.91	106.00	65.00
4/ /2006 (N=3)	8	76.11	101.00	69.00
12/ /2006 (N=3)	7	74.15	101.00	64.00
6/ /2007 (N=3)	8	69.21	94.00	59.00
10/ /2008 (N=3)	7	67.20	93.00	56.00
6/ /2009 (N=3)	9	65.61	89.00	56.00

b

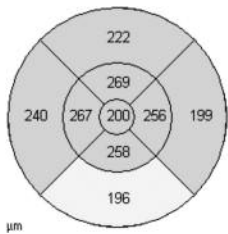
FIGURE 43: Macular Scan from Stratus TD-OCT. (A) Vertical macular B Scan. (B) Retinal Thickness Chart. (C) Retinal Thickness Map. The macula in this case shows some inferior thinning.



a

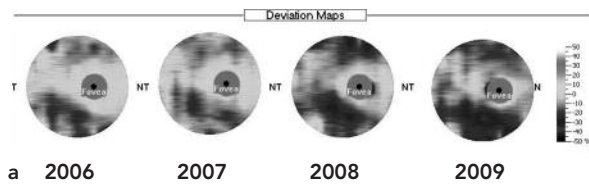


b

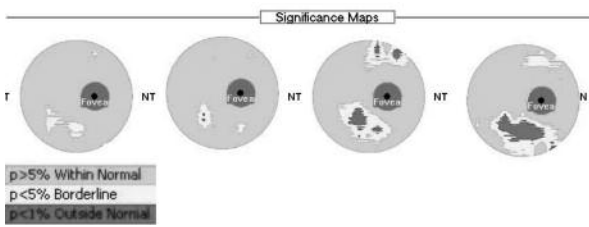


µm
c

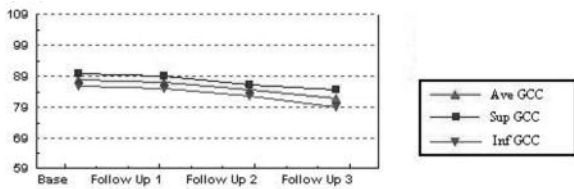
FIGURE 44: RTView SD-OCT Ganglion Cell Complex (GCC) Progression Scans of the macula. (A) Deviation maps showing thinning inferiorly in comparison with a normative database. (B) Significance maps in comparison with a normative database. (C) Graphic change of average (red), superior (blue), and inferior (green) GCC thickness.



a 2006 2007 2008 2009

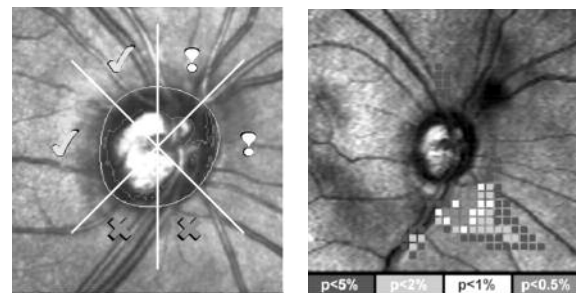


b 2006 2007 2008 2009



c

FIGURE 45: Other imaging modalities confirming the pre-perimetric inferior defect in 2004 (A) CSLO. (B) SLP.



a

b

TAKE HOME POINTS

1. OCT is capable of detecting damage to the RNFL before functional change occurs.
2. OCT is a tool that is able to quantify progression, even when a clinical fundus exam remains stable.
3. Some progression analyses are very useful in visualizing damage, especially for explaining to patients.

CASE 6: GLAUCOMA — FLUCTUATING FUNCTION BEFORE STRUCTURE

This was the left eye of a 75 year old male with a history of ocular hypertension vs. POAG since 2000 treated with Brimonidine-Timolol drops. A small focal superonasal scotoma appeared from 2002– 2005, disappeared from 2006–2008, and reappeared in 2009 with no overall progression (Figure 46). Until 2006 when the OCT showed a clock-hour defect at 5:00, this spot was considered a patient-dependent error or lid line mark. In retrospect, this mark was indicative of impending corresponding structural changes.

Best corrected visual acuity was 20/25 and the IOP was recorded as 22 mm Hg in 2005 and 28 mm Hg in 2009. The anterior segment examination was normal with open angles. The dilated fundus exam revealed an ONH with C/D = 0.8 in 2005 and 0.9 thinnest inferiorly in 2009 with no other abnormalities. In 2006, a disc hemorrhage could be seen at 5:00 (Figure 45).

Imaging with OCT, both TD (Fig. 48) and SD (Fig. 49) display a progressive 5:00 defect (Figures 47 and 49).

FIGURE 45: Color ONH Photographs in 2006. The black arrow points to a disc hemorrhage, which often indicates progression at that location.

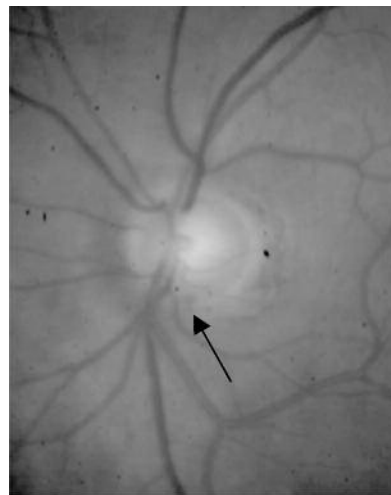
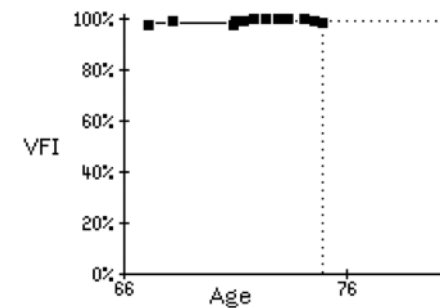
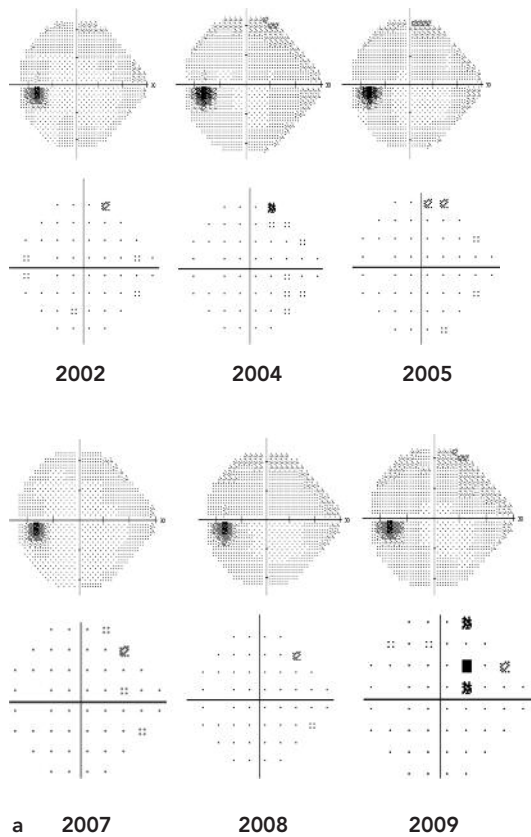


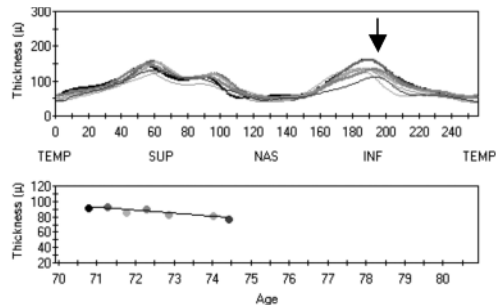
FIGURE 46: HVF from 2002-2009. (A) HVF grey scale (top) and pattern deviation (bottom) shows a fluctuating focal superior scotoma. (B) VFI progression shows no progression.



Rate of Progression: $+0.2 \pm 0.2\%/year$ (95% confidence)
Slope not significant

b

FIGURE 47: Stratus TD-OCT Progression Analysis. (A) RNFL Profiles color coded by date (top) and graph of average RNFL thickness (bottom) showing a significant rate of change. The black arrow indicates the inferior area that thins progressively from the first visits (black/purple line) to the last visit (dark blue line). (B) Dates of scans color coded along with signal strengths and quantitative measurements of each scan.



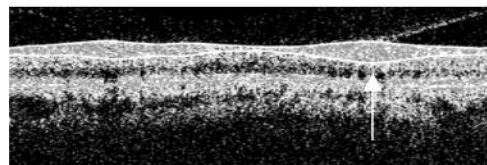
Rate of change: $-3.896 \pm 1.726 \mu/year^*$
Statistically significant $P < 1\%$, seek clinical correlates

a

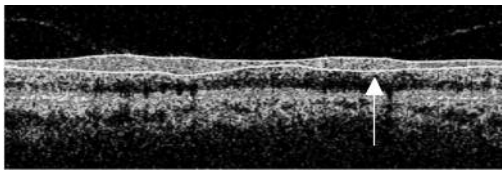
	SS,Q	AVG	SUP	INF
2/ /2005 (N=3)	9	93.08	119.00	122.00
8/ /2005 (N=3)	7	93.42	122.00	121.00
2/ /2006 (N=3)	7	86.98	119.00	106.00
8/ /2006 (N=3)	10	90.51	122.00	106.00
3/ /2007 (N=3)	9	83.33	106.00	106.00
5/ /2008 (N=3)	6	82.30	110.00	93.00
10/ /2008 (N=3)	7	78.61	112.00	85.00

b

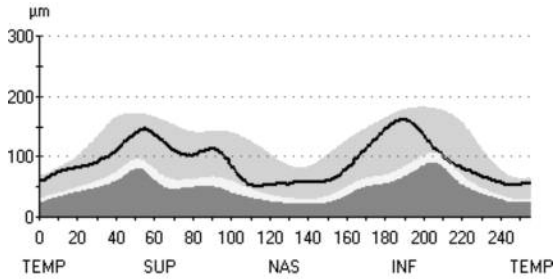
FIGURE 48: Stratus OCT TD-OCT Images in 2004 (A, C, and E) and 2008 (B, D, and F). Images (A) and (B) show the circumpaillary B scan in 2004 and 2009, respectively. Comparing (A) and (B) one can see the RNFL thinning inferiorly and inferiotemporally (between white arrows). Images (C) and (D) show the RNFL thickness profile comparison to a normative database in 2004 and 2009, respectively. Images (E) and (F) show clock-hours (left) and quadrants (right) in comparison to a normative database in 2004 and 2009, respectively.



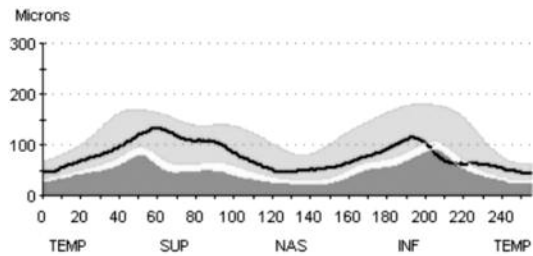
a 2005



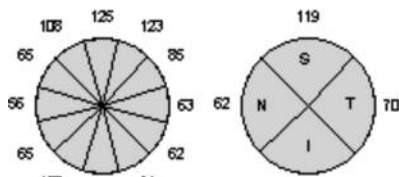
b 2008



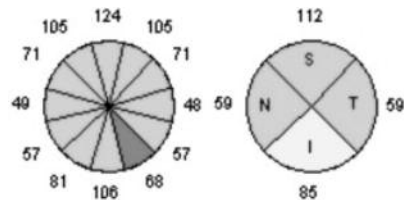
c 2005



d 2008

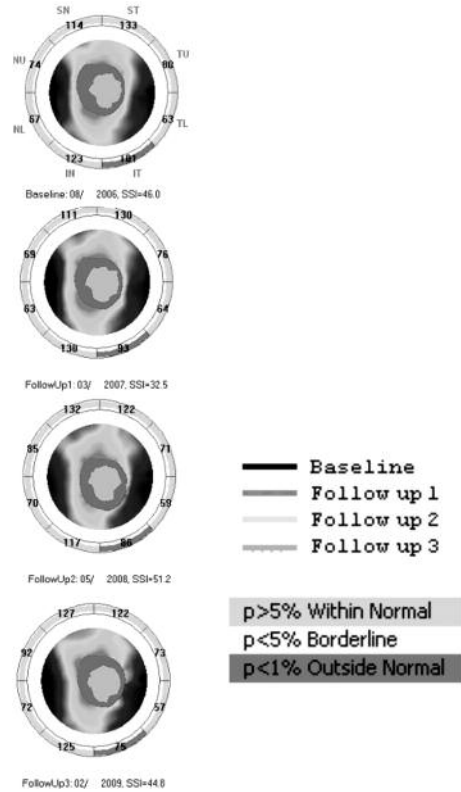


e 2005

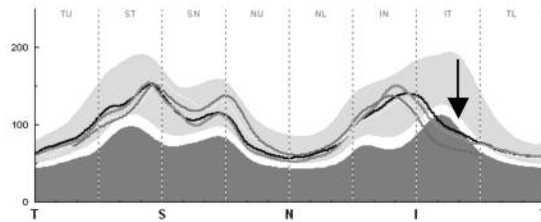


f 2005

FIGURE 49: RTView SD-OCT ONH Scan Progression from 2006-2009.



a 2006-2009



b

TAKE HOME POINTS

1. Beware of misleading HVF. Rely more on VF progression analyses, as they necessitate a greater number of exams.
2. Sometimes a focal scotoma will come and go because it is patient-dependent. OCT provides a reproducible, quantitative measurement that is less patient-dependent.
3. VF changes may occur before changes are seen on OCT.

CASE 7: GLAUCOMA — STABLE HEMIFIELD STRUCTURAL DAMAGE WITH BOTH STABLE AND FLUCTUATING FUNCTIONAL CHANGES

This was the right eye of a 65 year old female with a history of POAG treated with trabeculectomy in 2006. All images are taken after the surgical treatment, 2007–2009.

Best corrected visual acuity was 20/20 and the IOP was 6 mm Hg, and remained stable without drops. The anterior segment examination was normal other than a superior avascular bleb without leak and a patent peripheral iridotomy at 1:00. The dilated fundus exam revealed a, the increased cupping from 2007–2009 C/D = 0.8 to 0.9 with no other abnormalities.

From January 2007– February 2009, HVF displayed a dense inferior nasal step and arcuate scotoma. It also seemed that the patient’s glaucoma had progressed functionally to include both a superior nasal step and arcuate scotoma. However, when the patient returned in September 2009, the superior defects nearly disappeared.

Imaging with OCT, both TD (Fig. 52) displayed a stable RNFL thickness through this time period (Figures 53). Other SD-OCT technologies showed similar B scan profiles (Figures 54–57).

FIGURE 50: Color ONH Photographs in 2009.

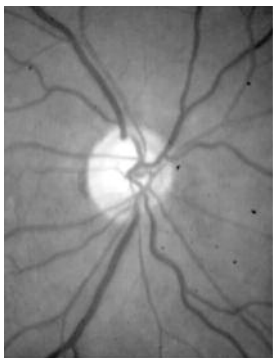
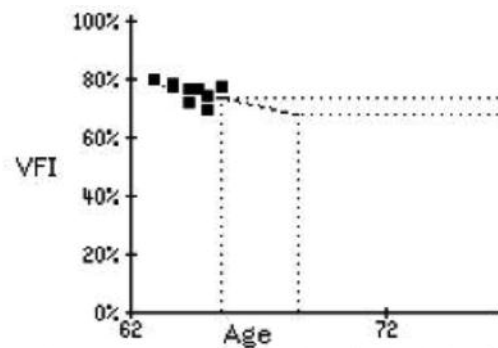
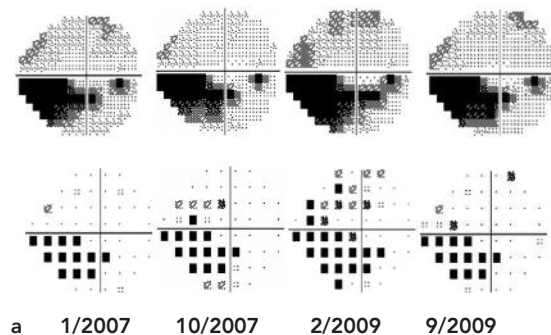


FIGURE 51: HVF from 2007-2009. (A) HVF grey scale (top) and pattern deviation (bottom) shows a fluctuating superior nasal step and arcuate scotoma. (B) VFI progression shows no progression.



Rate of Progression: $-1.9 \pm 3.0 \%$ /year (95% confidence)
Slope not significant

FIGURE 52: Stratus OCT TD-OCT Images in 2009 and progression analysis. Image (A) shows the circumpaillary B Scan. Image (B) shows the RNFL thickness profile in comparison to a normative database. Image C shows clock-hours (left) and quadrants (right) in comparison to a normative database. (A)-(C) all correspond with HVF with more superior RNFL structural damage leading to a dense inferior defect.

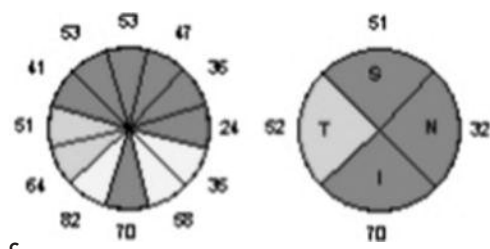
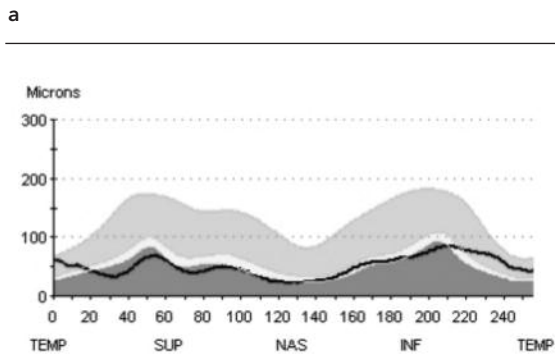
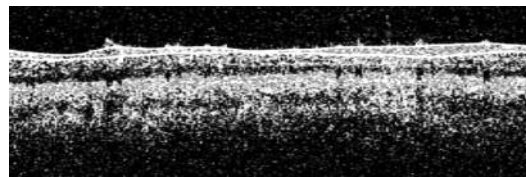
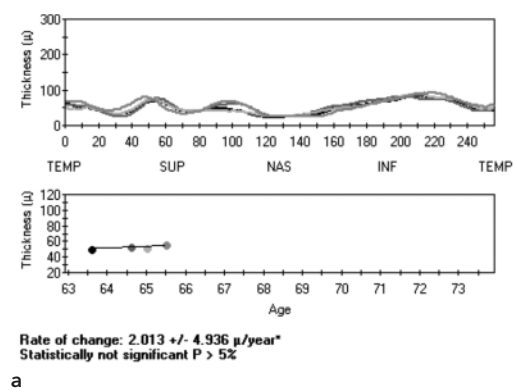


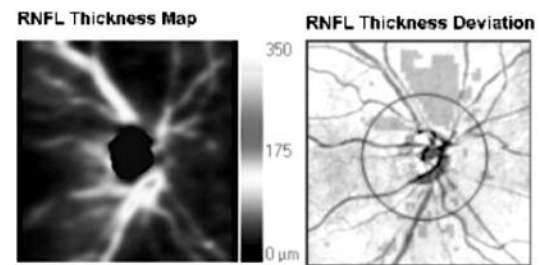
FIGURE 53: Stratus TD-OCT Progression Analysis. (A) RNFL Profiles color coded by date (top) and graph of average RNFL thickness (bottom) showing no change. (B) Dates of scans color coded along with signal strengths and quantitative measurements of each scan. Note, how stable the measurements stay throughout the time period.



	SS,Q	AVG	SUP	INF
10/ /2007 (N=3)	7	51.14	51.00	70.00
10/ /2008 (N=3)	7	53.68	53.00	72.00
2/ /2009 (N=3)	7	51.92	51.00	70.00
9/ /2009 (N=3)	7	55.88	56.00	70.00

a

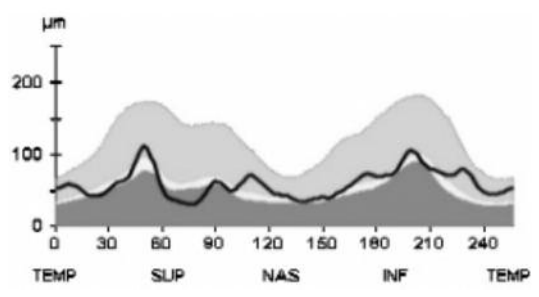
FIGURE 54: Optic Disc Cube 200x200 from Cirrus SD-OCT. (A) RNFL Thickness Map. (B) En-face fundus image showing the location of the peripapillary circle scan location and coloration based upon deviation from a normative database. (C) RNFL Tomogram extracted from the cube. (D) RNFL thickness profile compared to a normative database at the TSNIT locations. (E) RNFL Thickness – Average, Quadrants, and Clock Hours.



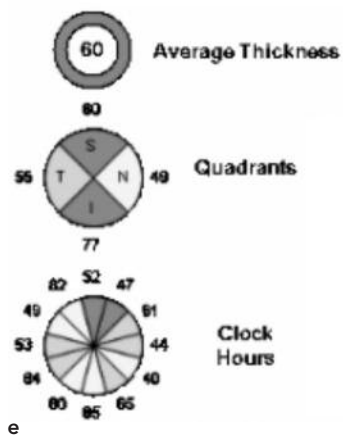
a



c

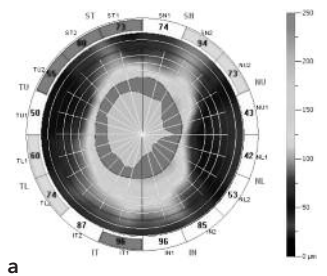


d

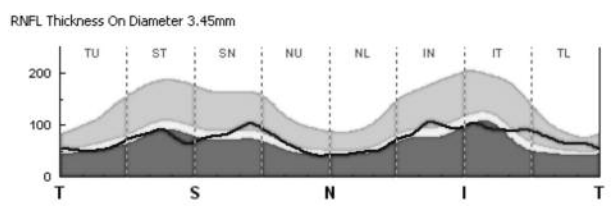


e

FIGURE 55: RTView SD-OCT NHM4 ONH Scan. (A) neuroretinal rim thinnest inferiorly. (B) ONH Scan with RNFL sector measurements along the 3.45mm diameter peripapillary circle. (C) RNFL Thickness Profile along the 3.45 mm circle.



a



b

FIGURE 56: Spectralis SD-OCT. (A) Peripapillary circle B scan highlighting the RNFL with red lines. (B) RNFL thickness profile compared to a normative database. (C) Sectoral RNFL measurements compared to a normative database.

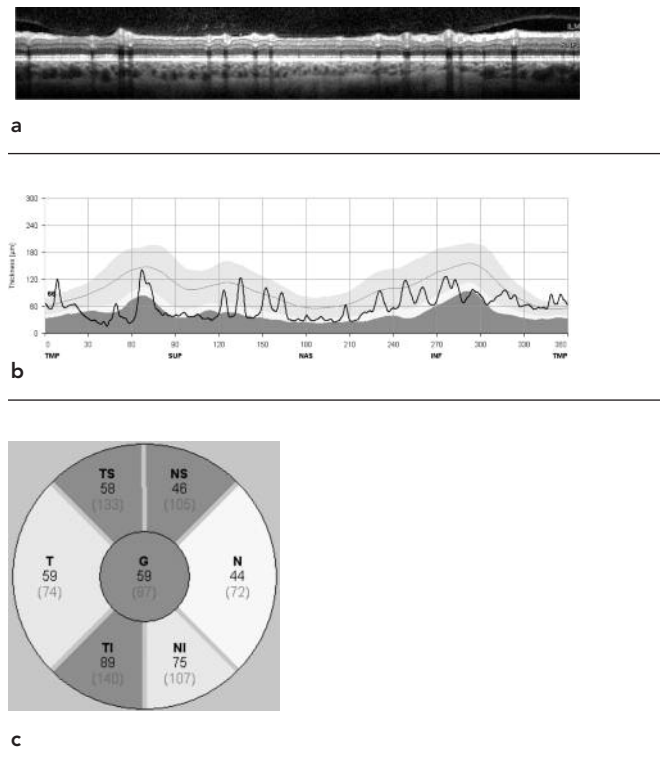
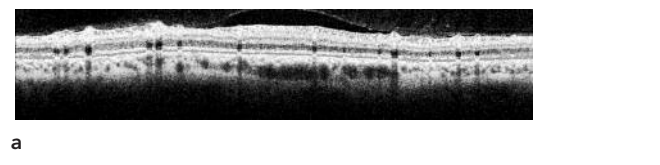


FIGURE 57: Peripapillary circle scan from TopCon SD-OCT.



TAKE HOME POINTS

1. Again, beware of misleading HVF — even large areas can fluctuate. Do not judge a single VF in isolation of the others that preceded it.
2. Currently, the various OCT technologies are not quantitatively comparable to one another.
3. OCT is an excellent quantitative, objective, and reproducible technology to monitor progression in glaucoma, or lack thereof. This statement is especially poignant in clinical management decisions.

CME ANSWERS

1. Retinal Nerve Fiber Layer (RNFL) thickness, ganglion cell complex (GCC). Optic nerve head parameters (ONH) may be useful as well, but there is insufficient evidence base to validate at this time.
2. Circumpapillary Scan, Macular Scan, and ONH Scan.
3. Increase in scanning speed enabling 3D imaging, improved resolution, post-processing capabilities, increased reproducibility, and better sensitivity and specificity in disease detection.

REFERENCES

1. Quigley HA, Broman AT. The number of people with glaucoma worldwide in 2010 and 2020. *Br J Ophthalmol* 2006;90:262–7.
2. Quigley HA. Number of people with glaucoma worldwide. *Br J Ophthalmol* 1996;80:389–93.
3. George R, Vijaya L. First World Glaucoma day, March 6, 2008: tackling glaucoma challenges in India. *Indian J Ophthalmol* 2008;56:97–8.
4. Abrams LS, Scott IU, Spaeth GL, Quigley HA, Varma R. Agreement among optometrists, ophthalmologists, and residents in evaluating the optic disc for glaucoma. *Ophthalmology* 1994;101:1662–7.
5. Wong EY, Keeffe JE, Rait JL, et al. Detection of undiagnosed glaucoma by eye health professionals. *Ophthalmology* 2004;111:1508–14.
6. Fingeret M, Medeiros FA, Susanna R, Jr., Weinreb RN. Five rules to evaluate the optic disc and retinal nerve fiber layer for glaucoma. *Optometry* 2005;76:661–8.
7. Gaasterland DE, Blackwell B, Dally LG, Caprioli J, Katz LJ, Ederer F. The Advanced Glaucoma Intervention Study (AGIS): 10. Variability among academic glaucoma subspecialists in assessing optic disc notching. *Trans Am Ophthalmol Soc* 2001;99:177–84; discussion 84–5.
8. Tielsch JM, Katz J, Quigley HA, Miller NR, Sommer A. Intraobserver and interobserver agreement in measurement of optic disc characteristics. *Ophthalmology* 1988;95:350–6.
9. Varma R, Steinmann WC, Scott IU. Expert agreement in evaluating the optic disc for glaucoma. *Ophthalmology* 1992;99:215–21.
10. Artes PH, Iwase A, Ohno Y, Kitazawa Y, Chauhan BC. Properties of perimetric threshold estimates from Full Threshold, SITA Standard, and SITA Fast strategies. *Invest Ophthalmol Vis Sci* 2002;43:2654–9.
11. Keltner JL, Johnson CA, Levine RA, et al. Normal visual field test results following glaucomatous visual field end points in the Ocular Hypertension Treatment Study. *Arch Ophthalmol* 2005;123:1201–6.
12. Kerrigan-Baumrind LA, Quigley HA, Pease ME, Kerrigan DF, Mitchell RS. Number of ganglion cells in glaucoma eyes compared with threshold visual field tests in the same persons. *Invest Ophthalmol Vis Sci* 2000;41:741–8.

13. Schuman JS, Pedut-Kloizman T, Hertzmark E, et al. Reproducibility of nerve fiber layer thickness measurements using optical coherence tomography. *Ophthalmology* 1996;103:1889-98.
14. Paunescu LA, Schuman JS, Price LL, et al. Reproducibility of nerve fiber thickness, macular thickness, and optic nerve head measurements using StratusOCT. *Invest Ophthalmol Vis Sci* 2004;45:1716-24.
15. Kim JS IH, Sung KR, Xu J, Wollstein G, Bilonick RA, Kagemann L, Duker JS, Fujimoto JG, Schuman JS. Retinal Nerve Fiber Layer Thickness Measurement Reproducibility Improved with Spectral Domain Optical Coherence Tomography. *Br J Ophthalmol* 2009;93:1057-63.
16. Williams ZY, Schuman JS, Gamell L, et al. Optical coherence tomography measurement of nerve fiber layer thickness and the likelihood of a visual field defect. *Am J Ophthalmol* 2002;134:538-46.
17. Bourne RR, Medeiros FA, Bowd C, Jahanbakhsh K, Zangwill LM, Weinreb RN. Comparability of retinal nerve fiber layer thickness measurements of optical coherence tomography instruments. *Invest Ophthalmol Vis Sci* 2005;46:1280-5.
18. Budenz DL, Michael A, Chang RT, McSoley J, Katz J. Sensitivity and specificity of the StratusOCT for perimetric glaucoma. *Ophthalmology* 2005;112:3-9.
19. Leung CK, Chan WM, Hui YL, et al. Analysis of retinal nerve fiber layer and optic nerve head in glaucoma with different reference plane offsets, using optical coherence tomography. *Invest Ophthalmol Vis Sci* 2005;46:891-9.
20. Kanamori A, Escano MF, Eno A, et al. Evaluation of the effect of aging on retinal nerve fiber layer thickness measured by optical coherence tomography. *Ophthalmologica* 2003;217:273-8.
21. Nouri-Mahdavi K, Hoffman D, Tannenbaum DP, Law SK, Caprioli J. Identifying early glaucoma with optical coherence tomography. *Am J Ophthalmol* 2004;137:228-35.
22. Kruse FE, Burk RO, Volcker HE, Zinser G, Harbarth U. Reproducibility of topographic measurements of the optic nerve head with laser tomographic scanning. *Ophthalmology* 1989;96:1320-4.
23. Dreher AW, Tso PC, Weinreb RN. Reproducibility of topographic measurements of the normal and glaucomatous optic nerve head with the laser tomographic scanner. *Am J Ophthalmol* 1991;111:221-9.
24. Rohrschneider K, Burk RO, Kruse FE, Volcker HE. Reproducibility of the optic nerve head topography with a new laser tomographic scanning device. *Ophthalmology* 1994;101:1044-9.
25. Ford BA, Artes PH, McCormick TA, Nicolela MT, LeBlanc RP, Chauhan BC. Comparison of data analysis tools for detection of glaucoma with the Heidelberg Retina Tomograph. *Ophthalmology* 2003;110:1145-50.
26. Mardin CY, Hothorn T, Peters A, Junemann AG, Nguyen NX, Lausen B. New glaucoma classification method based on standard Heidelberg Retina Tomograph parameters by bagging classification trees. *J Glaucoma* 2003;12:340-6.
27. Miglior S, Guareschi M, Albe E, Gomasasca S, Vavassori M, Orzalesi N. Detection of glaucomatous visual field changes using the Moorfields regression analysis of the Heidelberg retina tomograph. *Am J Ophthalmol* 2003;136:26-33.
28. Miglior S, Guareschi M, Romanazzi F, Albe E, Torri V, Orzalesi N. The impact of definition of primary open-angle glaucoma on the cross-sectional assessment of diagnostic validity of Heidelberg retinal tomography. *Am J Ophthalmol* 2005;139:878-87.
29. Zangwill LM, Chan K, Bowd C, et al. Heidelberg retina tomograph measurements of the optic disc and parapapillary retina for detecting glaucoma analyzed by machine learning classifiers. *Invest Ophthalmol Vis Sci* 2004;45:3144-51.
30. Hatch WV, Flanagan JG, Etchells EE, Williams-Lyn DE, Trope GE. Laser scanning tomography of the optic nerve head in ocular hypertension and glaucoma. *Br J Ophthalmol* 1997;81:871-6.
31. Lester M, Broadway DC, Mikelberg FS, Drance SM. A comparison of healthy, ocular hypertensive, and glaucomatous optic disc topographic parameters. *J Glaucoma* 1997;6:363-70.
32. Lester M, Mikelberg FS, Drance SM. The effect of optic disc size on diagnostic precision with the Heidelberg retina tomograph. *Ophthalmology* 1997;104:545-8.
33. Wollstein G, Garway-Heath DF, Hitchings RA. Identification of early glaucoma cases with the scanning laser ophthalmoscope. *Ophthalmology* 1998;105:1557-63.
34. Deleon-Ortega JE, Arthur SN, McGwin G, Jr., Xie A, Monheit BE, Girkin CA. Discrimination between glaucomatous and nonglaucomatous eyes using quantitative imaging devices and subjective optic nerve head assessment. *Invest Ophthalmol Vis Sci* 2006;47:3374-80.
35. Zangwill LM, Weinreb RN, Beiser JA, et al. Baseline topographic optic disc measurements are associated with the development of primary open-angle glaucoma: the Confocal Scanning Laser Ophthalmoscopy Ancillary Study to the Ocular Hypertension Treatment Study. *Arch Ophthalmol* 2005;123:1188-97.
36. Bowd C, Zangwill LM, Medeiros FA, et al. Confocal scanning laser ophthalmoscopy classifiers and stereophotograph evaluation for prediction of visual field abnormalities in glaucoma-suspect eyes. *Invest Ophthalmol Vis Sci* 2004;45:2255-62.
37. Bowd C, Medeiros FA, Zhang Z, et al. Relevance vector machine and support vector machine classifier analysis of scanning laser polarimetry retinal nerve fiber layer measurements. *Invest Ophthalmol Vis Sci* 2005;46:1322-9.
38. Essock EA, Zheng Y, Gunvant P. Analysis of GDx-VCC polarimetry data by Wavelet-Fourier analysis across glaucoma stages. *Invest Ophthalmol Vis Sci* 2005;46:2838-47.
39. Medeiros FA, Zangwill LM, Bowd C, Bernd AS, Weinreb RN. Fourier analysis of scanning laser polarimetry measurements with variable corneal compensation in glaucoma. *Invest Ophthalmol Vis Sci* 2003;44:2606-12.
40. Vessani RM, Moritz R, Batis L, Zagui RB, Bernardoni S, Susanna R. Comparison of quantitative imaging devices and subjective optic nerve head assessment by general ophthalmologists to differentiate normal from glaucomatous eyes. *J Glaucoma* 2009;18:253-61.

41. Greaney MJ, Hoffman DC, Garway-Heath DF, Nakla M, Coleman AL, Caprioli J. Comparison of optic nerve imaging methods to distinguish normal eyes from those with glaucoma. *Invest Ophthalmol Vis Sci* 2002;43:140-5.
42. Essock EA, Sinai MJ, Bowd C, Zangwill LM, Weinreb RN. Fourier analysis of optical coherence tomography and scanning laser polarimetry retinal nerve fiber layer measurements in the diagnosis of glaucoma. *Arch Ophthalmol* 2003;121:1238-45.
43. Hoffmann EM, Bowd C, Medeiros FA, et al. Agreement among 3 optical imaging methods for the assessment of optic disc topography. *Ophthalmology* 2005;112:2149-56.
44. Leung CK, Chan WM, Chong KK, et al. Comparative study of retinal nerve fiber layer measurement by StratusOCT and GDx VCC, I: correlation analysis in glaucoma. *Invest Ophthalmol Vis Sci* 2005;46:3214-20.
45. Medeiros FA, Zangwill LM, Bowd C, Weinreb RN. Comparison of the GDx VCC scanning laser polarimeter, HRT II confocal scanning laser ophthalmoscope, and stratus OCT optical coherence tomograph for the detection of glaucoma. *Arch Ophthalmol* 2004;122:827-37.
46. Schuman JS, Wollstein G, Farra T, et al. Comparison of optic nerve head measurements obtained by optical coherence tomography and confocal scanning laser ophthalmoscopy. *Am J Ophthalmol* 2003;135:504-12.
47. Lin SC, Singh K, Jampel HD, et al. Optic nerve head and retinal nerve fiber layer analysis: a report by the American Academy of Ophthalmology. *Ophthalmology* 2007;114:1937-49.

LINKING AXONS AND NEURONS: UNVEILING MYSTERIES OF THE MACULA AND MODELING NEUROPROTECTION

Randy Kardon, M.D. Ph.D.
University of Iowa, Hospitals and Clinics
Iowa City, IA

LEARNING OBJECTIVES

1. Understand the linear relationship between retinal nerve fiber layer thickness and corresponding visual field areas of sensitivity.
2. Understand the limitations of using the retinal nerve fiber layer thickness to diagnose and monitor optic nerve disorders.
3. Understand the advantages and disadvantages of using the retinal ganglion cell layer thickness determined by OCT for diagnosis and management of optic neuropathy.

CME QUESTIONS

1. Which of the following factors may confound the accurate OCT determination of RNFL thickness for diagnosing optic nerve damage?
 - a) Blood vessels
 - b) Proliferation of glial elements in the retina
 - c) Scan signal to noise
 - d) Developmental differences in the distribution of axon bundles in the retina
 - e) all of the above
2. Which of the following clinical conditions is likely to show the highest correlation between structure and function using OCT?
 - a) compressive optic neuropathy
 - b) NAION after 6 months
 - c) optic neuritis after 6 months from the acute attack
 - d) visual field loss in a patient with idiopathic intracranial hypertension
 - e) all of the above

3. Which of the following factors may significantly confound the correlation between ganglion cell layer thickness and corresponding locations of visual sensitivity?
 - a) the number of ganglion cell layers in the normal retina at the locations being evaluated
 - b) peripheral field location of damage
 - c) spatial variability in the mapping of ganglion cell location to corresponding visual field
 - d) extent of visual field damage
 - e) all of the above

KEY WORDS

Optical Coherence Tomography

Retinal Nerve Fiber Layer

Ganglion Cells

Glaucoma

Anterior Ischemic Optic Neuropathy

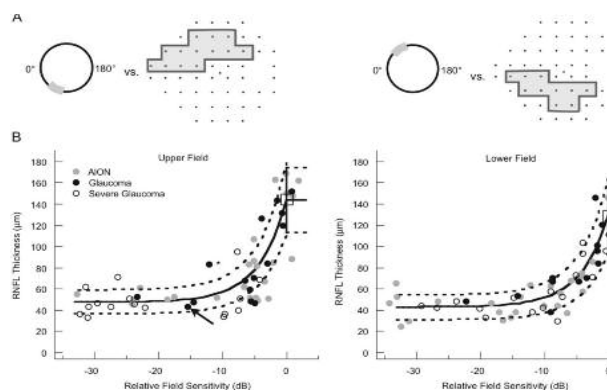
Optic Neuritis

Most clinicians, especially neuro-ophthalmologists and glaucoma specialists, have been trying to understand whether the information yielded by optical coherence tomography is really helping them to improve upon the clinical care of their patients. In this context, clinical decision-making has mainly focused on the status of the retinal nerve fiber layer (RNFL) thickness in relation to the threshold sensitivity of the corresponding area of visual field (see review, reference 1). Theoretically, it is expected that the degree of thinning of the RNFL will have a meaningful correlation with optic nerve function in a patient with loss of axons²⁻⁴ and less correlation of structure with function in locations where axons are still intact, but not functioning. In the latter case, either a return of function may still be possible, as in the case with some eyes with compressive optic neuropathy⁵, acute optic neuritis⁶⁻⁹, or ischemic optic neuropathy. Alternatively, the axons may have undergone irreversible dysfunction but not enough time has elapsed to produce atrophy and thinning of the RNFL¹.

The clinical interpretation becomes even more difficult in the setting of optic disc edema associated with visual field loss, since there may be swelling of some axons with atrophy of neighboring axons, confounding the relationship between RNFL thickness and corresponding visual field sensitivity, as long as axon swelling is present and atrophy is not yet complete. Another potential confounding variable is the status of other components that make up the thickness of the RNFL, besides axons, such as blood vessels and glial elements, which may influence the measured thickness of the RNFL^{1,10,11}.

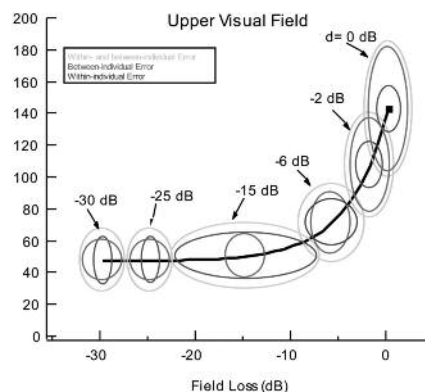
Attempts to quantify the relationship between structure and function between RNFL thickness and visual threshold at corresponding locations have discovered that there is a correlation (primarily studied in glaucoma and anterior ischemic optic neuropathy), but not as great as one would expect (refs). Factors such as measurement variability in both visual threshold and in RNFL thickness, the influence of non-neuronal elements on the RNFL thickness such as blood vessels and glial elements, and the inter-individual variation in mapping of RNFL bundles to their corresponding area of the visual field all confound the correlation in an individual patient. We have recently reviewed this topic¹ and have provided evidence for a linear model relating visual threshold (unlogged) and RNFL thickness in glaucoma and AION²⁻⁴. This is depicted in Fig 1 in semi-log plots.

FIGURE 1: Relationship of the retinal nerve fiber layer (RNFL) thickness to visual field loss in patients with glaucoma and AION. (A) A schematic illustrating the location of the corresponding disc sectors and field regions for the superior arcuate field (left panel) and inferior arcuate field (right panel). (B) RNFL thickness as a function of field loss for the upper field/inferior disc (left panel) and the lower field/superior disc (right panel). Data are shown for patients with AION ($n = 24$; filled gray), asymmetric glaucoma ($n = 15$; filled black), and severe glaucoma ($n = 16$; open symbols), and for the mean of a group of 60 age-similar controls (open square). The theoretical structure-function curves are fitted to a linear function, but plotted here on a semi-log plot. For the upper and lower visual field regions, three theoretical curves are shown (50th percentile=solid line, 95th percentile, and 5th percentile = dashed lines). From review reference 1 (with author permission).



While the relationship between RNFL thickness and visual field sensitivity appears to correspond to a linear model, there are still between and within subject components of measurement variability that impose limitations of this framework and its application to individual patients (see Figure 2). In addition, the dynamic range of both the RNFL and threshold sensitivity and their associated measurement variability limit meaningful relationships to be explored once 10 decibels of threshold loss have been exceeded or if the RNFL thickness drops below 60 microns for arcuate field loss.

FIGURE 2: The ellipses are the 95% confidence boundaries of the linear model of structure vs function with variability component shown for different glaucoma disease states, d , expressed in decibels of field loss. The 95% ellipses for the combined within- and between-individual variability (green), for between-individual variability excluding within-individual variability (red), and for within-individual variability excluding between-individual variability (blue) are shown for six levels of decibel visual field loss (from reference 4 with author permission).



In glaucoma studies, the RNFL thickness has been shown to have a very good sensitivity and specificity for diagnosing glaucoma, using Receiver-Operator Characteristic curve analysis (ROC). It is important to keep in mind that such analyses are always influenced by the criteria that are chosen as the gold standard for the presence or absence of the disease, the characteristics of the population being studied in terms of the distribution of severity of damage in the population included, and whether structure (disc appearance) or function (visual field sensitivity and the pattern of loss) is used as the criteria for the presence of glaucomatous or optic nerve disease.

A great deal of research has also been directed towards using the RNFL thickness to detect progression of glaucomatous damage over time (refs). Most of these studies have applied techniques that have also been used to study progression of visual field loss, namely a) significant change in RNFL status at a given time point from a prior baseline measurement or b) linear regression analysis of RNFL thickness over time. The main problems encountered in detecting progression using these

approaches are measurement variability and using population statistics to determine what constitutes a significant change over time. Individuals appear to vary considerably in their measurement variability, so applying population statistics (defining the variability of a given patient by applying the variability from a population of patients) to a given patient may not be optimal for individualizing the analysis of progression for a given patient. In addition, defining a statistically significant change over time may not always equate with what is a *clinically* significant change — one that would warrant a deviation in treatment. Because the rate of glaucomatous visual field progression varies considerably among treated and untreated patients and the rate is, in general, slow, the challenge in the future will be to identify as early as possible which patients are at the most risk for progression and focus aggressive treatment on those patients while not applying the same treatment to patients who are at low risk for significant progression over their remaining life expectancy.

For neuro-ophthalmology, the OCT landscape for optic nerve diseases other than glaucoma pose similar problems. These mostly encompass the following disorders and focus on questions regarding the application of OCT to diagnosis and treatment:

1. **Multiple Sclerosis:** In this setting OCT is being used to help substantiate the diagnosis of multiple sclerosis, determine whether OCT can be used to monitor the course and treatment of demyelinating disease and predict which patients are likely to progress at a faster rate, requiring a more tailored treatment approach⁶⁻⁹. There is also evidence that total macular thickness may also reflect neuronal loss in multiple sclerosis¹³. The main interest at present is whether acute optic neuritis is a good model for evaluating the efficacy of new CNS multiple sclerosis treatment strategies, such as the use of neuro-protectants and whether the use of OCT is a valid surrogate for modeling the status of multiple sclerosis and treatment strategy.
2. **Non-arteritic anterior ischemic optic neuropathy (NAION):** Structural features on OCT are being identified (such as neural opening size in the sclera) which might predict which patients are at the most risk for progressive visual field loss during the acute phase of NAION and who may respond to treatment interventions during the first 2 weeks (e.g. steroids). It may be possible to use OCT to help identify patients that are most likely to benefit from treatments aimed at preserving axons.
3. **Compressive optic neuropathy:** The presumption is that the greater number of axons that are present at the time of diagnosis, the higher potential for visual recovery if decompression is successful⁵. Here the confounding variables are how much time must elapse before axonal degeneration is detectable on OCT at the time of diagnosis and how many neurons/axons are required to support adequate visual function which may influence treatment decisions?
4. **Papilledema:** When the optic nerve appears swollen, the main questions applicable to OCT concern whether true papilledema is present vs. pseudopapilledema¹², whether the change in optic disc edema over time can be better quantified using thickening of the RNFL with OCT compared to the fundus appearance of the optic nerve and whether axon loss can be detected while the disc is still swollen and differentiated from a reduction in RNFL thickness due to lowering of intracranial pressure.
5. **Differentiation of optic neuropathy from retinopathy and identifying disorders in which both are present:** OCT scans of other portions of the posterior pole besides the RNFL can be very revealing. For example, acute or subacute visual field loss with a thickened macula on OCT but without obvious evidence of retinal edema on fundus exam may help point the diagnosis more correctly toward a branch or central retinal artery occlusion (CRAO), and away from anterior or posterior ischemic optic neuropathy, inflammatory, or compressive optic neuropathy. In the chronic state, an abnormally reduced total macular thickness keeping company with a thinned RNFL and pale nerve may also help make the diagnosis of a previous retinal artery occlusion, without requiring an electroretinogram (ERG) or neuro-imaging. Another example is a patient with possible neuroretinitis and persistent visual field loss; the combination of an OCT scan of the peripapillary RNFL and macula scan may help reveal the layer of the retina which is most likely to be the source of pathology explaining the visual field loss.

Most ophthalmologists use the macula OCT to diagnose disorders causing loss of the photoreceptors in the outer retina or disorders causing fluid accumulation in the retina (e.g. cystoid macular edema, diabetic macular edema, vitreal traction, perifoveal telangiectasia, choroidal neovascular membrane), or macular holes. Such patients may make their way into a neuro-ophthalmology clinic and a macular OCT may be an important diagnostic tool to narrow the differential and reduce cost of a work-up.

The factors discussed above pose limitations on relating the retinal nerve fiber layer to visual threshold and axon loss. This has prompted an interest in going to the source of the axons – the soma of retinal ganglion cells, which predominate in the macula. Here the question is whether the ganglion cell layer can be accurately quantified within the macula scan using current OCT technology and whether a change in the number of viable neurons can accurately be detected with current software. This also presupposes that the ganglion cells in the macula are adequate surrogates for disease affecting the visual field outside of the macula.

Segmentation of the ganglion cell layer within the central macula with spectral domain OCT has a number of potential advantages:

1. The retinal ganglion cells are densest in the macula and form a stratified multi-cellular layer within the central 6 degrees of visual field. Therefore, loss of axons and the corresponding soma in this location is likely to cause a thinning of the retinal ganglion cell layer.
2. The lack of large retinal vessels in this location makes their confounding contribution to the thickness of the ganglion cell layer very minimal, compared to the peripapillary retina, where they do influence the RNFL measurement.
3. The mapping of visual field location to corresponding ganglion cell soma is less complicated than the situation with the RNFL bundles and may show less inter-individual developmental variability. Simplistically, a focal light in the macula activates the ganglion cells directly underlying it. In the foveal and perifoveal location this is not strictly the case and some modification has to be made in this area of the visual field due to displaced ganglion cells.
4. Recent advances in OCT image analysis using both manual¹⁴ and automated analysis in three dimensions^{15,16} have provided a potential solution for delineation of the different neuronal layers in the macula (Figures 3–4).
5. Preliminary attempts to quantify the correlation between visual threshold and retinal ganglion cell thickness in the macula appear to subjectively correlate with the spatial pattern of visual field loss in the macula in patients with glaucoma (Figure 5) and anterior ischemic optic neuropathy. However, a quantitative correlation between ganglion cell thickness and corresponding overlying visual threshold has not yet been reported in detail.

FIGURE 3: Automated software 3D segmentation of the retinal layers of the normal macula using spectral domain SDOCT. Segmentation is shown for one of many successive slices of the volume macula scan. The software uses all surrounding volume image information to segment the layers.

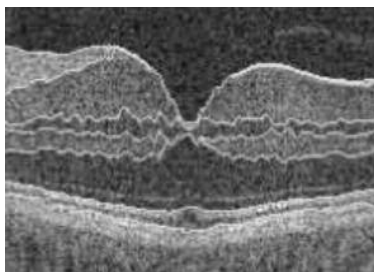


FIGURE 4: Thickness and thickness variability (standard deviation) maps of six macular intraretinal layers from the right eye of 15 normal subjects. The micron thickness of the different macula layers is color coded (red=thickest, blue=thinnest).

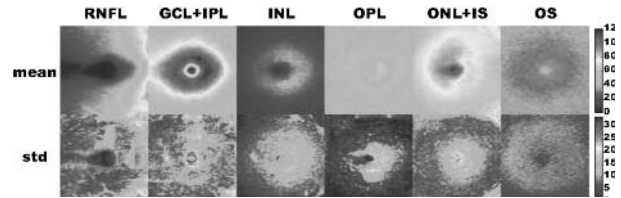
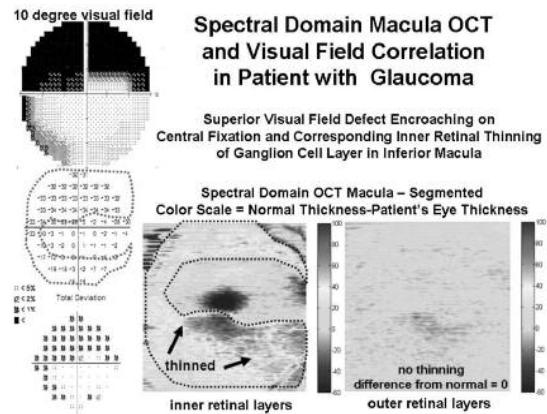


FIGURE 5: Example of a glaucoma patient whose visual field defect came close to the center of their visual field and was tested with a denser visual field testing program covering only 10 degrees of radius and which corresponds to the area of retina covered by the macula scan on the corresponding spectral domain OCT. The gray scale map shows visual sensitivity loss that was worst in the top part of the visual field (dark areas), but also shows some loss in the inferior field. The visual field sensitivity difference from normal plot is also shown below the gray scale with the abnormal area with decrease in sensitivity surrounded by a red dotted line. The statistical probability plot of the same visual field data is shown in the lower left corner. 3D-OCT was obtained on this eye and segmented into the inner retinal layer (ganglion cells and axons) and outer retinal layer containing the photoreceptors and bipolar cells. Note the high spatial correlation between the thinned layer containing the ganglion cells in the inferior macula (thinned areas are red and yellow and depicted as difference from normal) and the corresponding superior (and inferior) areas of visual field defect. However, there is no such thinning in the outer retina which is known not to be affected in most glaucomatous damage.



Challenges associated with OCT analysis of the macula that need to be overcome before clinical monitoring of optic nerve function is useful:

1. Total macula thickness is a measurement that is not likely to be specific and sensitive enough to detect small changes in the ganglion cell layer associated with optic neuropathy. This is why segmenting the different layers is likely to be a better approach.

2. Current commercially available OCT and associated software are not capable of segmenting the ganglion cell layer in three dimensions. At best, one manufacturer (Optoview) purports to segment the inner layers of the retina of the macula as a neural complex layer (RNFL, ganglion cell layer and inner plexiform layers), but this software analysis has not yet been rigorously validated. Recently Don Hood and colleagues reported to have manually segmented two dimensional line scans through the macula and have shown correlation of thinning of the ganglion cell+inner plexiform layer with corresponding loss of visual threshold in glaucoma, so this approach does have promise¹⁴. Our group has reported automated segmentation of retinal layers using a 3D graph search approach applied to volume OCT scans, as shown in Figures 3–5^{15,16}.
3. Outside of the central 6 degrees of the macula, the ganglion cell layer is less of a multi-cellular layer. In areas where there is only a single layer of ganglion cells it is not known if loss of soma will cause a measurable, significant thinning of the cellular layer or whether it will just be replaced by glial and Mueller cells, making structural thinning of the ganglion cell layer of the inner retina difficult to measure.
4. Focal peripheral visual field damage would be unlikely to affect the retinal ganglion cell layer in the macula, making it theoretically less sensitive to detection and monitoring of peripheral field pathology. On the other hand, most optic nerve diseases do show some degree of diffuse loss and although significant abnormalities in visual threshold may not be detected, there still may be a measurable decrease in retinal ganglion cell thickness in the macula, even though a visual field test may appear to show mainly extra-macular loss of sensitivity.
5. It is currently not known how much time it takes for a decrease in the thickness of the ganglion cell layer to occur after damage to the optic nerve at different distances from the globe. The time delay between permanent damage and atrophy of the ganglion cell layer would provide a framework for dating the time of injury.

In summary, recent improvements in OCT resolution and automated segmentation software has provided a means of relating visual pathway damage to structural changes in the RNFL and corresponding soma of the ganglion cells in the macula. Ganglion cell layer analysis in volume OCT data may provide yet another piece of the puzzle to understanding structure–function relationships and its application to diagnosis and monitoring of optic nerve and retinal diseases.

CME ANSWERS

1. e) all of the above; all of these factors may influence the ability to differentiate a normal RNFL from an abnormal thinning due to optic nerve damage
2. b) thinning of the RNFL reaches a maximum at 6 months following acute injury from AION. The other conditions may not show as good a correlation between structure and function.
3. e) all of the above.

REFERENCES

1. Hood DC, Kardon RH: A framework for comparing structural and functional measures of glaucomatous damage. *Prog Retin Eye Res* 2007;26(6):688–710.
2. Hood DC, Anderson SC, Wall M, Kardon RH: Structure versus function in glaucoma: an application of a linear model. *Invest Ophthalmol Vis Sci* 2007;48(8): 3662–3668.
3. Hood DC, Anderson S, Rouleau J, Wenick AS, Grover LK, Behrens MM, Odel JG, Lee AG, Kardon RH: Retinal nerve fiber structure versus visual field function in patients with ischemic optic neuropathy: a test of a linear model. *Ophthalmology* 2008;115(5):904–910.
4. Hood DC, Anderson SC, Wall M, Raza AS, Kardon RH. A test of a linear model of glaucomatous structure–function loss reveals sources of variability in retinal nerve fiber and visual field measurements. *Invest Ophthalmol Vis Sci* 2009;50(9):4254–4266.
5. Danesh–Meyer HV, Papchenko T, Savino PJ, Law A, Evans J, Gamble GD. In vivo retinal nerve fiber layer thickness measured by optical coherence tomography predicts visual recovery after surgery for parachiasmal tumors. *Invest Ophthalmol Vis Sci*. 2008 May;49(5):1879–85. Epub 2008 Feb 8.
6. Costello F, Hodge W, Pan YI, Metz L, Kardon RH. Retinal nerve fiber layer and future risk of multiple sclerosis. *Can J Neurol Sci* 2008;35(4):482–487.
7. Costello F, Hodge W, Pan Y, Eggenberger E, Coupland S, Kardon R: Tracking retinal nerve fiber layer loss after optic neuritis: a prospective study using optical coherence tomography. *Mult Scler* 2008;14(7):893–905.
8. Frohman EM, Fujimoto JG, Frohman TC, Calabresi PA, Cutter G, Balcer LJ. Optical coherence tomography: a window into the mechanisms of multiple sclerosis. *Nat Clin Pract Neurol*. 2008 Dec;4(12):664–75. Review.
9. Frohman EM, Costello F, Stüve O, Calabresi P, Miller DH, Hickman SJ, Sergott R, Conger A, Salter A, Krumwiede KH, Frohman TC, Balcer L, Zivadinov R. Modeling axonal degeneration within the anterior visual system: implications for demonstrating neuroprotection in multiple sclerosis. *Arch Neurol*. 2008 Jan;65(1):26–35. Review.
10. Hood DC, Salant JA, Arthur SN, Ritch R, Liebmann JM. The Location of the Inferior and Superior Temporal Blood Vessels and Interindividual Variability of the Retinal Nerve Fiber Layer Thickness. *J Glaucoma*. 2009 Aug 5. [Epub ahead of print]
11. Hood DC, Fortune B, Arthur SN, Xing D, Salant JA, Ritch R, Liebmann JM. Blood vessel contributions to retinal nerve fiber layer thickness profiles measured with optical coherence tomography. *J Glaucoma*. 2008 Oct–Nov;17(7):519–28.

12. Johnson LN, Diehl ML, Hamm CW, Sommerville DN, Petroski GF. Differentiating optic disc edema from optic nerve head drusen on optical coherence tomography. *Arch Ophthalmol*. 2009 Jan;127(1):45–9.
13. Burkholder BM, Osborne B, Loguidice MJ, Bisker E, Frohman TC, Conger A, Ratchford JN, Warner C, Markowitz CE, Jacobs DA, Galetta SL, Cutter GR, Maguire MG, Calabresi PA, Balcer LJ, Frohman EM. Macular volume determined by optical coherence tomography as a measure of neuronal loss in multiple sclerosis. *Arch Neurol*. 2009 Nov;66(11):1366–72.
14. Wang M, Hood DC, Cho JS, Ghadiali Q, De Moraes GV, Zhang X, Ritch R, Liebmann JM. Measurement of local retinal ganglion cell layer thickness in patients with glaucoma using frequency-domain optical coherence tomography. *Arch Ophthalmol*. 2009 Jul;127(7):875–81.
15. Haeker M, Wu X, Abramoff M, Kardon R, Sonka M: Incorporation of regional information in optimal 3-D graph search with application for intraretinal layer segmentation of optical coherence tomography images. *Inf Process Med Imaging* 2007;20: 607–618.
16. Garvin MK, Abramoff MD, Kardon R, Russell SR, Wu X, Sonka M. Intraretinal layer segmentation of macular optical coherence tomography images using optimal 3-D graph search. *IEEE Trans Med Imaging*. 2008;27(10):1495–1505.

PLATFORM PRESENTATION

GANGLION CELL LAYER VOLUME BY SPECTRALIS OPTICAL COHERENCE TOMOGRAPHY (OCT) IN MULTIPLE SCLEROSIS

Emma Davies¹, Dina Jacobs¹, James Wilson¹, Clyde Markowitz¹, Steven Galetta¹, Elliot Frohman², Peter Calabresi³, Laura Balcer¹

¹University of Pennsylvania School of Medicine, Philadelphia, PA, United States,

²University of Texas Southwestern Medical Center, Dallas, TX, United States,

³Johns Hopkins University School of Medicine, Baltimore, MD, United States

INTRODUCTION:

Anterior visual pathway neuronal loss in multiple sclerosis (MS) has been suggested by optical coherence tomography (OCT) measurements of macular volume. Software programs that segment retinal layers are used but not yet widely available. The purpose of this study was to pilot a manual method of estimating the retinal ganglion cell layer volume by Spectral-Domain OCT, and to explore the relation of this volume to visual function and prior history of optic neuritis (ON).

METHODS:

Patients with MS and control subjects underwent fast macular OCT scans (25 frames/eye) obtained with Spectral-Domain OCT technology. Ganglion cell layer volume was determined by manually outlining these structures for each frame of the OCT scan. Images were magnified by 400–800%; contrast was enhanced to maximize the accuracy of layer delineation. Visual function testing was performed using low-contrast (1.25% level) and high-contrast visual acuity (VA).

RESULTS:

Eyes of patients with MS ($n=16$, age 50 ± 6.3 years) had a lower ganglion cell layer volumes than did control eyes (MS: 0.76 mm^3 vs. controls: 1.06 mm^3 ; $p=0.0001$, t-test). MS eyes with a prior history of ON had the greatest degree of ganglion cell layer thinning. Lower ganglion cell layer volumes were associated with poorer performance on tests of low-contrast letter acuity ($r=0.60$, $p<0.001$), but not VA ($r=0.10$).

CONCLUSION:

This exploratory study demonstrates thinning of the retinal ganglion cell and associated layers in MS eyes. This finding is most pronounced in the setting of a prior history of ON, consistent with the occurrence of neuronal loss in addition to axonal loss in this setting. Low-contrast acuity is more sensitive than high-contrast VA to ganglion cell layer loss in this small cohort. Ongoing longitudinal studies piloting segmentation software will define the temporal relation of neuronal to axonal degeneration in MS, ON, and other optic neuropathies.

REFERENCES:

1. Burkholder B, Osborne B, Loguidice M, et al. Macular volume by optical coherence tomography as a measure of neuronal loss in multiple sclerosis. Archives of Neurology 2009, in press.
2. Dijk H, Kok P, Garvin M, et al. Selective loss of inner retinal layer thickness in type 1 diabetic patients with minimal diabetic retinopathy. Investigative Ophthalmology & Visual Science 50:3404–3409, 2009.
3. Wolf-Schnurrbush U, Ceklic L, Brinkmann C, et al. Macular thickness measurements in healthy eyes using six different optical coherence tomography instruments. Investigative Ophthalmology & Visual Science 50:3432–3437, 2008.

KEY WORDS:

Multiple Sclerosis (MS), Optical Coherence Tomography (OCT), Ganglion Cell Layer, Visual Function

FINANCIAL DISCLOSURE: NONE

EVIDENCE MEETS PRACTICE: TAKE-HOME POINTS ON OCT

Thomas R. Hedges III, MD

Tufts University
Boston, Massachusetts

LEARNING OBJECTIVES

1. To understand how OCT helps identify maculopathy that may mimic optic neuropathy.
2. To understand how OCT can aid in the management of various optic neuropathies.
3. To understand some of the limitations of OCT and how to avoid misinterpretation of OCTs.

CME QUESTIONS

1. OCT can identify all but which of the following macular lesions that may not be apparent clinically?
 - a. Occult outer retinopathy, including MEWDS
 - b. Stargardt's disease
 - c. Cone dystrophy
 - d. Solar maculopathy
2. OCT can clearly distinguish improvement of papilledema from evolution of papilledema into atrophic papilledema. True or False?
3. Nerve fiber layer analysis by OCT can distinguish mild papilledema from pseudopapilledema. True or False?

KEY WORDS

1. Optical Coherence Tomography
2. Occult Maculopathy
3. Optic Neuropathy
4. Papilledema
5. Optic Neuritis
6. Anterior Ischemic Optic Neuropathy

INTRODUCTION

I have been fortunate to have access to optical coherence tomography (OCT) since its inception thanks to collaboration between Joel Schuman and others at the New England Eye Center¹ with Jim Fugimoto at M.I.T.² At first, this appeared to be a tool primarily useful for retina specialists, but, as optic nerve analysis became more refined for the use in glaucoma, its use in other types of optic neuropathy became more apparent. However, there are still some difficulties with regard to this, which will be reviewed below. What turns out to be most useful in neuro-ophthalmic practice is the ability of OCT to identify and prove occult maculopathy mimicking optic

neuropathy, and this has had a significantly positive impact on my practice.

HOW I USE OCT IN MY NEURO-OPHTHALMIC PRACTICE

Proving Maculopathy That May Mimic Optic Neuropathy

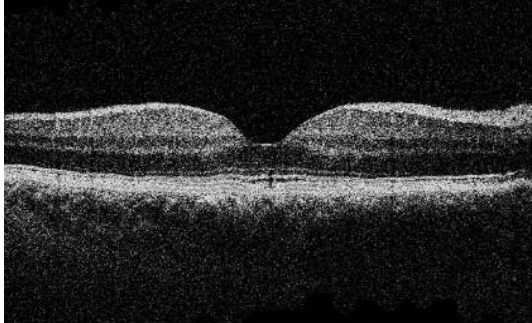
Years ago, the diagnosis of occult maculopathy mimicking optic neuropathy depended on subtle and often indirect findings. Frequently, this also required ruling out optic neuropathy, sometimes at significant expense. It was not unusual for neuro-ophthalmologists to become engaged in a dialogue with a retina specialist who insisted that a patient with unexplained visual loss had optic neuropathy, when the neuro-ophthalmologist was sure that the problem was indeed macular, but had no clear way of proving this. Central serous retinopathy was a common maculopathy, which could mimic optic neuropathy yet could easily be identified with fundus fluorescein angiography. However, now, with more refined OCT techniques, other retinal conditions mimicking optic neuropathy are more easily proven.

The diagnosis of macular hole and epiretinal membrane often required considerable discussion between neuro-ophthalmologists and retina colleagues in the past. Now macular hole is a favorite diagnosis for retina specialists now that it can be treated surgically. OCT reliably and consistently demonstrates macular holes and epiretinal membranes.³ Another group of conditions, now more easily identified using OCT, the occult outer retinopathies, includes multiple evanescent white-dot syndrome, acute zonal occult outer retinopathy, and acute idiopathic blind spot enlargement syndrome. These conditions are especially easy to identify with high-resolution OCT whereby the inner segment/outer segment junction is usually affected in the retinal areas corresponding to the clinical findings.⁴⁻⁸ These diagnoses are also made with more assurance using multifocal retinography. However, OCT is much easier and quicker for the patient and usually suffices.

We have also found that ultra-high resolution OCT helps in localizing the cause of microscotomas to the outer retina. However, we still do not have a better understanding of the pathophysiology of this condition. Hopefully, with more detailed OCT, the mechanism by which these micro scotomas occur will become apparent. The structural findings in some patients with microscotoma that we see with OCT do resemble those which are seen with phototoxic maculopathy⁹⁻¹¹ which can

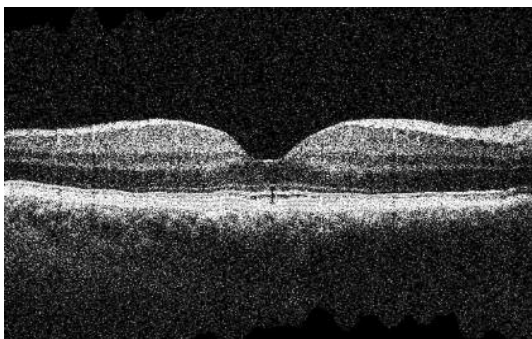
result in a very discrete area of inner segment/outer segment loss in such individuals. It also resembles what is occasionally seen in patients with epiretinal membrane.¹²

FIGURE 1. Inner segment/outer segment defect in a patient with a paracentral microscotoma.



Bilateral central visual loss in young people with apparently normal appearing retinas and optic nerves has been a diagnostic dilemma until recently. Frequently, these children have required a variety of rather expensive investigations. Although multifocal electroretinography can identify juvenile retinal degeneration or Stargardt's disease when it does occur, OCT does show distinctive macular outer retinal changes early on, and I think OCT will become the standard way of making this diagnosis in the future.¹³ Multifocal electroretinography may be difficult in young children, although we have been able to use this approach in some individuals as young as six years of age. We have also found that OCT is as sensitive in identifying hydroxychloroquine retinopathy as multifocal ERG.¹⁴ OCT allows neuro-ophthalmologists to make diagnosis of occult maculopathy much more efficiently and, this has saved me time and has saved patients considerable expense.

FIGURE 2. Perifoveal inner segment/outer segment loss in a patient with Plaquenil retinal toxicity. Note also the presence of epiretinal membrane on the right portion of the inner retina.



OPTIC NEUROPATHY IN THE PRESENCE OF RETINOPATHY

OCT can identify optic neuropathy when there is nerve fiber layer loss, and this may be the first clue that there is an insidious optic neuropathy occurring such as with optic nerve sheath meningiomas. In individuals with mild decrease in visual acuity, mild visual field constriction, mild color vision loss, and subtle visual field constriction, finding nerve fiber layer thinning provides more objective evidence that there is an optic neuropathy that requires further investigation. We have been impressed with how optic nerve head analysis by OCT will identify optic neuropathy in the presence of a known maculopathy. Even though such individuals may have visual field characteristics that are more typical of optic neuropathy, such as bitemporal hemianopia, frequently a concomitant maculopathy makes interpretation of subjective psychophysical tests difficult. Finding characteristic nerve fiber layer changes on OCT does help motivate me at least to obtain MRI scans when a retinal surgeon sends me a patient in whom the possibility of an optic neuropathy coexisting with maculopathy arises.

FUNCTIONAL LOSS OF VISION

OCT can provide further objective evidence of normal structure in patients suspected of having functional visual loss. However, one must remember that retinal nerve fiber layer degeneration does take time to develop, and a normal RNFL thickness does not always rule out a compressive optic neuropathy. However, in patients who have had functional visual loss for many months or years, a normal RNFL thickness, along with a normal macular scan, is strong, objective evidence that there is no structural pathology accounting for visual loss that is likely functional in nature.

OPTIC NERVE SWELLING

We have attempted to use OCT to differentiate mild papilledema from pseudopapilledema. OCT can show optic nerve head drusen, and, when there are significant drusen, one would expect the retinal nerve fiber layer to be thin.¹⁵ However, in those individuals with congenitally crowded optic nerve heads, without significant drusen, we have been impressed that OCT shows thickening of the nerve fiber layer, similar to that which occurs in mild papilledema.¹⁶ Therefore, we now use OCT to observe such individuals with suspected pseudopapilledema over time, just the way we used to use photographs for this purpose. If the OCT does not show any change in the nerve fiber layer thickness over time, then we can assume that such individuals were born with crowded nerves and thicker nerve fiber layers. The finding of thickened nerve fiber layer on circumferential OCTs in patients with pseudopapilledema is not surprising, considering that there is axoplasmic flow stasis in these individuals, just as there is in those with true papilledema. Of course, one must remember that patients with pseudopapilledema can

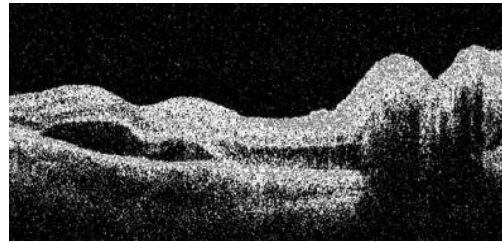
develop increased intracranial pressure and these two conditions may occur simultaneously. Recently, one report showed evidence that peripapillary subretinal fluid may be seen exclusively in patients with pathologic optic nerve swelling either from increased intracranial pressure or from ischemic optic neuropathy. Perhaps this may be the best way to distinguish mild papilledema from pseudopapilledema in the future.¹⁷

We also have been using OCT to followup patients with papilledema. However, the main problem with this has been in interpreting what appears to be normalization of the retinal nerve fiber layer thickness when there is concomitant optic atrophy, which also leads to reduction in the thickness of the nerve fiber layer over time. However, we have some indication that there may be a pattern of nerve fiber layer change, which may indicate that there is optic atrophy superimposed upon papilledema. When the thickness of the superior nerve fiber layer diminishes while the thickness of the inferior nerve fiber layer remains elevated, the likelihood of visual field loss appears to rise, indicating the onset of atrophic papilledema, rather than improvement in the papilledema.

One observation that OCT has allowed is the visualization of subretinal fluid in patients with papilledema.¹⁸ This may correlate with loss of visual acuity which is a reversible phenomenon. The degree of subretinal fluid in the foveal region seems to correlate with the degree of visual acuity loss, and, just as in patients with central serous retinopathy, the prognosis for recovery of visual acuity remains good and, in my practice, when there is loss of visual acuity and this can be demonstrated to be due to subretinal fluid by OCT, I do not feel that this is definitely an indication for urgent intervention surgically. The source of the fluid is not entirely clear. Because there is frequently a communication between the subfoveal fluid and the peripapillary subretinal fluid that we also described, the possibility that the fluid could be coming from the choroid remains the best possibility. There may be disruption of the connections between Bruch's membrane and the optic nerve which is disturbed because of the swelling of the nerve, allowing for serous fluid to leak under the retina in the peripapillary space and then, in some individuals, track into the subfoveal region.

Subretinal fluid has also been observed in patients with anterior ischemic optic neuropathy.¹⁹ We believe that, when there is loss of visual acuity in patients with AION associated with subfoveal fluid, this may have significant implications with regard to treatment. Patients with subretinal fluid from AION, like patients with subretinal fluid from papilledema, also have a good prognosis for spontaneous recovery of visual acuity as the subretinal fluid resorbs.

FIGURE 3. Foveal and peripapillary subretinal fluid in a patient with acute nonarteritic AION. The patient's vision spontaneously recovered from 20/400 to 20/40 over 3 months.



VITREOPAPAPILLARY TRACTION

OCT has also been very useful in our practice in patients with suspected optic disc swelling due to vitreopapillary traction.²⁰ Vitreopapillary traction may be difficult to prove by ophthalmoscopy alone. However, OCT clearly shows vitreous adhesions to the optic nerve head, and in some of these individuals, there may be simultaneous, vitreomacular traction. When the latter occurs, the resolution of the pseudopapilledema caused by vitreopapillary traction can be relieved surgically.

COMPRESSIVE OPTIC NEUROPATHY

There have been some interesting OCT findings in patients with compressive optic neuropathy.^{21, 22} However, from a practical point of view, we have not found OCT to be all that useful in managing patients with compressive optic neuropathy. We do not feel that OCT aids in the prognosis any more than ophthalmoscopic observation of the retinal nerve fiber layer does. Our main goal in managing patients with compressive optic neuropathy is to prevent any retinal nerve fiber layer loss, and visual field testing remains the main tool in identifying compressive optic neuropathy before optic atrophy develops. As opposed to patients with optic nerve head disease, glaucoma being the main example, visual field changes usually precede nerve fiber layer changes and we continue to follow all of our patients with compressive optic neuropathy primarily monitoring their visual fields.

OPTIC NEURITIS

From a practical point of view OCT is occasionally useful in managing patients with optic neuritis.²³⁻²⁹ Although OCT can serve as a biomarker for the progression of demyelinating disease, it may not always reflect the overall degree of demyelination occurring in such individuals. Certainly, OCT will be a useful in studies of the effectiveness of various drugs in the treatment of demyelinating disease from an investigational point of view, but for the day-to-day management of patients with MS, OCT is probably only going to be as useful as MRI scanning to monitor the overall condition of the patient. Although there have been reports of OCT helping to distinguish patients with neuromyelitis optica from those

with multiple sclerosis, the degree of nerve fiber layer dropout is reflected by the degree of visual loss demonstrated by visual acuity testing or visual field testing, so OCT so in and of itself is not all that useful in that regard.

CAVEATS

Although OCT has become very useful in my practice over the last several years, I try to remain aware of some of the limitations of OCT. OCT can be normal in patients with compressive optic neuropathy, and visual field testing remains the most important diagnostic tool in the diagnosis and followup of patients with compressive optic neuropathy. OCT can be normal in patients with some occult maculopathies, and multifocal electroretinography may be needed to identify maculopathy in these patients and to prevent extensive evaluations, searching for other diagnoses. A bad OCT is like a bad MRI or a bad CT scan. There may be errors in retinal nerve fiber layer analysis. Sometimes the algorithm used by the OCT machine will fail and false measurements of the retinal nerve fiber layer or the macula may occur. It is important to check the alignment of the circular scans when analyzing retinal nerve fiber layer measurements. If the scan is not properly placed which respect to the optic nerve head, inaccurate measurements may follow. This is especially problematic in patients with swollen optic nerves where the presence of subretinal fluid and marked elevation of the nerve fiber layer may provide measurements which are inaccurate because they are out of the range of the normal algorithm. Perhaps, in patients with optic nerve head swelling, a larger diameter should be used for retinal nerve fiber layer analysis. Also, there may be errors in macular analysis. To avoid this, because most macular diagnoses rely on a more qualitative evaluation of the OCT, I always obtain line scans, which incorporate the optic nerve head and the macula. This allows for a better view of the anatomic details of the macula, which are not always clear on the typical macular scans. OCT may identify concurrent optic nerve and macular disease. Therefore, I image the macula as well as the RNFL in every patient in whom I obtain OCT.

MY STANDARD PROTOCOL FOR OCT

My standard protocol is to obtain a retinal nerve layer scan, a macula scan, and a line scan of the macula and nerve. I have not found that the optic nerve head protocol is useful in analyzing optic nerve disease, and I have very little experience with this. Spectral domain OCT appears better than time domain for evaluating macular disease. However, the time domain appears to be more consistent with regard to retinal nerve fiber layer analysis, especially for serial analysis over time. High-speed ultra-high resolution OCT is best for occult maculopathy, especially for the occult outer retinopathies, and also in patients with micro scotomas.

CME ANSWERS

1. C
2. False
3. False

REFERENCES

1. Huang D, Swanson EA, Lin CP, Schuman JS, Stinson WG, Chang W, et al. Optical coherence tomography. *Science* 1991 Nov 22;254(5035):1178-81.
2. Fujimoto JG, Brezinski ME, Tearney GJ, Boppart SA, Bouma B, Hee MR, et al. Optical biopsy and imaging using optical coherence tomography. *Nat Med* 1995 Sep;1(9):970-2.
3. Ko TH, Witkin AJ, Fujimoto JG, et al. Ultrahigh-resolution optical coherence tomography of surgically closed macular hole. *Arch Ophthalmol* 2006;124:827-836.
4. Witkin AJ, Ko TH, Fujimoto JG, et al. Ultra-high resolution optical coherence tomography assessment of photoreceptors in retinitis pigmentosa and related diseases. *Am J Ophthalmol* 2006;142:945-952.
5. Pieroni CG, Witkin AJ, Ko TH, et al. Ultrahigh resolution optical coherence tomography in non-exudative age related macular degeneration. *Br J Ophthalmol* 2006 Feb;90(2):19-17.
6. Ko TH, Fujimoto JG, Duker JS, et al. Comparison of ultrahigh and standard resolution optical coherence tomography for imaging of macular pathology and repair. *Ophthalmol* 2004;111:2033-43.
7. Drexler W, Sattmann H, Hermann B, et al. Enhanced visualization of macular pathology with the use of ultrahigh-resolution optical coherence tomography. *Arch Ophthalmol* 2003;121(5):695-705.
8. Srinivasan VJ, Wojtkowski M, Witkin AJ, et al. High-definition and 3-dimensional imaging of macular pathologies with high-speed ultrahigh-resolution optical coherence tomography. *Ophthalmology* 2006;113:2054-2065.
9. Garg SJ, Martidis A, Nelson ML, et al. Optical coherence tomography chronic solar retinopathy. *Am J Ophthalmol* 2004;137:351-354.
10. Chen RW, Gorczynska I, Srinivasan VJ, et al. High-speed ultrahigh resolution optical coherence tomography findings in chronic solar retinopathy. *Retin Cases Brief Rep* 2008;2(2):101-102.
11. Kaushik, S, Gupta V, Gupta A. Optical coherence tomography findings in solar retinopathy. *Ophthalmic Surg Lasers Imaging* 2004;35(1):52-5.
12. Witkin AJ, Wojtkowski M, Reichel E, et al. Photoreceptor disruption secondary to posterior vitreous detachment as visualized using high-speed ultrahigh resolution optical coherence tomography. *Arch Ophthalmol* 2007 Nov;125(11):1579-1580.
13. Ergun E, Hermann B, Wirtitsch M, et al. Assessment of Central Visual Function in Stargardt's Disease/Fundus Flavimaculatus with Ultrahigh-Resolution Optical Coherence Tomography. *Investigative Ophthalmology and Visual Science*. 2005;46:310-316.
14. Rodriguez-Padilla JA, Hedges TR, Monson B, Srinivasan V, et al. High-Speed Ultra-High-Resolution Optical Coherence Tomography Findings in Hydroxychloroquine Retinopathy. *Arch Ophthalmol*. 2007;125:775-780.

15. Roh S, Noecker RJ, Schuman, JS, Hedges TR, Weiter JJ, Mattox C. Effect of optic nerve head drusen on nerve fiber layer thickness. *Ophthalmology* 1998; 105:878–885.
16. Karam EZ, Hedges TR. Optical coherence tomography of the retinal nerve fibre layer in mild papilloedema and pseudopapilloedema. *Br J Ophthalmol* 2005;89:294–298.
17. Johnson LN, Diehl ML, Hamm CW et al. Differentiating Optic Disc Edema From Optic Nerve Head Drusen on Optical Coherence Tomography . *Arch Ophthalmol*. 2009;127(1): 45–49.
18. Hoye VJ, Berrocal AM, Hedges TR, Amaro–Quiereza ML. Optical coherence tomography demonstrates subretinal macular edema from papilledema. *Arch Ophthalmol*. 2001;119: 1287–1290.
19. Hedges TR, Vuong, LN, Gonzalez–Garcia AO, Mendoza–Santiesteban CE, Amaro–Quiereza AL. Subretinal fluid from anterior ischemic optic neuropathy demonstrated by optical coherence tomography. *Arch Ophthalmol* 2008;126:812–815.
20. Hedges TR, Flattem NL, Bagga A. Vitreopapillary traction confirmed by optical coherence tomography. *Arch Ophthalmol* 124; 279–281: 2006.
21. Kanamori A, Nakamura M, Matsui N, et al. Optical coherence tomography detects characteristic retinal nerve fiber layer thickness corresponding to band atrophy of the optic discs *Ophthalmology* 2004; 111: 2278–2283.
22. Monteiro MLR, Leal BC, Rosa AAM, Bronstein MD. Optical coherence tomography analysis of axonal loss in band atrophy of the optic nerve. *Br J Ophthalmol* 2004;88:896–899.
23. Zaveri MS, Conger A, Salter A, et al. Retinal imaging by laser polarimetry and optical coherence tomography evidence of axonal degeneration in multiple sclerosis. *Arch Neurol* 2008 Jul;65(7):924–8.
24. Frohman EM, Dwyer MG, Frohman T, et al. Relationship of optic nerve and brain conventional and non–conventional MRI measures and retinal nerve fiber layer thickness, as assessed by OCT and GDx: a pilot study. *J Neurol Sci* 2009 Jul 15;282(1–2):96–105.
25. Costello F, Hodge W, Pan YI, et al. Tracking retinal nerve fiber layer loss after optic neuritis: a prospective study using optical coherence tomography. *Mult Scler* 2008 Aug;14(7):893–905.
26. Henderson AP, Trip SA, Schlottmann PG, Altmann DR, Garway–Heath DF, Plant GT, et al. An investigation of the retinal nerve fibre layer in progressive multiple sclerosis using optical coherence tomography. *Brain* 2008 Jan;131(Pt 1): 277–87.
27. Pulicken M, Gordon–Lipkin E, Balcer LJ, et al. Optical coherence tomography and disease subtype in multiple sclerosis. *Neurology* 2007 Nov 27;69(22):2085–92.
28. Gordon–Lipkin E, Chodkowski B, Reich DS, et al. Retinal nerve fiber layer is associated with brain atrophy in multiple sclerosis. *Neurology* 2007 Oct 16;69(16):1603–9.
29. Ratchford JN, Quigg ME, Conger A, et al. Optical coherence tomography helps differentiate neuromyelitis optica and MS optic neuropathies. *Neurology* 2009 Jul 28;73(4):302–8.